ABSTRACT

MICRONOME AND KSHV INFECTION: IDENTIFICATION AND FUNCTIONAL CHARACTERIZATION OF CELLULAR MICRORNAS DURING VIRUS ENTRY

by

Hosni A. M. Hussein

April 2018

Director of Dissertation: Dr. Shaw M. Akula

Major Department: Department of Microbiology and Immunology

Kaposi's sarcoma-associated herpesvirus (KSHV), is the most recently identified human herpesvirus and causes a variety of human malignancies. KSHV is etiologically associated with Kaposi's sarcoma (KS), primary effusion lymphoma (PEL), and multicentric Castleman disease (MCD). MicroRNAs (miRNAs) are small non-coding RNA molecules that play important post-transcriptional regulatory roles in gene expression and can greatly influence virus-host cell interactions. KSHV is one of a few examples of viruses that encode their own miRNAs. KSHV encodes 12 pre-miRNAs which are processed to yield 25 mature miRNAs. To date, extensive work has been conducted on the expression and roles of cellular and KSHV-encoded miRNAs during virus latency, replication, and angiogenesis. However, little is currently known about the roles of microRNAs (miRNAs) in KSHV entry. In the following studies, we investigated the induction of cellular miRNA expression in response to initial stages of KSHV infection and their roles in virus entry. We employed deep sequencing to analyze miRNA expression in KSHV-infected BJAB cells at 15min post infection (PI) and compared this to uninfected BJAB cells. The expression profile of cellular miRNAs was significantly altered in response to KSHV entry. Interestingly, expression of these KSHV-induced miRNAs noted during early stages of infection

does not require virus replication, as UV-inactivated KSHV could induce the expression of cellular miRNAs to comparable levels as live wild-type KSHV. A synthetic mimic for miR-36, a novel cellular miRNA expressed in response to KSHV infection, was able to significantly inhibit virus entry by targeting the expression of interferon induced transmembrane protein 1 (IFITM1). The effect of miR-36 on KSHV infection of cells was at a post-binding stage of virus entry. Similarly, miR-36 mimic inhibits infection of closely related DNA viruses: Epstein-Barr virus (EBV), and herpes simplexvirus-2 (HSV-2). IFITM1 was observed to have a crucial role in the *in vitro* and *in vivo* infection of *γ-herpesviruses*. IFITM1-specific siRNA inhibits *γ-herpesviruses* infection in BJAB cells and BALB/c mice. Taken together, our studies provide new insights and appreciation for the role of the host cellular miRNAs to inhibit internalization of KSHV which may contribute to the development of miRNA-based antiviral therapy.

MICRONOME AND KSHV INFECTION: IDENTIFICATION AND FUNCTIONAL CHARACTERIZATION OF CELLULAR MICRORNAS DURING VIRUS ENTRY

A Dissertation

Presented to the Faculty of the Department of Microbiology and Immunology

The Brody School of Medicine, East Carolina University

In Partial Fulfillment of the Requirements for the Degree

Doctor of Philosophy in Microbiology and Immunology

by

Hosni Ahmed Mohamed Hussein

April 2018

MICRONOME AND KSHV INFECTION**:** IDENTIFICATION AND FUNCTIONAL CHARACTERIZATION OF CELLULAR MICRORNAS DURING VIRUS ENTRY

by

Hosni Ahmed Mohamed Hussein

APPROVED BY:

DIRECTOR OF DISSERTATION: _____
Shaw M. Akula, Ph.D.

COMMITTEE MEMBER: _____
Paul P. Cook, M.D.

COMMITTEEMEMBER: _____
Ronald S. Johnson, Ph.D.

COMMITTEE MEMBER: _____
Richard A. Franklin, Ph.D.

COMMITTEE MEMBER: _____
Isabelle M. Lemasson, Ph.D.

COMMITTEE MEMBER: _____
Baohong Zhang, Ph.D.

CHAIR OF THE DEPARTMENT OF MICROBIOLOGY AND IMMUNOLOGY:

_____
Everett C. Pesci, Ph.D.

DEAN OF THE GRADUATE SCHOOL:

_____
Paul J. Gemperline, Ph.D.

DEDICATION

This work is dedicated to my parents and my wife. Thank you ALL for your understanding and patience. Without your love, support and encouragement, I would not have made any success in my life.

ACKNOWLEDGMENTS

I would like to thank my mentor, Dr. Shaw Akula for guidance, patience, and continued support. One simply could not wish for a better mentor. Additionally, I would like to thank my committee members: Dr. Cook, Dr. Jonson, Dr. Lemasson, Dr. Zhang, and Dr. Franklin for their valuable feedback and suggestions. I must also acknowledge members of the Akula lab, past and present, for their willingness to offer encouragement and a helping hand.

TABLE OF CONTENTS

LIST OF TABLES

LIST OF FIGURES

LIST OF ABBREVIATIONS

3’ UTR	3 prime untranslated region
5’ UTR	5 prime untranslated region
α3β1	alpha 3 beta 1; an RGD binding integrin
αVβ3	alpha V beta 3; an RGD binding integrin
αVβ5	alpha V beta 5; an RGD binding integrin
α9β1	alpha 9 beta 1; an integrin identified as a receptor for DLD in KSHV gB
Ago	argonaute protein
AIDS	acquired immunodeficiency syndrome
BCBL cells	body-cavity-based lymphoma cell line
BJAB	Human Burkitt lymphoma B cell line
BL	Burkitt’s lymphoma
cDNA	cloned DNA
CFU	colony forming unit
CSA	chondroitin sulfate A
Ct	threshold cycle
DC-SIGN	dendritic cell-specific intercellular adhesion molecule-3-grabbing non-integrin
DGCR8	DiGeorge syndrome critical region gene 8
DMEM	Dulbecco’s modified Eagle’s medium
DMSO	dimethyl sulfoxide
DNA	deoxyribonucleic acid
dsRNA	double-stranded RNA
EBV	Epstein-Barr virus
EDTA	ethylenediaminetetraacetic acid
EEs	early endosomes
ELISA	enzyme-linked immunosorbent assay

EphA2	ephrin receptor tyrosine kinase A2
ERK1/2	extracellular signal-related kinase ½
FAK	focal adhesion kinase
FBS	fetal bovine serum
HAART	highly active antiretroviral therapy
HCV	hepatitis C virus
HCMV	human cytomegalovirus
HCoV-OC43	human coronavirus OC43
HFF	human foreskin fibroblast cells
HHV-4	human herpesvirus 4
HHV-8	human herpesvirus 8
HIV	human immunodeficiency virus
HL	Hodgkin lymphoma
HMVEC-d	human dermal microvascular endothelial cells
HVS	herpesvirus Saimiri
HS	heparan sulfate
HSV-1	herpes simplex virus-1
HSV-2	herpes simplex virus-2
HPV16	human papillomavirus 16
IFITM1	interferon-inducible transmembrane 1
IFNs	interferons
IgG	immunoglobulin G antibody molecules
IL	interleukin
ISGs	IFN-stimulated genes
KICS	KSHV inflammatory cytokine syndrome
KSHV	Kaposi’s sarcoma-associated herpesvirus

KS	Kaposi’s Sarcoma
KSHV-MCD	KSHV multicentric Castleman disease
LANA	latency-associated nuclear antigen
LEs	late endosomes
MAPK	mitogen activated protein kinase
MCD	multicentric Castleman's disease
MHV-68	murine gammaherpesvirus 68
miRNA	microRNA
MOI	multiplicity of infection
mRNA	messenger RNA
NaOH	Sodium hydroxide
NF-κB	nuclear factor-kappa B
NCR	non-coding region
nt	nucleotide
ORF	open reading frame
ORF50	immediate early gene encoding for RTA
PABP	poly-A binding protein
PAGE	polyacrylamide gel electrophoresis
P-bodies	processing bodies
PBS	phosphate buffered saline
PCR	polymerase chain reaction
PEL	primary effusion lymphoma
PFU	plaque forming units
PI	post infection
PI-3K	phosphatidylinositol 3-kinase
pre-miRNA	precursor miRNA

pri-miRNA	primary mirRNA
PVDF	polyvinylidene difluoride
qPCR	quantitative real time PCR
qRT-PCR	quantitative reverse transcription PCR
RE	replication element
RISC	RNA-induced silencing complex
RITS	RNA-induced transcriptional silencing
RNAi	RNA-interference
RNA	ribonucleic acid
RT	room temperature
RTA	replication and transcription activator
SDS-PAGE	sodium dodecyl sulfate-polyacrylamide gel electrophoresis
siRNA	small inhibitory RNA
SIR	superinfection resistance
snRNA	small nuclear RNA
ssRNA	single-stranded RNA
TPA	12-O-tetradecanoyl phorbol-13-acetate
UTR	untranslated region
UV-KSHV	UV-inactivated KSHV
VEGF	vascular endothelial growth factor
VSV	vesicular stomatitis virus
VZV	varicella zoster virus
xCT	human cysteine transporter system xCT

CHAPTER 1: REVIEW OF LITERATURE

Kaposi's Sarcoma-Associated Herpesvirus

Kaposi's sarcoma-associated herpesvirus (KSHV) also known as human herpesvirus 8 (HHV-8) is an enveloped double-stranded DNA virus originally discovered by Chang and Moore at Columbia University in Kaposi's Sarcoma (KS) tissues that were taken from acquired immunodeficiency syndrome (AIDS) patients (Bechtel et al., 2005; Chang et al., 1994; Jenner and Boshoff, 2002).

KSHV belongs to *Gammaherpesvirinae*, a sub-family of the *Herpesviridae* family, and the genus *rhadinovirus* which is also known as *Rhadinoviridae* or *gamma-2 herpesviruses* (Taylor and Blackbourn, 2011; West and Damania, 2010; Zhu et al., 1999). KSHV is closely related to the primate *gamma-2 herpesvirus*, herpesvirus saimiri (HVS) and the human gamma-1 herpesvirus, Epstein-Barr virus (EBV; HHV-4) (Taylor and Blackbourn, 2011; Westmoreland and Mansfield, 2008). KSHV consist of ~165kb dsDNA genome and encodes for more than 90 ORFs as well as 25 microRNAs (miRNAs) (Arias et al., 2014; Bai et al., 2014). The majority of KSHV ORFs are conserved herpesvirus genes expressed by many other members of the family (Dourmishev et al., 2003). Additionally, the KSHV genome has its unique ORFs which are known as K genes and are specific to KSHV (Bai et al., 2014; Sharma-Walia et al., 2006). Both KSHV and EBV are oncoviruses, distinguished by their ability to establish a lifelong persistent infection in lymphocytes.

Owing to the absence of an appropriate experimental model for human γ-herpesviruses, *in vivo* studies on KSHV and EBV are limited (Cho et al., 2013). The murine gammaherpesvirus 68 (MHV-68), a member of the subfamily of *Gammaherpesvirinae* from wild rodents, has been developed as an experimental model for these studies (Simas and Efstathiou, 1998). Similar to KSHV and EBV, MHV-68 has genetic similarity and exhibits two distinct phases of life cycle (latent and lytic replication) (Flano et al., 2000). Thus, MHV-68 is regarded as a substitute for

the human γ-herpesvirus and has been widely used for *in vitro* and *in vivo* studies on KSHV and EBV (Cipkova-Jarcuskova et al., 2013; Wu et al., 2012). Studies described in Chapter 4 use MHV-68 as a model virus to understand the biology of KSHV entry.

KSHV is an oncogenic virus, able to induce cellular transformation (Ganem, 2010; Jones et al., 2012). *In vitro* and *in vivo* studies have demonstrated that KSHV has a broad tropism and is able to infect a variety of cell types (Hertel, 2011). *In vivo*, KSHV can infect a variety of cell lineages including macrophages, keratinocytes, endothelial cells, and B-Cells, serving as the main reservoir (Ganem, 1998; Renwick et al., 2002). *In vitro*, KSHV can establish infections in a much broader range of cells, including human B cells, endothelial cells, epithelial cells, fibroblasts, mesenchymal stem cells, dendritic cells, and macrophages (Mesri et al., 1996; Rappocciolo et al., 2006; Wu et al., 2006b).

KSHV pathogenesis: Associated-diseases, epidemiology, and treatment

Studies strongly implicate an etiological association of KSHV primarily with KS, and also with two other B cell malignancies: primary effusion lymphoma (PEL) and KSHV-associated Castleman Disease (KSHV-MCD) (Neipel and Fleckenstein, 1999; Sharp and Boshoff, 2000).

KSHV infection affects a wide range of the population with different geographical distributions; however, the prevalence of infection varies between geographical locations (Whitby et al., 1998). Sub-Saharan Africa has the greatest percentage of KSHV infection (seropositivity rates >50%), where KSHV transmission is linked to horizontal transmission & intrafamilial/community spread via saliva. Such transmission modes have led KS to become the most prevalent cancer among men in Africa (Cao et al., 2014; Dedicoat et al., 2004; Dukers and Rezza, 2003; Mbulaiteye et al., 2005; Mbulaiteye et al., 2004). Mediterranean, Middle Eastern, and Caribbean countries have intermediate prevalence (seropositivity 20-30%), while KSHV infection is less common in Europe, Asia, and the United States (seropositivity <9%) (Dukers and Rezza, 2003; Uldrick and Whitby, 2011).

Treatment of KSHV-associated diseases is not based on standard guidelines, instead, the therapy depends on disease context such as the distribution of the lesions, variant, and immune competence in cases of KS (Fatahzadeh, 2012). Therapeutic options include surgical excision, chemotherapy, radiotherapy, antiviral therapy, antibodies specific to cytokines receptors, or elimination of immunosuppressive therapy in case of transplant-associated KS (Hengge et al., 2002; Schwartz, 2004; Szajerka and Jablecki, 2007). Since the advent of the highly active antiretroviral therapy (HAART), there has been a sharp decline in the incidence of KS in AIDS patients (Franceschi et al., 2010; Gabarre and Bossi, 2003; Gantt et al., 2014).

Other drugs that are being used to treat KSHV-associated pathogenesis are as follows: ganciclovir (GCV), valganciclovir for KS, (Murphy et al., 2017; Schwartz, 2004); foscarnet cidofovir, bortezomib, bleomycin for PEL (Dittmer et al., 2012; Lim et al., 2005; Murphy et al., 2017); and rituximab, siltuximab, tocilizumab for KSHV-MCD (Murphy et al., 2017; Song et al., 2010; Williams, 2013).

KS: Disease forms and geographic variation

KS is a multifocal malignancy originally described by Hungarian dermatologist Moritz Kaposi in 1872 (Stanescu et al., 2007). KS is the most prevalent cancer in HIV-infected patients and mainly affecting endothelial cells and manifested as skin lesions (Hussein et al., 2015; Stanescu et al., 2007). KS is characterized by three histological features: angiogenesis, inflammation, and proliferation (Ensoli et al., 2001). KSHV DNA has been shown to be present in all four forms of KS: classical KS (CKS), epidemic KS (AIDS-KS), endemic-KS (EKS), and transplantation-associated KS (TKS) (Ablashi et al., 2002; Cai et al., 2010b; Ganem, 2010; Pugalagiri et al., 2013).

There are variations in the incidence of KS among different populations which in part has been attributed to the availability of HAART (Uldrick and Whitby, 2011). In developed countries such as the United States, KSHV infection and KS is dramatically decreased because of the

availability of HAART. On the other hand, KS is the most common cancer in African countries where access to HAART is still limited (Coen et al., 2014; Engels et al., 2008; Gabarre and Bossi, 2003).

Virus entry: KSHV utilizes distinct receptors to successfully infect target cells

KSHV infects target cells in sequential steps (Akula et al., 2003; Kaleeba and Berger, 2006). Initially, the virus attaches to the host cell surface molecule, heparan sulfate (HS) (Bryan et al., 2005; Spear and Longnecker, 2003). Attachment of KSHV to target cells is critical for a successful virus infection as it allows envelope associated proteins to make meaningful interactions with other cell surface receptor molecules which trigger the actual entry of the virus. The internalization of the virus is either by fusion or receptor-mediated endocytosis (Spear and Longnecker, 2003).

KSHV infects cells by different entry mechanisms in a cell type-dependent manner. Clathrin-mediated endocytosis seems to be one of the common mechanisms that KSHV utilizes to enter cells (Akula et al., 2003; Greene et al., 2007; Walker et al., 2016). KSHV utilizes different cell surface receptor molecules including Ephrin Receptor Tyrosine Kinase A2 (EphA2), dendritic cell-specific ICAM-3 grabbing nonintegrin (DC-SIGN), and different combinations of integrins such as α3β1, αVβ3, αVβ5, and α9β1 (Chakraborty et al., 2012; Chandran, 2010; Hensler et al., 2014; Hussein et al., 2015). These cell surface molecules are usually referred to as the entry receptors. Numerous studies have deemed these receptor molecules, particularly integrins to be valuable for KSHV infection of cells (Akula et al., 2002; Hensler et al., 2014; Rappocciolo et al., 2008).

KSHV has a biphasic life cycle

The KSHV life cycle is biphasic comprising two sequential phases of replication: latent and lytic (Ohsaki and Ueda, 2012). Each phase of KSHV replication is characterized by its unique gene

expression profile (Uppal et al., 2015). Shortly after KSHV infection, the virus replication switches to the latent phase with only a small percentage (<3%) of infected cells supporting lytic replication (Steitz et al., 2011). A dynamic balance between latent and lytic phases of KSHV replication is critical to a successful virus infection, establishment of latency, and tumorigenesis (Frappier, 2015; Kang et al., 2011a).

The KSHV latent phase of replication is characterized by a persistent virus infection with a restricted expression of viral genes. The key role of the latent phase is to keep the virus dormant to evade the immune system, yet maintaining replication of the viral genome (White et al., 2012; Zhong et al., 1996). The few KSHV genes that are expressed during the latent phase are latency-associated nuclear antigen (LANA), vCyclin, vFLIP, and vIL-6. These genes are oncogenes and essential to maintaining the viral episome, promoting cell survival, and inhibiting apoptosis; all of which are a necessity to KSHV-induced pathogenesis (Cavallin et al., 2014; Mesri et al., 2014; Zhi et al., 2015).

The molecular mechanisms by which KSHV reactivates from the latent phase and enters lytic replication are largely un-known (Traylen et al., 2011). However, a crucial role has been described for mitogen-activated protein kinase (MAPK) signaling in KSHV reactivation (Cohen et al., 2006; Ford et al., 2006). During the Lytic phase the virus actively replicates with full viral gene expression and production of progeny virions (Toth et al., 2013). Once KSHV is reactivated, expression of lytic genes occurs in a sequential manner. Lytic genes can be divided into three groups: immediate early (IE), early (E), and late (L) genes (Uppal et al., 2014). Expression of IE genes occur immediately after reactivation and mainly encode transcription factors that are essential for the expression of viral and cellular genes. E genes encode for proteins that are required for viral DNA replication (viral polymerases, helicase, and primase) (Curreli et al., 2002). L genes encode for viral structural proteins and are expressed at the end of lytic replication. The final steps in the lytic phase are virus assembly and the release of mature virions (Chang and Kung, 2014).

KSHV gene regulation is critical to virus entry

Viruses hijack preexisting host cell signaling pathways to infect target cells and to generate a cellular state that is more receptive to virus infection and replication. One of the best examples is KSHV, which is known to activate many cell signaling pathways (Nemerow and Cheresh, 2002). Activation of these signaling pathways enables KSHV to reprogram host-cells to be susceptible to virus infection and to regulate cellular genes important to virus entry, escaping from the endosome, and trafficking inside the cytoplasm to reach the nuclear pore. KSHV regulates many cellular genes including vascular endothelial growth factor receptor 3 (VEGFR-3), lymphatic vessel endothelial hyaluronan receptor 1 (LYVE1), and Rac1 (Kumar and Chandran, 2016). These genes are essential to cell survival, proliferation, migration, angiogenesis, and contribute to KSHV-associated cellular transformation (Direkze and Laman, 2004; Hong et al., 2004; Hussein et al., 2016; Wang et al., 2004)

KSHV regulation of cellular genes occurs as early as 5min post infection of cells (Akula et al., 2003). The initial trigger to regulate cellular genes is due to the interactions of envelope-associated glycoproteins with cell surface receptors (Akula et al., 2002; Naranatt et al., 2003; Sharma-Walia et al., 2005; Sharp et al., 2002). KSHV-regulated genes have been shown to be critical to virus entry, infection, and virus-associated diseases (Chandrasekharan et al., 2016; Direkze and Laman, 2004; Emuss et al., 2009; Engels et al., 2008; Giffin et al., 2015)

Interactions with a variety of cell surface molecules allow KSHV to phosphorylate and activate focal adhesion kinase (FAK). Phosphorylation of FAK leads to activation of several focal adhesion-associated signaling molecules, including tyrosine kinase Src, phosphatidylinositol-3 kinase (PI3K), Rho GTPases (RhoA, Rac, and Cdc42), Dia2, and other effector molecules, such as AKT, ezrin, protein kinase C (PKC), MAPK, NF-kB, and p38MAPK which are a necessity for the internalization of virus (Akula et al., 2002; Hussein et al., 2015; Pan et al., 2006; Sharma-Walia et al., 2005; Xie et al., 2005). KSHV-activation of Src results in the induction of hypoxia-induced factors (HIFs) which in itself is important for KSHV-mediated

induction of VEGFR-1 (Carroll et al., 2006). KSHV regulation of the above cellular genes is critical to virus entry, infection and virus-associated diseases. The virus activates these genes at the early stage of infection to program host-cells to be more susceptible to virus entry and infection (Chandrasekharan et al., 2016; Direkze and Laman, 2004; Emuss et al., 2009; Engels et al., 2008; Giffin et al., 2015). The focus of this dissertation is on understanding the biology of KSHV entry.

Interferon-induced transmembrane proteins 1

Human interferon-inducible transmembrane 1 (hIFITM1) is a member of interferon-induced protein family including IFITM1, IFITM2, IFITM3, IFITM5, and IFITM10. Human IFITMs genes are located on chromosome 11 and are highly inducible by type I and II interferons (IFNs) (Friedman et al., 1984; Hickford et al., 2012; Reid et al., 1989).

As with other members of the IFITMs family, IFITM1 has two transmembrane domains (TM1 and TM2) which are separated by a highly conserved intracellular loop (Perreira et al., 2013). IFITM1 is expressed on the surface of many tissues and cell types (Lewin et al., 1991; Li et al., 2017; Tanaka et al., 2005). Such ubiquitously expressed IFITM1 modulates several cellular functions including immunological responses, proliferation, adhesion, germ cell maturation, and development (Hickford et al., 2012; Lewin et al., 1991). IFITM1 is induced by interferons and has been shown to be critical for the anti-viral responses (Brass et al., 2009; Deblandre et al., 1995; Evans et al., 1990; Smith et al., 2006).

IFITM1 and virus entry

Recent reports demonstrated that IFITM1 plays a significant role during entry of many viruses including influenza A H1N1 Virus, West Nile Virus and Dengue Virus, HIV, HCV, HSV2, EBV, and KSHV (Brass et al., 2009; Hussein and Akula, 2017a; Narayana et al., 2015; Yu et al., 2015b). Based on IFITMs topologies, several mechanisms have been proposed to explain their

role(s) in virus entry. However, the exact molecular mechanisms by which IFITMs inhibit or enhance virus entry remains to be determined. These proteins have been shown to inhibit virus binding to corresponding cellular receptors, blocking virus escape from endosomes, and acting as pattern recognizing receptors that activate downstream cellular signal pathways (Brass et al., 2009). IFITMs inhibit fusion between viral and endosomal membranes by blocking the creation of hemifusion, reducing membrane fluidity, and disrupting intracellular cholesterol homeostasis (Amini-Bavil-Olyaee et al., 2013; Li et al., 2013a).

IFITM1 has been shown to inhibit syncytia formation by viral proteins. Likewise, IFITM2 and IFITM3 inhibit fusion of viral glycoproteins with cell membranes in a cell type-specific manner. Interestingly, inhibition of virus entry by IFITMs has been shown to be specific to viral glycoproteins (Brass et al., 2009). On the other hand, over-expression of IFITM1 partially inhibited the infection of vesicular stomatitis virus but had no significant effect on the infection of influenza virus (Alber and Staeheli, 1996). Similarly, IFITM1 has no inhibitory effect on the infection of Rift Valley fever virus which has been shown to be significantly inhibited by IFITM2 and IFITM3. The authors of this study reported that a large fraction of IFITM1 proteins localized in vesicular compartments differ from those occupied by IFITM2 and IFITM3 (Mudhasani et al., 2013). Likewise, Warren et al reported that IFITM1, IFITM2, and IFITM3 had no inhibitory effect on infection of human papillomavirus 16 (HPV16), human cytomegalovirus (HCMV) and adenovirus type 5 (Ad5). They determined IFITM1 and IFITM3 to modestly enhance HPV16 infection of many cell types (Warren et al., 2014). In accordance with the above results, Zhao *et al.,* have shown type I IFN-α, IFN-γ, and type II IFN-λ to significantly promote infection of the human coronavirus, HCoV-OC43 by the induction of IFITM proteins. The authors reported that the IFITM2 or IFITM3 act as entry factors facilitating HCoV-OC43 infection of Huh7.5 cells (Zhao et al., 2014). The results suggest that roles of IFITMs during virus infection could be virus and/or cell-type specific.

The above variations in the mode of action between IFITM1, IFITM2 and IFITM3 during virus infection could be explained by the fact that IFITM1 primarily localized to the plasma membranes and early endosomes, while IFITM2 and IFITM3 were mainly expressed on late endosomes, lysosomes, and autolysosomes (Feeley et al., 2011; Huang et al., 2011; Perreira et al., 2013; Yount et al., 2010). Chapter 3 of this work describes a crucial role for IFITM1 in the biology of KSHV entry.

miRNAs: Biogenesis and mechanism of action

MicroRNAs (miRNAs) are a class of highly conserved small non-coding RNAs of ~ 22 nucleotides in length. The first discovered miRNA is lin-4 which was identified by Ambros and Ruvkun labs in 1993 from *Caenorhabditis elegans* (*C. elegans*) (Lee et al., 1993; Wightman et al., 1993) . miRNA lin-4 was described to regulate lin-14 mRNA translation during the early larval stage of the worm (Lee et al., 1993; Rougvie, 2001; Wightman et al., 1993). Subsequent work revealed that the miRNAs act as post-transcriptional regulators of gene expression in many organisms (Chen, 2005; Cock et al., 2010; Cuperus et al., 2011; Ninova et al., 2016; Wienholds and Plasterk, 2005). The current release of the miRBase database (miRBase release 21) contains 28645 microRNA loci from 223 species which produce 35828 mature microRNAs (Kozomara and Griffiths-Jones, 2014; Van Peer et al., 2014). The miRBase database is gradually increasing with over 2000 human miRNA sequences currently deposited in the most recent release of the mirBAse database (miRBAse 21) (Hammond, 2015; Kozomara and Griffiths-Jones, 2014).

Transcription of miRNA genes is mainly mediated by RNA Polymerase II and to a lesser extent by RNA polymerase III (Ha and Kim, 2014; Ketting, 2010; Lee et al., 2004; Macfarlane and Murphy, 2010). In general, miRNA genes are transcribed as several kilobase long transcripts called primary miRNAs (Pri-miRNAs) (Cai et al., 2004). Pri-miRNAs are processed in the nucleus to ~ 60-70- nucleotide long miRNAs precursors (Pre-miRNAs) by the

microprocessor, a complex of proteins composed of the RNAs III enzyme Drosha and its binding protein DGCR8 (Han et al., 2006). Subsequently, Pre-miRNAs are transported by Exportin-5 from the nucleus to the cytoplasm where they are trimmed by Dicer, another RNAs III enzyme (Chendrimada et al., 2005; Okada et al., 2009). Dicer products are 19-25 nt long RNA duplexes with a 3' 2-nt overhang. These miRNA duplexes are then loaded into the RNA-induced silencing complex (RISC) which includes the Ago proteins. The majority of miRNAs are produced by the canonical method described above, however, there are many alternative pathways for miRNAs biogenesis (Havens et al., 2012; Sibley et al., 2012; Yang and Lai, 2011). These include miRNAs that are generated in a microprocessor, or Dicer independent-ways (Coll et al., 2010; Eckenfelder et al., 2017; Herrera-Carrillo and Berkhout, 2017; Shapiro et al., 2010).

Once loaded to RISC, one strand of the miRNAs duplexes called the passenger strand gets ejected, while the other strand referred to as the guide strand directs the Ago proteins to the respective mRNA target(s) (Hutvagner and Zamore, 2002a, b; Khvorova et al., 2003). The seed region, positions 2-8 from the 5' end of the guide strand is critical for miRNA binding to its target (Bartel, 2009). Mutations in the seed region of miRNAs have been shown to strongly impact the ability of miRNA to bind its targets (Kertesz et al., 2007; Mencia et al., 2009). The majority of miRNAs bind to 3'-UTR of mRNA targets, however, miRNAs can also bind to the CDS and 5'-UTR of their targets (Gu et al., 2009).

The fate of miRNA targets depend on the level of complementarity between the miRNA and mRNA target. Low complementarity induces translational silencing, while high complementarity triggers degradation of mRNA (Bartel, 2004; Lewis et al., 2005). In both cases, miRNAs lead to a decrease in expression of respective proteins. A single miRNA can regulate hundreds of targets in an efficient way, conversely, multiple miRNAs can cooperatively regulate a single target (Zhou et al., 2013). Besides their role in the suppression of gene expression, miRNAs can also activate gene expression. The liver-specific miRNA, miR-122, has been shown to significantly enhance hepatitis C virus (HCV) infection and gene expression via

binding to the 5'-UTR of the viral RNA and protecting it from exonuclease activity (Li et al., 2013b). Similarly, miR-10a and miR-369-3p bind and activate expression of the ribosomal protein and TNF-α mRNAs respectively (Orom et al., 2008; Vasudevan and Steitz, 2007).

The accumulated evidence implicate miRNAs as gene regulators for about 60% of protein-coding genes. miRNA regulations have been shown to be critical for many vital mechanisms including maintenance of homeostasis, disease pathogenesis, and immunological responses to infection (Eulalio et al., 2012).

KSHV encodes miRNAs

Viruses have no miRNA processing machinery, yet many viruses encode miRNAs in their genomes including viruses from herpesviruses, adenovirus, polyomavirus, and retrovirus families (Cullen, 2011; Gourzones et al., 2012; Kincaid and Sullivan, 2012; Lieber and Haas, 2011; Nourse et al., 2012; Zhang et al., 2014). The majority of herpesviruses that infect humans encode their own miRNAs including viruses from Table 1 (Kincaid and Sullivan, 2012; Pfeffer et al., 2005; Wong et al., 2012).

One of the best examples of viruses that encode their own miRNA is KSHV. KSHV-encoded miRNAs have been described independently by several groups as early as 2005 (Cai et al., 2005; Pfeffer et al., 2005; Samols et al., 2005). Subsequent work revealed that the KSHV genome encodes 13 pre-miRNAs which are processed by cellular machinery to yield 25 mature miRNAs (**Table 1**) (Gottwein et al., 2011; Guo et al., 2017; Qin et al., 2017b). Names, sequences, and locations of KSHV encoded miRNAs and their precursors are provided in **Table 2** (Lin et al., 2010). Interestingly, KSHV-miRNAs have been shown to dominate the small RNA sequencing data generated from KSHV infected B-cell line BC-3 (Umbach and Cullen, 2010).

Tha majority of known KSHV-miRNAs are located in the latent locus and expressed during the latent phase of virus infection (Cai et al., 2005; Samols et al., 2005). KSHV-miR-K12-

10 and KSHV-miR-K12-12 are expressed more during the lytic phase and located within ORF and 3′UTR of kaposin, respectively (Lin et al., 2010). The rest of KSHV-miRNAs are expressed strictly during the latent phase from a ~ 4-kb noncoding sequence located between the kaposin and ORF71 (v-FLIP) genes (Cai et al., 2005; Gottwein et al., 2006; Qin et al., 2017b).

KSHV-encoded miRNAs promote virus latency and pathogenesis

Upon the discovery that KSHV encodes a considerable number of miRNAs, the initial focus has been to study the contributions of these miRNAs to KSHV infection and pathogenesis (Samols et al., 2007). Subsequent work revealed that KSHV-encoded miRNAs are able to regulate the expression of both viral and cellular genes that are essential to virus infection and the associated diseases (Dolken et al., 2010; Guo et al., 2017; Happel et al., 2016; Li et al., 2016a; Qin et al., 2017b; Samols et al., 2007).

KSHV-encoded miRNAs are expressed abundantly during the latent phase of virus infection. As latency is the default phase of KSHV infection, several studies have focussed their interests in determining the functions of these miRNAs in supporting viral latency (Chen et al., 2013; Gottwein, 2012; Lei et al., 2010). In 2009, Bellare and Ganem reported that the KSHV-miR-K12-9-5p inhibits virus reactivation by targeting the expression of replication and transcription activator (RTA), a KSHV immediate early gene, which is crucial to viral reactivation from latency (Bellare and Ganem, 2009). Moreover, elevated expression of RTA has been reported in cells infected with a mutant KSHV lacking 14 of the virus-encoded miRNAs (Lei et al., 2010). Similar studies conducted by Lu *et al.,* using a mutant virus indicated that the KSHV miRNAs maintain virus latency via targeting many genes including RTA and cellular retinoblastoma (Rb)-like protein 2 (Rbl2) gene which regulate epigenetic reprogramming (Lu et al., 2010).

KSHV miRNAs inhibit apoptosis of latently infected cells via targeting of apoptotic genes (Cai et al., 2005; Guo et al., 2017; Qin et al., 2017b). Suffert *et al.,* reported that the HEK293

epithelial cells and DG75 cells expressing KSHV miRNAs were protected from apoptosis (Suffert et al., 2011). Subsequently, they determined KSHV miRNAs, miR-K12-1, -3 and -4-3p, to target Casp3 and block apoptosis. Inhibition of these miRNAs with specific oligonucleotides directed to the seed regions enhances apoptosis of KSHV-infected cells (Suffert et al., 2011). Moreover, KSHV miRNAs modulate angiogenesis, signaling pathways, cell cycle, cell migration, and adhesion which are critical to KSHV dissemination and pathogenesis (Gallaher et al., 2013; Li et al., 2016a; Li et al., 2016b; Liu et al., 2017b; Samols et al., 2007). By this way, KSHV miRNAs promote tumorigenesis.

KSHV miRNAs also enhance immune evasion and viral pathogenesis by regulating host immune responses. Several groups independently reported that the KSHV miRNAs impact the functions of immune effector cells and thus alter the secretion pattern of many cytokines including IL-8, IL-10, and IL-6 (Boss and Renne, 2010; Gallaher et al., 2013; Nachmani et al., 2009; Qin et al., 2010). The aberrent expression of these cytokines is a necessity to KSHV-associated diseases (Polizzotto et al., 2012; Tamburro et al., 2012).

Roles of cellular miRNAs in KSHV entry, replication, and pathogenesis

Beside encoding its own miRNAs, KSHV infection of the cell has been shown to significantly alter the expression of many cellular miRNAs. These miRNAs, in turn, regulate KSHV entry, replication, pathogenesis, and immune evasion (Choi et al., 2015; Qin et al., 2014). A miRNA microarray profiling of six paired KS and matched adjacent healthy tissues revealed that 170 cellular miRNAs that were differentially expressed in KS tissues compared to healthy tissues (Wu et al., 2015). A large number (n=101) of these miRNAs including miR-125b-1-3p and miR-1183 were downregulated, while the rest (69 miRNAs) were upregulated and that included miR-126-3p, miR-199a-3p, and miR-16-5p (Wu et al., 2015). In a similar study, Catrina Ene *et al.,* reported 185 differentially expressed miRNAs (76 were upregulated and 109 were downregulated) in KS tissues *versus* normal skin. The most significantly downregulated miRNAs

in this study were cellular miRNAs: miR-99a, miR-200 family, miR-199b-5p, miR-100, and miR-335 (Catrina Ene et al., 2014). Similar studies reporting profiling of cellular miRNAs in KSHV-associated diseases has been conducted by several independent groups (Chugh et al., 2013; Lagos et al., 2010; O'Hara et al., 2008; O'Hara et al., 2009).

Similar to KSHV-encoded miRNAs, cellular miRNAs can also promote viral latency by inhibiting reactivation (Frappier, 2015; Yan et al., 2016). Many of the cellular miRNAs like miR-498, miR-320d, miR-557, miR-766, miR-1227, miR-1258, and miR-1301 have been shown to target mRNA of viral lytic activator RTA (Murphy et al., 2008; Yan et al., 2013; Yan et al., 2014). KSHV-induced cellular miRNAs are also involved in KSHV-induced angiogenesis. KSHV-K15, a viral oncoprotein has been shown to induce cell migration and angiogenesis via upregulation of cellular miR-21 and miR-31 (Tsai et al., 2009). Similarly, downregulation of miR-221/miR-222 cluster by KSHV infection has been reported to enhance the migration pattern of endothelial cells (Wu et al., 2011). In a way, KSHV-induced cellular miRNAs work in unision with the KSHV encoded miRNAs to promote latency and tumorigenesis.

The majority of the above work has been dedicated to studying the induction and contributions of miRNAs after the virus has succesfully established latency. For the first time, studies from our lab explored the ability of KSHV to alter expression of cellular miRNAs during early stages of infection; as early as 15min PI (Hussein and Akula, 2017b). We identified several cellular novel miRNAs which are upregulated during the initial stages of KSHV entry (Chapter 2). One of these miRNAs, miR-36, was able to inhibit the entry of not only KSHV but also related viruses, EBV and HSV-2 (Hussein and Akula, 2017a). miR-36 inhibits virus entry via targeting the expression of IFITM1, that functions as non-specific antiviral protein.

Cellular miRNAs mediate immunity against viral pathogens

Several viruses have been shown to significantly alter the expression of cellular miRNAs in infected cells (Bruscella et al., 2017; Skalsky and Cullen, 2010). This could be in part due to the

mechanism by which cells mount antiviral responses, or viral factors that inhibit cellular responses and change the intracellular milieu to support virus replication and infection (Bruscella et al., 2017; Cullen, 2013; Gottwein, 2013; Swaminathan et al., 2013; Trobaugh et al., 2014).

In general, the contributions of small RNAs to the antiviral response in chordates remains elusive compared to plants, arthropods, and nematodes (Cullen, 2010; tenOever, 2013). However, accumulating evidence indicates a crucial role for cellular miRNAs in antiviral immunity (Gantier et al., 2007; Skalsky and Cullen, 2010). Levels of miRNAs have been shown to correlate with the expression of interferons during virus infection (Lindsay, 2008; Pedersen et al., 2007). Pederson *et al.,* have shown that Interferon β induced by hepatitis C virus (HCV) rapidly modulates the expression of numerous cellular miRNAs. In turn, several of these miRNAs have been shown to target the HCV genome (Pedersen et al., 2007). Similarly, Dicer-deficient mice are more susceptible to infection with cytomegalovirus and vesicular stomatitis virus (VSV) (Ostermann et al., 2012; Otsuka et al., 2007). These studies demonstrate that the miRNAs are critical to mounting rapid antiviral responses such as interferon and interferon-inducing genes.

Cellular miRNAs have been shown to directly target the genome and transcripts of many viruses including HIV, HCV, HBV, VSV, and KSHV viruses (Chen et al., 2011; Forster et al., 2015; Jopling et al., 2005; Nathans et al., 2009; Skalsky and Cullen, 2010). Kang *et al.,* reported cellular miR-1293 to target KSHV IL-6, an essential protein for KSHV-mediated diseases, especially in the inflammatory cytokine syndrome associated with KSHV infection in AIDS patients (Kang et al., 2011b). Interestingly, KSHV has also evolved mechanisms to use cellular miRNAs to evade antiviral innate immune responses. miR-123, a cellular miRNA induced by KSHV in endothelial cells target the p300 transcriptional co-activator which negatively regulate the expression of interferon-stimulated genes and enhance virus replication (Lagos et al., 2010; Qin et al., 2014).

Studies from our recently concluded work described a crucial role for the KSHV-induced cellular miR-36 to inhibit virus infection in both B and endothelial cells which are the main targets of KSHV infection *in vivo* (Hussein and Akula, 2017a). Interestingly, miR-36 was able to inhibit infection of not only KSHV, but also EBV, and HSV-2 viruses. We were able to detect up-regulation of miR-36 as early as 15 minutes post-KSHV infection (Hussein and Akula, 2017b). Subsequently, we found that miR-36 inhibits virus infection by targeting the expression of IFITM1 protein (Hussein and Akula, 2017a). Chapters 2, 3, and 4 are aimed at describing our findings on miR-36, and IFITM1 on KSHV infection, *in vitro* and *in vivo*.

Targeting miRNAs for anti-viral and anti-cancer therapies

Cellular and viral miRNAs are attractive targets to design pathogen-specific antiviral therapies (Bofill-De Ros et al., 2017; Bruscella et al., 2017; Skalsky and Cullen, 2010). miRNA-based therapies could be formulated in two different forms: mimicking miRNA functions using miRNA-specific oligonucleotide mimics or silencing miRNA functions by miRNA-specific antisense oligonucleotide inhibitors (anti-miRNA) (Baigude and Rana, 2014; Reid et al., 2016; Tang and Tang, 2013).

There are several miRNA-based therapies currently being tested in human clinical trials (Christopher et al., 2016; Titze-de-Almeida et al., 2017). One of the most common examples of miRNA-based antiviral therapy is miR-122 antisense oligonucleotide inhibitor (miravirsen, Santaris Pharma, Hørsholm, Denmark). Miravirsen has been shown to be promising for treatment of HCV infection (de Jong and Jacobson, 2014; Janssen et al., 2013a; Janssen et al., 2013b). Interestingly, Miravirsen administration to 36 patients with chronic HCV genotype 1 infection resulted in a reduction of 1.2 to 3.0 log international units (IUs)/mL in HCV RNA levels in a dose-dependent manner without induction of virus resistance (Janssen et al., 2013b). In a recent and more promising study, Van der Ree *et al.,* reported that the administration of 2mg/kg

or 4mg/kg RG-101, a hepatocyte targeted N-acetylgalactosamine conjugated anti-miR-122 oligonucleotide, induced a significant reduction in HCV RNA levels (van der Ree et al., 2017).

As discussed above, miRNAs are able to directly target the viral genome, thus ubiquitously expressed miRNA can be harnessed to generate safe and effective live-attenuated vaccines (tenOever, 2013). Incorporation of tissue-specific miRNA target sequences into attenuated vaccines prevent the virus from replicating in this tissue (Drury et al., 2017; tenOever, 2013). Insertion of neuronal-specific miR-124 target sites into poliovirus genome inhibits the replication of the virus in the central nervous system. The engineered virus strain was able to elicit a strong protective immunity without producing neurovirulence in infected animals (Barnes et al., 2008). A similar approach has been applied to engineer safe and effective live attenuated vaccine strains for West Nile virus, dengue virus, influenza virus, VSV, and measles virus (Brostoff et al., 2016; Drury et al., 2017; Heiss et al., 2011; Kelly et al., 2010; Leber et al., 2011; Perez et al., 2009).

Similar to treating viral infections, miRNA-based therapies to treat for many cancers including that of lung cancer, pancreatic cancer, prostate cancer, colon cancer, ovarian cancer, and breast cancer are currently at preclinical and clinical phases of development (Christopher et al., 2016; Henry et al., 2011; Ibrahim et al., 2011; Liu et al., 2011; Pecot et al., 2013; Pramanik et al., 2011; Trang et al., 2011). miR-221 silencing using chol-anti-miR-221 blocks hepatocellular carcinoma and promote mouse survival. Chol-anti-miR-221 was able to inhibit tumor cell proliferation and increase the markers of apoptosis and cell-cycle arrest (Park et al., 2011). Studies described under chapters 2-4, we hope, will yield antiviral therapy to prevent KSHV and associated herpesviral infections by targeting IFITM1 by employing mi-36-specific oligonucleotide mimics.

Table1. Numbers of Pre-miRNA hairpins and mature miRNAs encoded by human herpesviruses.

Sub-Family	Viruses	Number of pre-miR Hairpins*	Number of mature miRNAs*	References
α-herpesviruses	HSV-1 (Herpes simplex virus 1)	18	27	(Cui et al., 2006; Jurak et al., 2010)
	HSV-2 (Herpes simplex virus 2)	18	24	(Jurak et al., 2010; Tang et al., 2009; Umbach et al., 2010)
β-herpesviruses	CMV (cytomegalovirus)	15	26	(Meshesha et al., 2012; Stark et al., 2012)
	Human herpesvirus 6B	4	8	(Tuddenham et al., 2012)
γ-herpesviruse	EBV (Epstein Barr virus)	25	44	(Cai et al., 2006; Cosmopoulos et al., 2009; Landgraf et al., 2007; Pfeffer et al., 2004)
	KSHV (Kaposi's sarcoma-associated herpesvirus)	13	25	(Cai et al., 2005; Lin et al., 2010; Qin et al., 2017b; Umbach and Cullen, 2010)

*Numbers of viral pre-miRNAs and mature RNAs based on the most recent release of miRBase (miRBase 21: http://www.mirbase.org/index.shtml).

Table 2. Names and sequences of KSHV-encoded miRNAs and their precursors*.

Pre-miRNA	Mature miRNAs	Start	End	Strand
KSHV-miR-K12-1 CGAUUACAGGAAACUGGGUGUAAGC UGUACAUAAUCCCCGGCAGCACCUG UUUCCUGCAACCCUCGU	**KSHV-miR-K12-1-5p** AUUACAGGAAACUGGGUGUAAG C	121847	121847	-
	KSHV-miR-K12-1-3p GCAGCACCUGUUUCCUGCAACC			
KSHV-miR-K12-2 GGGUCUACUUCGCUAACUGUAGUCC GGGUCGAUCUGAGCCAUUGAAGCAA GCUUCCAGAUCUUCCAGGGCUAGAG CUGCCGCGGUGACACC	**KSHV-miR-K12-2-5p** AACUGUAGUCCGGGUCGAUCUG	121674	121674	-
	KSHV-miR-K12-2-3p GAUCUUCCAGGGCUAGAGCUG			
KSHV-miR-K12-3 GGCUAUCACAUUCUGAGGACGGCAG CGACGUGUGUCUAACGUCAACGUCG CGGUCACAGAAUGUGACACC	**KSHV-miR-K12-3-5p** UCACAUUCUGAGGACGGCAGCG A	121544	121613	-
	KSHV-miR-K12-3-3p UCGCGGUCACAGAAUGUGACA			
KSHV-miR-K12-4 AUAACUAGCUAAACCGCAGUACUCU AGGGCAUUCAUUUGUUACAUAGAAU ACUGAGGCCUAGCUGAUUAU	**KSHV-miR-K12-4-5p** AGCUAAACCGCAGUACUCUAGG	121413	121482	-
	KSHV-miR-K12-4-3p UAGAAUACUGAGGCCUAGCUGA			
KSHV-miR-K12-5 UGACCUAGGUAGUCCCUGGUGCCCU AAGGGUCUACAUCAAGCACUUAGGA UGCCUGGAACUUGCCGGUCA	**KSHV-miR-K12-5-5p** AGGUAGUCCCUGGUGCCCUAAG G	121263	121332	-
	KSHV-miR-K12-5-3p UAGGAUGCCUGGAACUUGCCGG U			
KSHV-miR-K12-6 CUUGUCCAGCAGCACCUAAUCCAUC GGCGGUCGGGCUGAUGGUUUUCGG GCUGUUGAGCGAG	**KSHV-miR-K12-6-5p** CCAGCAGCACCUAAUCCAUCGG	120761	120822	-
	KSHV-miR-K12-6-3p UGAUGGUUUUCGGGCUGUUGAG			
KSHV-miR-K12-7 GCGUUGAGCGCCACCGGACGGGGA UUUAUGCUGUAUCUUACUACCAUGA UCCCAUGUUGCUGGCGCUCACGG	**KSHV-miR-K12-7-5p** AGCGCCACCGGACGGGGAUUUA UG	120355	120426	-
	KSHV-miR-K12-7-3p UGAUCCCAUGUUGCUGGCGC			
KSHV-miR-K12-8 CGCGCACUCCCUCACUAACGCCCCG CUUUUGUCUGUUGGAAGCAGCUAGG CGCGACUGAGAGAGCACGCG	**KSHV-miR-K12-8-5p** ACUCCCUCACUAACGCCCCGCU	119943	119943	-
	KSHV-miR-K12-8-3p CUAGGCGCGACUGAGAGAGCA			
KSHV-miR-K12-9 GGGUCUACCCAGCUGCGUAAACCCC GCUGCGUAAACACAGCUGGGUAUAC GCAGCUGCGUAAACCC	**KSHV-miR-K12-9-5p** ACCCAGCUGCGUAAACCCCGCU	119300	119365	-
	KSHV-miR-K12-9-3p CUGGGUAUACGCAGCUGCGUAA			
KSHV-miR-K12-10a CUGGAGGCUUGGGGCGAUACCACCA CUCGUUUGUCUGUUGGCGAUUAGU GUUGUCCCCCCGAGUGGCCAG	**KSHV-miR-K12-10a-5p** GGCUUGGGGCGAUACCACCACU	117967	118036	-
	KSHV-miR-K12-10a-3p UAGUGUUGUCCCCCCGAGUGGC			

KSHV-miR-K12-10b CUGGAGGCUUGGGGCGAUACCACCACUCGUUUGUCUGUUGGCGAUUGGUGUUGUCCCCCCGAGUGGCCAG	**KSHV-miR-K12-10b** UGGUGUUGUCCCCCCGAGUGGC			
KSHV-miR-K12-11 CGCUUUGGUCACAGCUUAAACAUUUCUAGGGCGGUGUUAUGAUCCUUAAUGCUUAGCCUGUGUCCGAUGCG	**KSHV-miR-K12-11-3p** GGUCACAGCUUAAACAUUUCUAGG	120576	120576	-
	KSHV-miR-K12-11-5p UUAAUGCUUAGCCUGUGUCCGA			
KSHV-miR-K12-12 GAUGGCCGGCACGCGGUGUCAACCAGGCCACCAUUCCUCUCCGCAUUAAAGCACUCGGUGGGGGAGGGUGCCCUGGUUGACACAAUGUGCCGCGCAUC	**KSHV-miR-K12-12-5p** AACCAGGCCACCAUUCCUCUCCG	117674	117771	-
	KSHV-miR-K12-12-3p UGGGGGAGGGUGCCCUGGUUGA			

*Name and sequences based on the most recent release of miRBase (miRBase 21: http://www.mirbase.org/index.shtml).

CHAPTER 2: PROFILING OF CELLULAR MICRORNAS IN RESPONSE TO EARLY STAGES OF KSHV INFECTION

Hosni A.M. Hussein & Shaw M. Akula*

Department of Microbiology & Immunology, Brody School of Medicine at East Carolina University, Greenville, NC 27834.

This manuscript has been published:

Arch Virol. 2017 Nov;162(11):3293-3303. doi: 10.1007/s00705-017-3478-y

Address correspondence to: Shaw M. Akula, Department of Microbiology & Immunology, Brody School of Medicine, East Carolina University, Greenville, North Carolina, USA 27834. Phone: (252)744-2702; Fax: (252) 744-3104; Email: akulas@ecu.edu

ABSTRACT

Kaposi's sarcoma-associated herpesvirus (KSHV) causes a variety of cancers, including Kaposi's sarcoma (KS), primary effusion lymphoma (PEL), and multicentric Castleman disease (MCD). Host cellular microRNAs (miRNAs) play important post-transcriptional regulatory roles in gene expression and can greatly influence virus-host cell interactions. This study investigated cellular miRNA expression profiles operating in response to early stages of KSHV infection of human Burkitt lymphoma B cells (BJAB). We employed deep sequencing to analyze miRNA expression in KSHV-infected BJAB cells 15min post infection (PI) as compared to the uninfected BJAB cells. A total of 32 known miRNAs and 28 novel miRNA candidates were differentially expressed in KSHV-infected and uninfected BJAB cells. Interestingly, miRNA expression profiles during early stages of viral infection yielded comparable results when UV-inactivated KSHV was used. The deep sequencing results were further confirmed by performing *real-time* reverse transcription PCR. The predicted target genes regulated by both known and novel miRNAs were mainly involved in assisting virus entry, inducing critical cell signaling, initiating transcription of immediate early genes, promoting latent infection, and modulating the host immune response. For the first time, we provide some insight into the host cellular miRNA expression profiles in response to early stages of KSHV infection of human B cells. Furthermore, this study offers a valuable basis for further investigation on the roles of cellular miRNAs in the KSHV entry process.

INTRODUCTION

Kaposi's sarcoma-associated herpesvirus (KSHV) or human herpesvirus-8 (HHV-8) is an oncogenic virus classified under the family of *herpesviridae* (subfamily: *γ2-herpesvirinae*) (Chang et al., 1994). KSHV is among the list of viral pathogens estimated to cause 12-25% of human cancers worldwide (La Ferla et al., 2013; Morrison et al., 2015). KSHV primarily causes Kaposi's sarcoma (KS) (Schalling et al., 1995) and is also etiologically associated with other lymphoproliferative diseases such as primary effusion lymphoma (PEL) and multricentric Castleman disease (MCD) (Hamden et al., 2005; Soulier et al., 1995). Prevalence of KSHV infection is directly correlated to KS incidence and varies according to geographic location, ethnicity, and distinct behavioral risk factors (Labo et al., 2014).

The KSHV genome consists of linear double-stranded DNA (dsDNA) and the virus displays two modes of replication in the infected cells: latent and lytic replication phase (Ford et al., 2006; Lukac et al., 1998). The default pathway of KSHV infection both *in vivo* and *in vitro* is latent (dormant) infection (Steitz et al., 2011); at any given instance, only a subpopulation (<3%) of infected cells display evidence of lytic gene expression (Cai et al., 2010a; Dyson et al., 2008; Sun et al., 1999). Establishing latency allows KSHV to evade the host's immune surveillance, maintain persistent life-long infections, and promote tumorigenesis (Yang et al., 2015). Using PCR arrays, we identified crucial cellular genes that can reactivate latent KSHV infections (Bryan et al., 2006).

MicroRNAs (miRNAs) are important regulators of gene expression (Trionfini and Benigni, 2017) that are short (~22 nucleotides long), endogenous, non-coding RNAs (Krol et al., 2010; Treiber et al., 2012). The human genome encodes thousands of miRNAs (Kozomara and Griffiths-Jones, 2011). KSHV is among the limited number of viruses that encode their own miRNAs (Pfeffer et al., 2004). There are several published works that describe virus and cellular encoded miRNAs in KSHV pathogenesis (Chen et al., 2016; Krause et al., 2016; Liu et al., 2017b). However, to date, no publication has profiled the expression of cellular miRNAs during

early stages of KSHV infection. KSHV internalization involves well-orchestrated interactions between the virus and the host cell at different levels: surface receptor molecules, host defense, endocytosis, capsid transport, and finally the replication of the viral genome (Bryan et al., 2005). Thus, the present study aimed to investigate cellular miRNA expression profiles operating in response to early stages of KSHV infection of cells. The study also aimed to predict target genes which might be useful in understanding host cellular mechanism as it pertains to promoting or inhibiting virus entry.

MATERIALS AND METHODS

Cell culture and virus

Human Burkitt lymphoma B cell line (BJAB) was used in this study. BJAB was propagated in phenol red–free RPMI medium (Invitrogen, Carlsbad, CA) containing 10% charcoal-stripped fetal bovine serum (Atlanta Biologicals, Lawrenceville, GA), L-glutamine, and antibiotics (Akula et al., 2005).

KSHV and UV-KSHV

Wild-type KSHV (Akula et al., 2004) and UV-inactivated KSHV (UV-KSHV) was used in this study. Replication-incompetent KSHV was prepared by exposing it for 20min under a UV light source (365 nm) (Naranatt et al., 2003). Both KSHV and UV-KSHV were concentrated and gradient purified using nycodenz (Sigma) as per standard protocols described earlier (Akula et al., 2002). To confirm the successful inactivation of KSHV by exposing it to UV light, we performed infection of BJAB cells using 10 MOI of KSHV exposed to normal light while another lot of 10 MOI of KSHV that was exposed to UV-light source. After 30 min post infection, cells were lysed, RNA extracted, cDNA synthesized, and the expression of ORF50 monitored by qRT-PCR using specific primers as per earlier studies (Dyson et al., 2010). Expression of ORF50 was used as a scale to measure KSHV infection of cells. ORF50 is expressed

immediately upon KSHV infection of cells (Dyson et al., 2010; Krishnan et al., 2004). As reported in earlier studies (Walker et al., 2014), the lowest limit of detection in the standard samples was 6–60 copies for the ORF50 gene.

KSHV infection of cells and RNA extraction

BJAB cells were infected with 10 multiplicity of infection (MOI) (Hamden et al., 2004; Walker et al., 2014). The cells were left uninfected or infected for 15min prior to washing the cells twice in PBS and processed appropriately for RNA extraction. Total RNA was extracted using TRIzol (Invitrogen, Carlsbad, CA). The RNA concentration was measured with a NanoDrop ND-2000 spectrophotometer (Thermo Fisher Scientific< Waltham, MA), and then verified for quality using an Agilent 2100 Bioanalyzer (Agilent Technologies, Santa Clara, CA). Only RNA samples with integrity number greater than 9 were used in the following steps.

sRNA library construction and sequencing

The total RNA samples were fractionated by 15% denaturing polyacrylamide gel electrophoresis, and then sRNA fragments between 16 and 30nt in length were isolated from the gel. The sRNA molecules were ligated to a 5′ adaptor and a 3′ adaptor by T4 RNA ligase (Promega, Madison, WI). Subsequently, the adapter-ligated sRNAs were converted to cDNA by RT-PCR using Superscript III kit (Invitrogen). The library was enriched by PCR employing specific primers and the products were then purified. The PCR products contained within the library were assessed by Agilent Bioanalyzer DNA 1000. The miRNA enriched samples were extracted from the above constructed sRNA libraries using a 3% Pippin prep (Sage Science) gel cassettes. Libraries were sequenced on an Illumina HiSeq 2000 using TruSeq SBS sequencing kit ver 3and SCS version 1.4.8 data collection software (Sun et al., 2016).

miRNA-seq data analysis

The miRNA sequence data for each sample was processed and analyzed as per standard procedures described earlier (Ning et al., 2014). The analysis was further confirmed by the use omiRas, a web server for the annotation, comparison, and visualization of interaction networks of non-coding RNAs (Muller et al., 2013). The differential expression of miRNAs was calculated on the basis of the difference (cutoff, ±2.0-fold or more) observed between different groups (uninfected versus KSHV infected cells 15min post infection). The *P* value of differentially expressed miRNAs was estimated via *z* score by using a Benjamini-Hochberg FDR corrections of 0.05 as described earlier (Klipper-Aurbach et al., 1995).

Real-time qRT-PCR analysis of the expression of miRNAs

The quality of RNA was tested using a spectrophotometer. Only the RNA samples with 260/280 ratios of 1.8 to 2.0 were used in the study. Approximately 500ng of RNA was reverse transcribed in a 25µl reaction volume using the All-in-one^{TM} miRNA qRT-PCR detection kit (GeneCopoeia, Rockville, MD). Briefly, the cDNA was synthesized in a 25µl reaction mix containing 5µl of 5x reaction buffer, 2.5U/µl Poly A Polymerase, 10ng/µl MS2 RNA, and 1µl RTase Mix. The reaction was performed at 37°C for 60 min and terminated at 85°C for 5 min. cDNA that was produced in the RT reaction was diluted ten-fold and was used as the template for the PCR reaction in an Applied Biosystems ViiA 7 Real-Time PCR System (Life Technologies, USA). In this system, MS2 RNA was used as an external reference for the quality of the extracted miRNAs, and RNU6B was used for normalization. The expression levels of miRNAs were measured employing qRT-PCR with the SYBR green detection and specific forward primer for the mature miRNA sequence and the universal adaptor reverse primer (GeneCopoeia, USA).

miRNA target prediction

The target genes for each differentially expressed miRNA were predicted using the miRanda (http://www.microrna.org/), MicroRNA Target prediction (miRTar; mirtar.mbc.nctu.edu.tw/human/index.php), and DIANA tool (http://diana.imis.athena-innovation.gr/DianaTools/index.php) algorithms. To further authenticate the biological function of the predicted target genes, a Kyoto Encyclopedia of Genes Genomes (KEGG) pathways enrichment analysis was performed using the KOBAS 3.0 annotation tool (Wu et al., 2006a).

Real-time qRT-PCR analysis of the expression of putative target genes. The experimental approach was done as per earlier protocols (Dyson et al., 2012). The primer sets used to monitor expression DLG5 was 5'-CTATGACGCCCTTCGGAAGAG-3' (sense) and 5'-TCATGGTGGATCGCCTCAAAC-3' (antisense). The primers used to monitor expression of IRF5, CPLX1, and SPTBN4 is described in earlier studies (Barnes et al., 2001; Kurokawa et al., 2015; Sanchez-Mut et al., 2013).

Western blotting

BJAB cells were KSHV infected for 30min. The cells were washed twice in PBS prior to lysing them using gold lysis buffer (GLB) (Akula et al., 2004). Equal amounts (25µg) of protein were resolved by SDS 12% PAGE, blotted on to a PVDF membrane (EMD Millipore), blocked in blocking buffer overnight at 4°C, incubated with sheep anti-IRF5 polyclonal antibody (R&D systems, Minneapolis, MN), rabbit anti-DLG5 polyclonal antibody (Abcam, Cambridge, MA), mouse anti-CPLX1 monoclonal IgG (R&D systems), or goat anti-SPTBN4 polyclonal antibody (Abgent, San Diego, CA) for 2h at room temperature followed by incubating with appropriate HRP-conjugated antibodies (KPL, Gaithersburg, MD) for 60min at RT, and finally developed using chemiluminescent reagent (NEN Life Science, Boston, MA). Membranes were 'stripped'

for reprobing with mouse anti-actin antibodies (Clone AC-74; Sigma-Aldridge) and appropriate secondary antibodies.

RESULTS

Construction and sequencing data analysis of sRNA libraries

The purpose of this study was to understand the changes in the expression profile of miRNAs during early stages of KSHV infection of cells. Accordingly, we used BJAB cells to study such changes induced during KSHV infection of cells. Human B cells is one of the major *in vivo* targets of KSHV infection (Myoung and Ganem, 2011; Naranatt et al., 2004) and that is the prime reason we chose to work with BJAB cells. To identify miRNA changes in BJAB cells infected with KSHV, two small RNA (sRNA) libraries pooled from uninfected and KSHV-infected groups were constructed at 15min post infection (PI). We performed high-throughput sRNA sequencing using the Illumina platform on sRNA libraries obtained from KSHV-infected BJAB cells, and compared the results to those obtained using uninfected cells. As shown in **Table 1**, a total of 17,093,083 and 12,203,413 raw reads were obtained from the uninfected and KSHV-infected groups, respectively, at 15min PI. After removing low-quality sequences, adapter sequences, and sequences smaller than 16nt, 15,296,253 and 12,278,645 clean reads were identified in the uninfected and KSHV-infected cells, respectively, at 15min PI. All of the clean reads were annotated and classified as miRNA, rRNA, tRNA, piRNA, snoRNA, scRNA, and snRNA (**Table 2**). The majority of the length distribution of the sRNAs were 22–23nt in length (**Fig 1**), which is consistent with the typical size of mature miRNAs (Liu et al., 2015). These results indicate that miRNAs have been enriched successively from all the libraries.

Differential expression analysis of known miRNAs

To identify known miRNAs in BJAB cells, we aligned the sRNAs from our libraries to the known mature miRNAs in the Sanger miRBase 21.0 database using BLASTN searches to obtain the

miRNA count as well as the base bias at the first position. At 15min PI, approximately 2220 unique sequences in the uninfected library (**Supplementary Table 1**) and 2020 unique sequences in the KSHV-infected library (**Supplementary Table 2**) were annotated as sRNA candidates. A total of 757 and 672 known miRNA genes were identified in the uninfected (**Supplementary Table 3**) and KSHV-infected (**supplementary Table 4**) BJAB cell libraries, respectively. Using a *P*-value<0.01 and a $\left|\log2 \text{ (fold change)}\right| > 2$ as the cut-off values, a total of 32 known miRNAs were differentially expressed in the two groups, and heat maps showing the relative expression of miRNAs in uninfected versus KSHV-infected cells at 15min PI is provided in **Fig. 2**.

Prediction and differential expression of novel miRNAs

After removing the snRNAs, snoRNAs, rRNAs, and known miRNAs, we aligned the remaining unannotated reads against the *H. sapiens* genome to predict novel miRNAs in the BJAB cells. Using miRDeep software, 125 novel miRNAs were predicted at 15min PI of BJAB cells (**Supplementary Table 5**). According to the cut-off values of the differential expression analysis discussed previously, 28 miRNAs were differentially expressed during the early stages of KSHV infection of cells. A total of fourteen miRNAs were upregulated and fourteen were downregulated in KSHV-infected cells ($p<0.01$) (**Fig. 3**). The original sequences of the novel miRNAs with appropriate IDs and specific primers are provided in the **Table 3**.

Authentication of differentially expressed miRNAs by qRT-PCR and target prediction

To validate the sequencing data, we selected five known miRNAs and twenty eight novel miRNA candidates for qRT-PCR analysis. All 34 miRNAs showed expression profiles that were consistent with the sRNA sequencing data. The expression of known miRNAs that were confirmed by qRT-PCR were hsa-miR-3164, hsa-miR-3130-5p, and hsa-miR-3140-3p, hsa-miR-29c-3p, and hsa-miR-103a-2-5p. The selection of the five known miRNAs was based on the

relevance of their targets to KSHV pathogenesis (**Table 4**). The expression of the known miRNAs, hsa-miR-3164, hsa-miR-3130-5p, and hsa-miR-3140-3p were downregulated while hsa-miR-29c-3p and hsa-miR-103a-2-5p were upregulated (**Fig. 4a**). The expression of fourteen novel miRNAs were upregulated while the other fourteen were downregulated in KSHV-infected BJAB cells (**Fig. 4b**). We also tested the ability of UV-treated KSHV (UV-KSHV) to alter the expression miRNAs during the course of infection. The UV-KSHV was inactivated successfully as it could no longer establish an infection in BJAB cells. There was a robust expression of the immediate-early gene, ORF50, in KSHV-infected BJAB compared to the UV-KSHV (**Supplemental Fig. 1**). Interestingly, we observed comparable results when BJAB cells were infected for 15min PI with UV-KSHV (**Supplemental Fig. 2**). These results may imply that the miRNA-based response to early stages of KSHV infection in cells is purely dependent on interactions between the virus envelope-associated and other structural proteins with the host cell machinery and not the viral genome.

To understand the molecular function and biological processes of these known and novel miRNAs during early stages of KSHV infection, three independent algorithms, miRanda, MIRTar, and DIANA, were used to predict the targets for each of the miRNAs that were differentially expressed. The annotated target genes regulated by known miRNAs relevant to KSHV pathogenesis were mainly involved in regulating cell signaling, initiating transcription of IE genes, promoting latent infection, and modulating the host immune response (**Tables 4).** We identified 84 target genes for 24 (out of a total of 28) of the identified novel miRNAs **(Supplemental Fig. 3**). These predicted target genes for the respective novel miRNAs were those that were directly associated with viral uptake. In fact, we validated the expression pattern of 4 putative targets of the novel miRNAs by qRT-PCR and Western blotting (**Supplemental Fig. 4A, B**). The paradigm explaining KSHV infection and the resultant changes in the expression pattern of miRNAs and their putative targets is shown schematically.

DISCUSSION

Deep sequencing approach has become an effective tool to analyze the expression profiles of miRNAs in animals and plants. Cellular miRNAs are implicated in the pathogenesis of numerous diseases, including those caused by various pathogens like bacteria and viruses. Some cellular miRNAs inhibit virus replication by regulating host immune responses or targeting viruses (Slonchak et al., 2014), while other miRNAs can also promote viral replication by modulating the cellular environment (Jopling et al., 2005; Norman and Sarnow, 2010). The KSHV genome actually encodes for at least 25 mature viral miRNAs (Happel et al., 2016). Recent studies unraveled the ability of KSHV miRNAs to regulate latency, angiogenesis, and the spread of the infected cells. Likewise, these viral miRNAs interfere with the host immune system by modulating both viral and cellular gene expression, and the actual tumorigenesis (Qin et al., 2017a; Tan et al., 2015). However, little is known about the manner in which the expression profile of cellular miRNAs is altered during the early stages of KSHV infection. To this end, we used deep sequencing to identify cellular miRNAs with significantly altered abundances in response to early stages of KSHV infection of BJAB human B cells.

KSHV entry is a rapid process (Akula et al., 2003). In as early as 5min PI, KSHV is internalized by endocytosis (Akula et al., 2003) and by 30min PI, KSHV immediate early transcript (*orf50*) is expressed in infected cells (Krishnan et al., 2005). KSHV infection of target cells resulted in the generation of various sRNA populations, including siRNAs, miRNA, and piRNAs as described earlier (Hussain et al., 2011; Vodovar et al., 2012). In our study, we determined KSHV infection of cells as early as 15min PI could significantly alter expression of miRNAs. The lengths of the clean reads in KSHV-infected and uninfected cells were mostly 22–23 nt (**Fig. 1**) These observations are consistent with previous analyses of miRNAs from animals and plants (Jia et al., 2017; Zhang et al., 2015). Our study, for the first time describes the expression profiles of both known and novel miRNAs as a result of KSHV infection of cells at an early time point. We also observed the typical 26-30nt long sRNAs representing the

piRNAs to be altered during early stages of KSHV infection (**Table 2**). The histone-derived piRNAs are dynamically expressed throughout the cell cycle (Girardi et al., 2017), suggesting a role for the KSHV-altered piRNA pathway in the regulation of histone gene expression, and perhaps also in selectively regulating non-self (viral) genes (Iwasaki et al., 2015).

Virus infection of cells can alter many cellular mechanisms including apoptosis and replication of the virus genome. Herein, for the first time, we identified the ability of KSHV to significantly alter miRNA expression profile as early as 15min PI. In human B cells, a large number of miRNAs exhibit altered profiles during early stages of KSHV infection of cells (**Fig. 2; Table 3**). We identified a total of 32 known and 28 novel miRNAs to be differentially expressed during KSHV infection of B cells. The results from deep sequencing was authenticated by performing *qRT-PCR* (**Fig. 4**). Implications of known miRNAs differentially expressed during KSHV infection of human B cells is provided in **Table 4**. Table 4 was constructed based on relevant target genes critical to the biology of KSHV internalization. Interestingly, the known miRNA, hsa-miR-3164; novel miRNAs, chrX_2892, chr2_257, and chr2_37 were significantly down-regulated upon KSHV infection of cells (**Fig. 4**). Over all, there were miRNAs upregulated and downregulated in these cells during KSHV infection. The net proposed effects of these miRNAs (both known and novel) are as follows: (i) assists virus entry; (ii) induces critical cell signaling; (iii) initiates transcription of IE genes; (iv) promotes latent infection; and (v) protects the virus from host immune response.

The present study not only describes the manner in which KSHV alters expression of miRNAs during as early stages of KSHV infection of BJAB cells but also poses a new question: What are the roles of such miRNAs induced specifically by KSHV at such early time points during KSHV infection? Changes in the host cell miRNAs in response to virus infection may be a mechanism that coordinates gene expression critical to the outcome of a viral pathogen: a productive infection versus a robust immune response. Future studies are aimed at understanding the regulatory role of miRNAs in the biology of KSHV entry.

In summary, we used deep sequencing to identify and examine the host cell miRNAs expressed by BJAB cells that may play a significant role in internalization of KSHV. To our knowledge, this is the first study delineating the changes to the miRNA expression profiles as a result of early stages of KSHV infection of cells. Such a profiling can help inform additional studies to better understand the mechanisms responsible for the specific changes observed in the expression of cellular miRNAs and their roles in the of KSHV pathogenesis.

COMPLIANCE WITH ETHICAL STANDARDS

We thank Dr. Blossom Damania (University of North Carolina at Chapel Hill) to have kindly provided us with the BJAB cells.

Conflict of interest

The authors declare no conflict of interest.

Ethical approval

This article does not contain any studies with human participants or animals performed by any of the authors.

Table 1: Basic statistics of miRNA-sequences obtained at 15min PI.

Treatment	Total Read	Clean/trimmed read	Percentage
UnInfected	17,093,083	15,296,253	89.5%
KSHV Infected	12,403,413	12,278,645	99.0%

Table 2: Mapping of clean reads.

Classifications	uninfected	KSHV-infected
miRNA	5,000,000	4,000,000
rRNA	2,000	2,000
tRNA	0	0
piRNA	289,000	167,000
snoRNA	240,000	130,000
scRNA	0	0
snRNA	8,000	8,000
Total Reads	5,539,000	4,299,000

Table3: Novel miRNAs altered during KSHV infection of cells.		
ID/Name	**Sequence**	**Primer**
chr10_2863	GGCGTGGAGCCGGGCT	AGATTCTATAGACGCGGCGTGGAGCCG
chr11_3509	CCGGGAGCCCCCTCCAT	ATATTTATAGACGCCCGGGAGCCCCCTC
chrX_2892	GTTTAGACGGGTTTC	GCGACGCGCGCAGACTATTAAGGCTTAG
chr16_5060	CCAGCCAGGCCCCACCA GGAA	ACAGACAGATCATAACCAGCCAGGCCCCA
chr10_1855	TATATGATGTGCCTGGAT TGCTTCTGATTC	CGCGCGCAGTATATGATGTGCCTGGATTG
chr11_4565	CCCCGGCTCCTCCACAA	ACAGCAGATCATAAGCCCCGGCTCCTC
chr14_245	TCCCTGGGCTCTGCCTCC TC	GACAGACAGATCATTCCTGGGCTCTGCCT
chr16_401	TGCTCTGACCCACCCCTC TTGCCTAGCAGG	CACACATATGCTCTGACCCACCCCTCTTG
chr16_5060	CCAGCCAGGCCCCACCAG GAA	ACGACAGATCATAACCAGCCAGGCCCCA
chr17_2719	GGCGGACGCCTGAAGTGT	ACACAGATCATACAGGCGGACGCCTGAAG
chr17_2844	TGAGAAGGTGGTGTGGAGT	CACAGAGCTCACAGTGAGAAGGTGGTGT
chr17_455	TTGGCTGTTTAGTCTCGGG CAA	GAGCACGCGCAGTTGGCTGTTTAGTCTC
chr1_5426	GGGCGGCGGCGGCGGCGG CGGCGGGC	TTATAGATCATAAGGGCGGCGGCGGCG
chr2_257	CGGGCGTGGTGGTGGGAA	GCAGTCAGATCATAACGGGCGTGGTGGT
chr2_37	CCCGGCTCCTCCACTC	CAGTCAGATCATAAGCCCGGCTCCTCCA
chr6_4966	TTGATCGAGGAGCGCG GTTAC	CAGTCAGACTCACGCAGTTGATCGAGGAG
chr6_6774	GAGGTCCCCGGTTTG	ACTTGACAGATCACAAGGAGGTCCCCGGT
chr7_6319	AAGCGGGTGCTCTGC	AGACAGATCACAAGCAGAAGCGGGTGCTC
chr7_955	CCAGGGCCAGCAGGG AATGTCA	ATATCAAGCAGCCAGGGCCAGCAGGGA
chr9_4744	GAAGTCCTGGCAACGT GGACAGAAGGAATGG	GTGAAGTCCTGGCAACGTGGACAGAAGGA
chr1:hsa	TGGCAGCAAGGAAGG CAGGGGTT	AGAGTGACGCTGGCAGCAAGGAAGGCA
chr1:hsa	CCTCCTGCCCTCCTTG CTGTAGA	AGATGACGCCCTCCTGCCCTCCTTG
chr17:hsa	ACTATTAAGGCTTAGGGCA	CGTGACGCGCGCAGACTATTAAGGCTTAG
chr17:hsa	CGCCGACGGACAGAC AGACAGTGCAGTCACC	TGTGTCGCCGACGGACAGACAGACAGT
chr17:hsa	TGAGTGTACTGTGGGC TTCGGAGA	GACGACGCTGAGTGTACTGTGGGCTTC
chr5:hsa	TGGCTGGCCGCGCTCT TCGCAC	AACTAGTCTGGCTGGCCGCGCTCTTC
chr5:hsa	CGCAGGAGCCGCGGAG GGCCGGA	ATGTACTAGTCCGCAGGAGCCGCGGA
chr16_609	GCAGACTCGACCTCCC AGGCTTA	GCGACGCCAGCATTCAGACTGACAGATG
chr16_863	GAGCCGGAGAACTCGG GAGGGAGA	GATTCGACGCCGCAGGTTTAGACGGGT

Table 4. Implications of Known miRNAs induced during early stages KSHV infection of cells.

miRNAs	Target	Function of the target	Implications
Upregulated			
hsa-miR-4742-3p	ZFAND5	Bind AU-rich elements (AREs) and regulate many inflammatory mediators including tumor necrosis factor (TNF) and COX2 (He et al., 2012).	Inhibits host immune response to KSHV infection.
hsa-miR-29c-3p	SPARC	Inhibits cell growth and promotes apoptosis (Nian et al., 2015).	Promotes cell survival.
hsa-miR-449b-5p	SIRT1	Induces apoptosis (Ferreira et al., 2014).	Promotes cell survival.
hsa-miR-15a-5p	BCL2	Inhibits apoptosis (Vogler et al., 2017).	Limit cell division and promote viral latency.
hsa-miR-103a-2-5p	NFAT5	Is crucial for immune response and is a key regulator of T cell activation (Muller and Rao, 2010).	Limits host cell immune response to KSHV infection.
hsa-miR-1226-5p hsa-miR-1343	SEPT8	Upregulates MAPK signaling (Shiryaev et al., 2012).	Promotes latent infection of cells.
hsa-miR-133a	CDC42	Induces filopodial formation and cell migration (Ye et al., 2013).	Inhibits cell migration.
hsa-miR-1323	PTENP1	Negatively regulates AKT/PKB signaling pathway (Song et al., 2012).	Enhances AKT/PKB associated signaling.
Downregulated			
hsa-miR-3164	DCAF7	Regulates protein kinase associated signaling (Glenewinkel et al., 2016).	Induces intracellular protein kinase signaling.
hsa-miR-3130	ORC4	ORC4 is a component of the Pre-replicative complex (pre-RC) crucial to replication of the genome (Wiebusch et al., 2003).	This may allow for the initial lytic replication of the KSHV genome that is observed in cells.
hsa-miR-3140-3p	DNAJC10	Enhances membrane fusion (Jain et al., 2008).	May assist viral membrane fusion during the course of entry.

FIGURE LEGENDS

Figure 1. Length distribution and count of sRNA sequences. The x-axis indicates length distribution of clean sequence reads in two sRNA libraries pooled at 15min PI from uninfected and KSHV-infected BJAB cells. The y-axis indicates the count of reads for sequences of each length, the most of reads are 22 and 23 nt in length.

Figure 2. Differential expression of known miRNAs. Heat map showing 32 known miRNAs that are differentially expressed between uninfected and KSHV-infected BJAB cells at 15min PI. Red color indicates highly expressed miRNAs, and miRNAs with low expression are indicated in blue. The absolute signal intensity ranged from 0 to 12.

Figure 3. Differential expression of novel miRNAs. Twenty eight differentially expressed novel miRNAs between uninfected and KSHV-infected BJAB cells at 15min PI have been predicted using miRdeep software. The x-axis indicates the ID/name of novel miRNAs and y-axis indicates fold change in expression of these miRNAs. Student's *t* test was performed to compare expression of a specific miRNA in KSHV-infected cells compared to the uninfected cells. All the changes plotted are statistically significant (*P* value of 0.05 or less).

Figure 4. qRT-PCR confirmation of differentially expressed miRNAs. Expression of miRNAs detected by next-generation sequencing was confirmed using qRT-PCR. The qRT-PCR data was plotted for (**A**) 5 known miRNAs and (**B**) 28 novel miRNAs that are differentially expressed in KSHV-infected BJAB cells compared to uninfected cells at 15min PI. The relative expression of miRNAs was measured in terms of threshold cycle value (Ct) and normalized to snRNA RNU6B. The x-axis indicates the ID/name of miRNAs and y-axis indicates fold change in expression of these miRNAs. Bars represent average ± s.d. of three individual experiments. Student's *t* test was performed to compare expression of a specific miRNA in KSHV-infected

cells compared to the uninfected cells. All the changes plotted are statistically significant (*P* value of 0.05 or less).

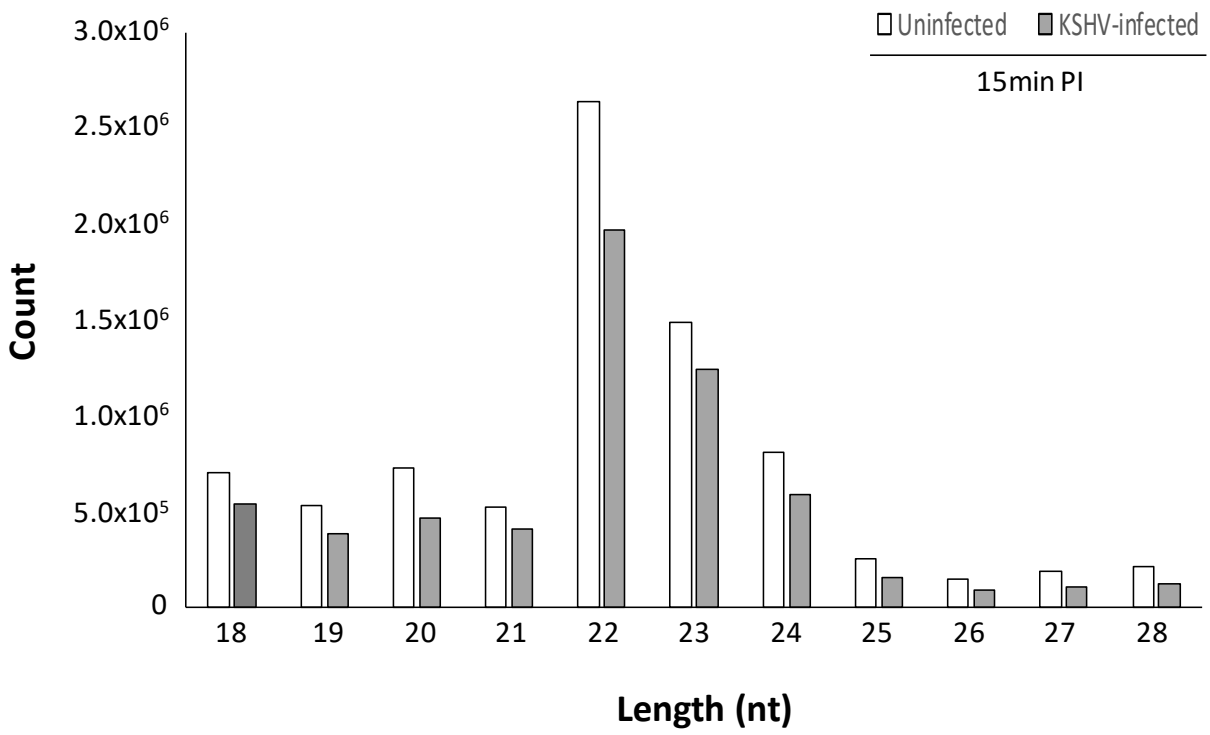
Uninfected
KSHV-infected
15min PI
3.0x10^6
2.5x10^6
2.0x10^6
1.5x10^6
1.0x10^6
5.0x10^5
0
Count
18
19
20
21
22
23
24
25
26
27
28
Length (nt)

Figure 1

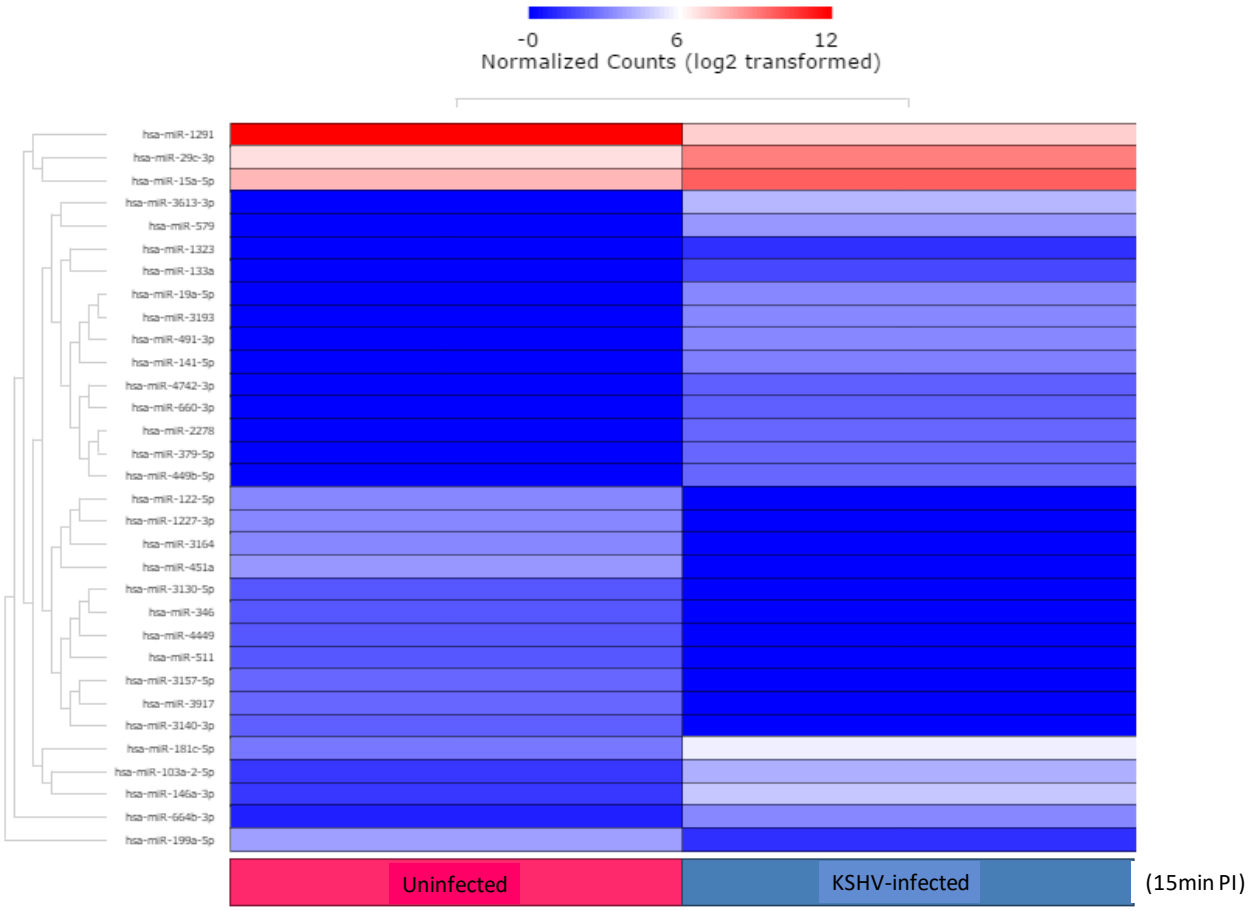
-0
6
12
Normalized Counts (log2 transformed)
hsa-miR-1291
hsa-miR-29c-3p
hsa-miR-15a-5p
hsa-miR-3613-3p
hsa-miR-579
hsa-miR-1323
hsa-miR-133a
hsa-miR-19a-5p
hsa-miR-3193
hsa-miR-491-3p
hsa-miR-141-5p
hsa-miR-4742-3p
hsa-miR-660-3p
hsa-miR-2278
hsa-miR-379-5p
hsa-miR-449b-5p
hsa-miR-122-5p
hsa-miR-1227-3p
hsa-miR-3164
hsa-miR-451a
hsa-miR-3130-5p
hsa-miR-346
hsa-miR-4449
hsa-miR-511
hsa-miR-3157-5p
hsa-miR-3917
hsa-miR-3140-3p
hsa-miR-181c-5p
hsa-miR-103a-2-5p
hsa-miR-146a-3p
hsa-miR-664b-3p
hsa-miR-199a-5p
Uninfected
KSHV-infected
(15min PI)

Figure 2

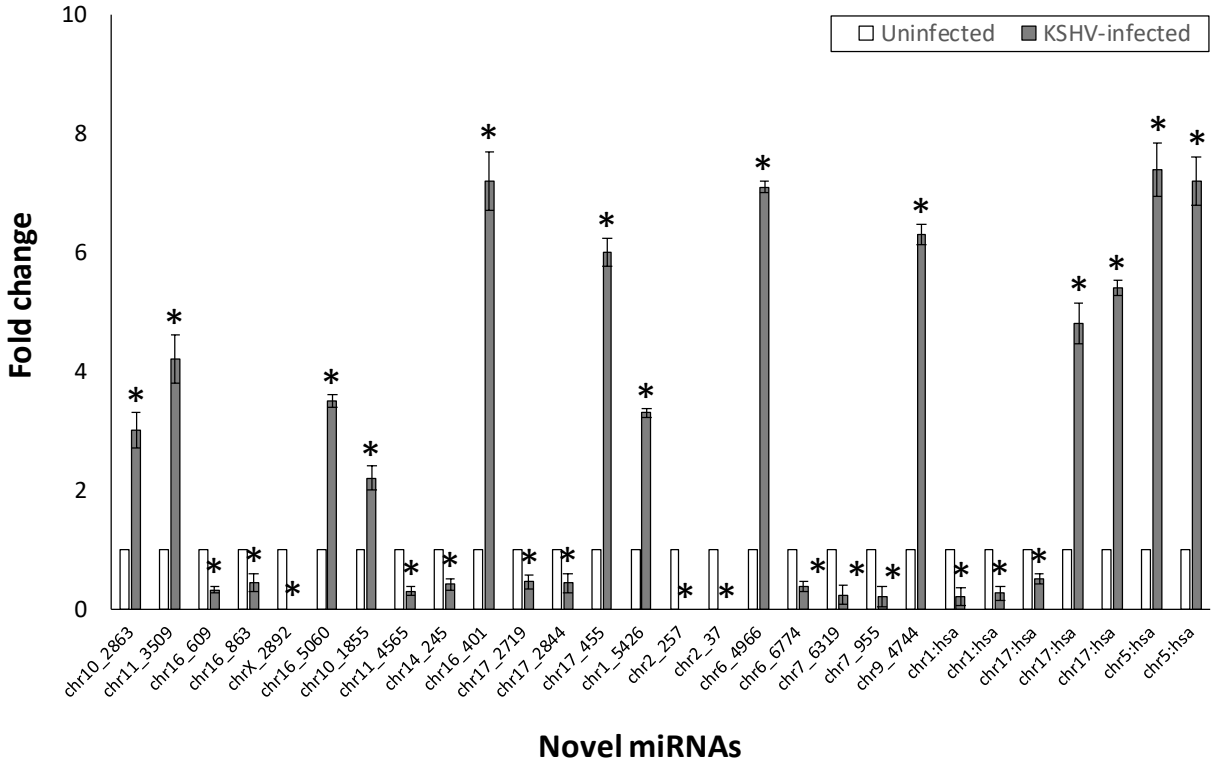
Uninfected
KSHV-infected
Fold change
10
8
6
4
2
0
chr10_2863
chr11_3509
chr16_609
chr16_863
chrX_2892
chr16_5060
chr10_1855
chr11_4565
chr14_245
chr16_401
chr17_2719
chr17_2844
chr17_455
chr1_5426
chr2_257
chr2_37
chr6_4966
chr6_6774
chr7_6319
chr7_955
chr9_4744
chr1:hsa
chr1:hsa
chr17:hsa
chr17:hsa
chr17:hsa
chr5:hsa
chr5:hsa
Novel miRNAs

Figure 3

(**A**)

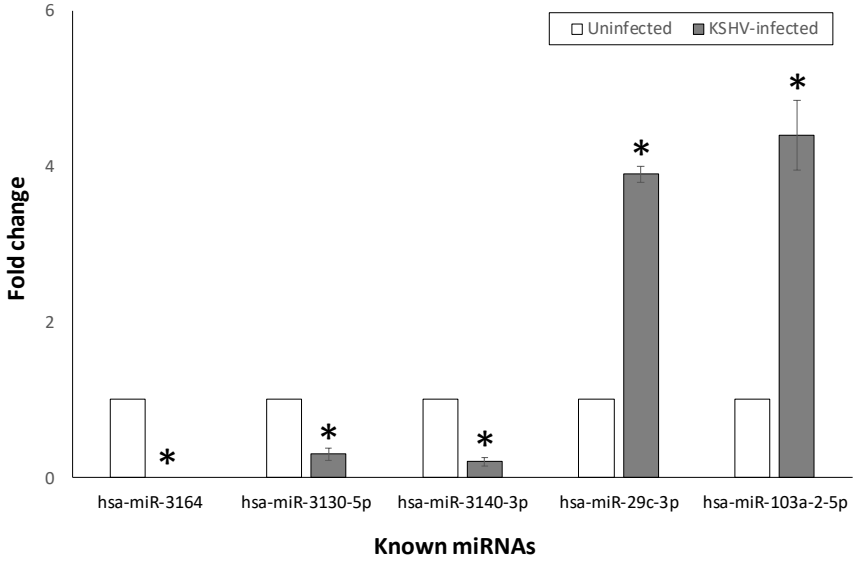
Uninfected
KSHV-infected
Fold change
6
4
2
0
hsa-miR-3164
hsa-miR-3130-5p
hsa-miR-3140-3p
hsa-miR-29c-3p
hsa-miR-103a-2-5p
Known miRNAs

(**B**)

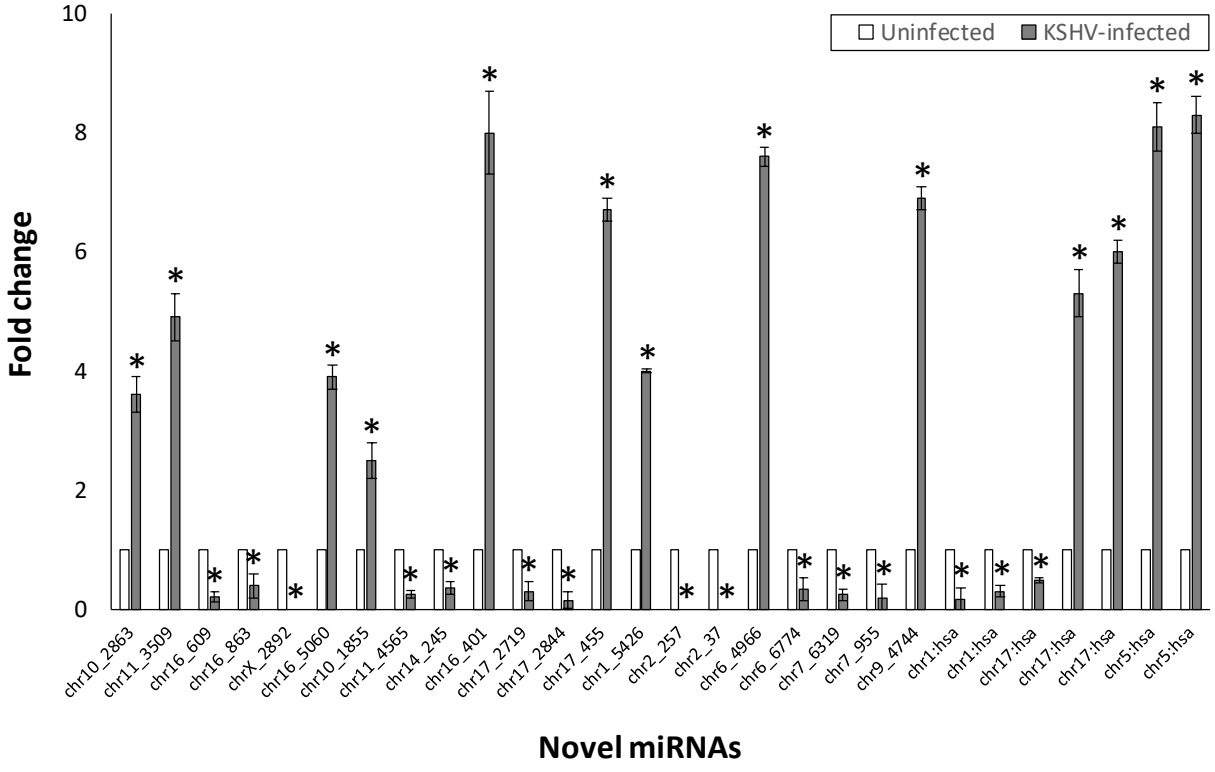
Uninfected
KSHV-infected
Fold change
10
8
6
4
2
0
chr10_2863
chr11_3509
chr16_609
chr16_863
chrX_2892
chr16_5060
chr10_1855
chr11_4565
chr14_245
chr16_401
chr17_2719
chr17_2844
chr17_455
chr1_5426
chr2_257
chr2_37
chr6_4966
chr6_6774
chr7_6319
chr7_955
chr9_4744
chr1:hsa
chr1:hsa
chr17:hsa
chr17:hsa
chr17:hsa
chr5:hsa
chr5:hsa
Novel miRNAs

Figure 4

SUPPLEMENTAL DATA:

The supplementary data for this manuscript includes the following and they can be downloaded at the following link:

https://link.springer.com/article/10.1007%2Fs00705-017-3478-y#SupplementaryMaterial

Supplementary Table 1. sRNA candidates in uninfected BJAB cells.

Supplementary Table 2. sRNA candidates in KSHV-infected BJAB cells.

Supplementary Table 3. Mature miRNA in uninfected BJAB cells at 15min PI.

Supplementary Table 4. Mature miRNA in KSHV-infected BJAB cells at 15min PI.

Supplementary Table 5. Predicted Novel miRNA in KSHV-infected BJAB cells at 15min PI.

Supplementary Figure 1. UV exposure inactivates KSHV. BJAB cells were infected with 10MOI of KSHV or UV-KSHV for 30 min prior to monitoring infection of cells by qRT-PCR conducted to measure the expression of ORF50. Bars represent average ± s.d. of three individual experiments. Data was plotted to represent the change in RNA copy numbers of KSHV-ORF50 used as an indicator of a successful infection. Student's *t* test was performed to compare expression of ORF50 RNA in KSHV-infected cells compared to the UV-KSHV infected cells. All the changes plotted are statistically significant (*P* value of 0.05 or less).

Supplementary Figure 2. UV-KSHV modulates expression of miRNAs. The qRT-PCR data was plotted for the 28 novel miRNAs that are differentially expressed in UV-KSHV-infected BJAB cells compared to uninfected cells at 15min PI. The x-axis indicates the ID/name of novel miRNAs and y axis indicates fold change in expression of these miRNAs. The relative expression of miRNAs was measured in terms of threshold cycle value (Ct) and normalized to snRNA RNU6B. Bars represent average ± s.d. of three individual experiments. Student's *t* test

was performed to compare expression of a specific miRNA in KSHV-infected cells compared to the uninfected cells. All the changes plotted are statistically significant (*P* value of 0.05 or less).

Supplementary Figure 3. Putative targets for novel miRNAs expressed during early stages of KSHV infection of BJAB cells. 24 novel miRNA that are validated to be differentially expressed by KSHV infection have been predicted to modulate expression of 84 target genes with confirmed roles during early stages of virus infection. MIRanda, DIANA, and miRTar tools were used for identifying miRNA-target interactions.

Supplementary Figure 4. Validation of miR-targets by qRT-PCR (**A**) **and Western blotting** (**B**)**.** (**A**) Expression of IRF5, DLG5, CPLX1 and SPTBN4 were detected by qRT-PCR at 15 minutes post KSHV infection. The qRT-PCR data was plotted for fold changes for the expression of IRF5, DLG5, CPLX1, and SPTBN4 in BJAB cells infected with 10 MOI of KSHV compared to uninfected cells. Bars represent average ± s.d. of three individual experiments. Student's *t* test was performed to compare expression of specific target genes in KSHV-infected cells compared to the uninfected cells. All the changes plotted are statistically significant (*P* value of 0.05 or less). (**B**) Western blotting analysis demonstrate changes in the expression levels of identified putative targets for novel miRNAs expressed during early stages of KSHV infection. BJAB cells were either left uninfected or infected with 10 MOI of KSHV for 30 min. The cells were then lysed and the expression of IRF5, DLG5, CPLX1 and SPTBN4 protein levels was monitored using appropriate antibodies and normalized to β-actin protein levels. The link between miRNAs and putative target genes is depicted by a schematic. Red and green lines denote inhibition and enhancement, respectively.

CHAPTER 3: miRNA-36 INHIBITS KSHV, EBV, HSV-2 INFECTION OF CELLS VIA STIFLING EXPRESSION OF INTERFERON INDUCED TRANSMEMBRANE PROTEIN 1 (IFITM1)

Hosni A.M. Hussein & Shaw M. Akula*

Department of Microbiology & Immunology, Brody School of Medicine at East Carolina University, Greenville, NC 27834.

This manuscript has been published:

Sci Rep. 2017 Dec;7(1):17972. doi: 10.1038/s 41598-017-18225-w

Address correspondence to: Shaw M. Akula, Department of Microbiology & Immunology, Brody School of Medicine, East Carolina University, Greenville, North Carolina, USA 27834. Phone: (252)744-2702; Fax: (252) 744-3104; Email: akulas@ecu.edu

ABSTRACT

Kaposi's sarcoma-associated herpesvirus (KSHV) is etiologically associated with all forms of Kaposi's sarcoma worldwide. Little is currently known about the role of microRNAs (miRNAs) in KSHV entry. We recently demonstrated that KSHV induces a plethora of host cell miRNAs during the early stages of infection. In this study, we show the ability of host cell miR-36 to specifically inhibit KSHV-induced expression of interferon induced transmembrane protein 1 (IFITM1) to limit virus infection of cells. Transfecting cells with miR-36 mimic specifically lowered IFITM1 expression and thereby significantly dampening KSHV infection. In contrast, inhibition of miR-36 using miR-36 inhibitor had the direct opposite effect on KSHV infection of cells, allowing enhanced viral infection of cells. The effect of miR-36 on KSHV infection of cells was at a post-binding stage of virus entry. The highlight of this work was in deciphering a common theme in the ability of miR-36 to regulate infection of closely related DNA viruses: KSHV, Epstein-Barr virus (EBV), and herpes simplexvirus-2 (HSV-2). Taken together, we report for the first time the ability of host cell miRNA to regulate internalization of KSHV, EBV, and HSV-2 in hematopoietic and endothelial cells.

INTRODUCTION

Kaposi's sarcoma-associated herpesvirus (KSHV) causes Kaposi's sarcoma (KS)(Chang et al., 1994). To a lesser extent, KSHV is etiologically associated with rare neoplastic disorders like primary effusion lymphoma (PEL), and multicentric Castleman disease (MCD)(Soulier et al., 1995). KS is a malignant vascular tumor characterized by lesions occurring mainly on the skin, but can also affect the mucosa and visceral organs(Makharoblidze et al., 2015). Hallmarks of KS are angiogenesis, cell proliferation, and inflammation(Cancian et al., 2013). KSHV is among the list of viral pathogens estimated to cause 12-25% of human cancers worldwide(Morrison et al., 2015).

KSHV has a biphasic life cycle comprised of latent and lytic phases of replication that are distinguished based on divergent gene expression profiles(Uppal et al., 2015). The dynamics between latent and lytic phases of replication allows the virus to persist for the duration of the host's lifetime(Frappier, 2015). Notably, KSHV establishes latency in the majority of infected cells(Steitz et al., 2011); at any given instance, only a subpopulation (<3%) of infected cells display evidence of lytic gene expression(Sun et al., 1999). MicroRNAs (miRNAs) are one of the main classes of non-coding RNAs(Keshavarzi et al., 2017). These are small non-coding RNAs that regulate expression of genes in cells(Wang et al., 2017). The human genome encodes thousands of miRNAs(Kozomara and Griffiths-Jones, 2011). Of late, miRNAs have emerged as a pivotal component of host cell responses to a pathogen including viruses, bacteria, and fungi(Liu et al., 2017a).

KSHV, human immunodeficiency virus 1 (HIV-1), Epstein-Barr virus (EBV), and herpes simplex virus type 1 (HSV-1) are few examples of the limited number of viruses that encode their own miRNAs(Swaminathan et al., 2013; Zhang et al., 2014). KSHV encodes 12 pre-miRNAs which are processed to yield 25 mature miRNAs(Qin et al., 2017a). The roles of these KSHV-encoded miRNAs is to establish and/or maintain KSHV latency, enhance angiogenesis, spread infected cells, and interfere with the host immune system; all of which are crucial to

oncogenesis(Cai et al., 2005). Extensive work has been conducted on KSHV encoded miRNAs and the manner by which KSHV replication alters cellular miRNAs(Chen et al., 2016; Tan et al., 2015). However, there is limited work along the lines of understanding the effects of cellular miRNAs in response to early stages of KSHV infection of cells; specifically internalization of the virus. Recently, we employed deep sequencing for the first time, to analyze the miRNA expression profile in KSHV-infected BJAB cells during early stages of infection(Hussein and Akula, 2017c). In this study, we attempted to decipher how the cellular miRNA-36 (miR-36) alters KSHV infection in physiologically relevant cells: human B, and endothelial cells. We focused on the expression and effects of cellular miR-36 in response to KSHV infection because it was consistently elevated at 15 and 30min post infection (PI). Our data showed that the over-expression of cellular miR-36 inhibits KSHV infection of cells by dampening expression of interferon induced transmembrane protein 1 (IFITM1). Interestingly, the effect of IFITM1 on the closely related virus, Epstein-Barr virus (EBV) and a distant relative, herpes simplex virus-2 (HSV-2) followed the same pattern as in KSHV. These results reveal a layer of common theme in the regulation of host cell genes by miRNAs in the internalization of KSHV and related viruses.

RESULTS

KSHV infection of cells induces host cell miR-36 during early stages of KSHV infection

In a recently concluded study, we described a significant increase in the expression of host cell encoded miR-36 as early as 15 min PI of cells(Hussein and Akula, 2017c). In the present study, we monitored expression of this miR-36 at early time points during KSHV infection of human B and endothelial cells. We employed human B (BJAB) and endothelial (HMVEC-d) cells as they are physiologically relevant cells to KSHV biology. Expression of miR-36 gradually increased from 5min PI and peaked at 30min PI in KSHV infected BJAB (**Fig. 1A**) and HMVEC-d cells (**Fig. 1B**). Uninfected BJAB and HMVEC-d cells did not express miR-36 (**Fig. 1A, B**).

Expression of known miRNAs, hsa-let-7c and hsa-miR-3130-5p, were not significantly altered when compared to miR-36 during early stages of KSHV infection of cells (**Fig. 1A, B**). Treatment of cells with 10units/ml of heparinase I/III for 2h at 37°C prior to KSHV infection of cells resulted in a significant drop in the expression of miR-36 in BJAB (**Fig. 1C**) and HMVEC-d cells (**Fig. 1D**). Also, infection of both BJAB and HMVEC-d cells with UV.KSHV could induce the expression of miR-36 to comparable levels as the wild-type KSHV (**Fig. 1C, D**). These results demonstrate KSHV to induce host cell miR-36 very early upon infection. The key features of miR-36 including the secondary structure are provided in **Table 1** and **supplemental Figure 1**, respectively.

miR-36 inhibits KSHV infection in BJAB and HMVEC-d cells

To evaluate the biological effects of miR-36 in target cells, we analyzed the effects of miR-36 mimic and inhibitor on KSHV infection. The range of doses tested in this study is comparable to those reported in the earlier studies(Jin et al., 2015; Montgomery et al., 2014; Noh et al., 2017; Seimandi et al., 2005; Shao et al., 2017). The doses of the mimic and inhibitor used in the study did not significantly induce cell death in BJAB and HMVEC-d cells (**Fig. 2A, B**). Transfection of BJAB (**Fig. 2C**) and HMVEC-d (**Fig. 2D**) cells with miR-36 mimic significantly reduced KSHV infection of cells as monitored by the expression of *ORF50* gene as early as 30min PI. KSHV entry is a quick process and the IE gene, *ORF50*, is expressed immediately upon infection(Dyson et al., 2010). KSHV infection was not significantly altered in BJAB (**Fig. 2C**) and HMVEC-d (**Fig. 2D**) cells that were either transfected with scrambled miRNA control (miR-NC) or mock transfected. Interestingly, the effect of miR-36 mimic on KSHV infection of BJAB and HMVEC-d cells could be significantly reversed by co-transfecting cells with 10nM of miR-36 inhibitor (**Fig. 2E**). Co-transfection of cells with miR-NS did not alter the effects of miR-36 mimic (**Fig. 2E**). To ascertain that the effect of miR-36 mimic was at a post-binding stage of infection, we performed a binding assay. The binding assay performed on BJAB and HMVEC-d cells

demonstrated that miR-36 mimic and the miR-36 inhibitor did not block KSHV from binding the target cells (**Fig. 2F**). Incubating KSHV with heparin but not CSA significantly blocked KSHV from binding cells (**Fig. 2F**). Our results clearly implicate miR-36 to inhibit KSHV infection of cells. To extend our understanding of the role of miR-36 on other related viruses, we tested the effect of miR-36 mimic and the miR-36 inhibitor on EBV and HSV-2 infection of BJAB cells. Interestingly, miR-36 mimic could significantly block EBV and HSV-2 infection of BJAB cells and this inhibition could be specifically reversed by the miR-inhibitor (**Fig. 3**).

miR-36 targets IFITM1

By using the DIANA and MiRmap tool algorithms, we identified a putative miR-36 binding site located in the 3'-UTR of IFITM1 mRNA (**Supplemental Figure 2**). To confirm the ability of miR-36 to specifically inhibit IFITM1 expression, we monitored the expression of IFITM1 in target cells that were untransfected, transfected with miR-36 mimic, or miR-NC prior to infection. Transfection of BJAB and HMVEC-d cells with miR-36 mimic significantly lowered the expression of IFITM1 at 15min PI compared to untransfected cells and cells transfected with miR-NC (**Fig. 4A**). Transfection of cells with miR-36 mimic could specifically inhibit IFITM1 expression from 5min till 48h PI (data not shown). These results authenticate the fact that IFITM1 expression may well be regulated by miR-36.

In order to determine the bona fide target of miR-36, a luciferase reporter assay was performed. In this assay, two quantifiable genes encoding luciferase proteins were put on a vector. The IFITM1 3′ UTR with the target region was placed downstream GLuc to regulate its translation, and SEAP was placed under no regulation for normalization. 293 cells were co-transfected with the IFITM1 3′ UTR vector plasmid and miR-36 mimic. miR-36 mimic significantly decreased the relative luciferase activity compared to the cells that were transfected with miR-NC (**Fig. 4B**). In contrast, transfection of cells with miR-inihibitor reversed the ability of miR-36 mimic from lowering the luciferase activity (**Fig. 4B**). There was

an inverse correlation observed in the expression of miR-36 and IFITM1 during the course of KSHV infection of BJAB (**Fig. 4C**) and HMVEC-d (**Fig. 4D**) cells. These results suggest that miR-36 directly targets IFITM1 and thereby downregulates its expression.

IFITM1 expression enhances KSHV, EBV, and HSV-2 infection of cells

IFITM1 protein expression was significantly elevated with KSHV infection of BJAB and HMVEC-d cells (**Fig. 5A**). The expression of IFITM1 increased in KSHV infected cells as early as 5min PI which was elevated by 15min and 10min PI in BJAB and HMVEC-d cells, respectively, but declined sharply by 30 min PI (**Fig. 5A**). To confirm a role for IFITM1 in KSHV infection of target cells, we transiently transfected BJAB and HMVEC-d cells with pQCXIP/IFITM1 and the expression of IFITM1 was confirmed by flow cytometry (**Fig. 5B**). KSHV infection of the above IFITM1 expressing BJAB and HMVEC-d cells was a measure of the expression of *ORF50* at 30min PI. The idea was to strictly understand the effects of IFITM1 expression on early stages of KSHV infection. BJAB (**Fig. 5C**) and HMVEC-d (**Fig. 5D**) cells expressing IFITM1 supported a significantly enhanced KSHV infection compared to those cells that were left untransfected, mock transfected, or transfected with the empty vector. Surprisingly, IFITM1 expression also enhanced HSV-2 and EBV infection of BJAB and HMVEC-d cells (**Fig. 5C, D**). Interestingly, co-transfection of the above cells with miR-36 mimic could significantly drop KSHV infection of cells compared to miR-NC (**Fig. 5C, D**).

To further confirm the role of IFITM1 in KSHV infection of cells, we first transfected cells with siRNA specific for IFITM1. Northern blotting was performed at 0, 12, 24, and 48 hours after transfection as per the standard protocols to monitor IFITM1 mRNA expression (**Fig. 6A**). The levels of IFITM1 mRNA was significantly suppressed in BJAB and HMVEC-d cells by siRNA when compared with a (NS)siRNA control (**Fig. 6A**). A IFITM1 mRNA inhibition of 82% ± 7%, 74% ± 9%, and 45% ± 6% was observed in BJAB cells at 12, 24, and 48 hours, respectively, after siRNA transfection (**Fig. 6A**). A IFITM1 mRNA inhibition of 78% ± 9%, 65% ± 7%, and 34%

± 7% was observed in HMVEC-d cells at 12, 24, and 48 hours, respectively, after siRNA transfection. IFITM1 expression levels were not significantly altered by the (NS)siRNA controls in both the cells tested, demonstrating the specificity of the siRNA used (**Fig. 6A**). IFITM1 expression in target cells transfected with siRNA specific to IFITM1 was significantly lowered at 15min post KSHV infection (**Fig. 6B**). In contrast, KSHV induced IFITM1 expression in untransfected or cells transfected with (NS)siRNA were not altered (**Fig. 6B**). On the same lines, KSHV infection in cells silenced for the expression of IFITM1 was significantly lower compared to cells that were untransfected or transfected with (NS)siRNA (**Fig. 6C**). Silencing the expression of IFITM1 also decreased EBV and HSV-2 infection of the above cells (**Fig. 6C**). The above viral infections were monitored by performing *qRT-PCR*. Taken together, the results clearly implicate a role for IFITM1 in enhancing KSHV, EBV, and HSV-2 infection of cells.

DISCUSSION

Since miRNAs discovery over 20 years ago, miRNAs have been established as key players in the molecular mechanisms of mammalian biology including the maintenance of normal homeostasis and the regulation of disease pathogenesis. Host miRNAs also play a crucial role in mounting an immune response against microbial infections including those caused by viruses(Eulalio et al., 2012). Several viruses belonging to herpesvirus, polyomavirus, hepadnavirus, adenovirus, and retrovirus encode miRNAs(Swaminathan et al., 2013; Zhang et al., 2014). Virus-encoded miRNAs (vmiRNA) identified in virus-infected cells significantly influence viral replication and disease progression by modulating viral as well as host cellular mRNA. Many of the cellular miRNAs affect viral replication either directly by binding to the viral genome or indirectly by targeting host factors related to replication(Shrivastava et al., 2015). There are several published works that describe virus and cellular encoded miRNAs in KSHV pathogenesis(Chen et al., 2016; Keshavarzi et al., 2017). However, to date, there is no report on the role of cellular miRNAs during early stages of KSHV infection.

Recent studies from our laboratory using a combination of deep sequencing and qRT-PCR identified cellular miR-36 to activate as early as 15min PI(Hussein and Akula, 2017c). In the current studies, we employed physiologically relevant human B cells (BJAB) and endothelial cells (HMVEC-d) to make the study more meaningful to KSHV biology. Accordingly, using specific primers we analyzed the expression profile of cellular miR-36 during the first 30min of KSHV infection of cells. A successful viral entry was a measure of KSHV to enter cells and express immediate early gene, *ORF50*. The expression of *ORF50* was monitored by qRT-PCR(Dyson et al., 2010; Walker et al., 2014). KSHV infection of BJAB and HMVEC-d cells rapidly triggered the expression of miR-36 as early as 5min PI that peaked at 30min PI (**Fig. 1**). Expression of miR-36 in KSHV infected BJAB is higher than those in HMVEC cells. This could be attributed to the inherited variations observed between different cells in the manner by which they respond to virus infection(Maisch et al., 2002). Moreover, the expression level of miRNAs has been shown to vary among tissues, cell types, and even between cells of the same lineage(Lagos-Quintana et al., 2002; Teruel-Montoya et al., 2014).

Cellular miR-36 is triggered by UV.KSHV infection of cells while treating target cells with heparinase I/III prior to infecting cells with the wild-type KSHV failed to induce expression of miR-36. Treatment of cells with heparinase I/III cleave heparan sulfate (HS) at different sites and liberate them from the cell surface(Stringer and Gallagher, 1997). KSHV binds to a target cell via interacting with HS expressed on the cell surface(Akula et al., 2001b). Taken together, our results indicate the following: (i) it is the interactions between the virus envelope proteins and the host cells that trigger miR-36 response; and (ii) binding of KSHV to cells is critical to miR-36 expression in cells. miR-36 mimic specifically inhibited KSHV infection of BJAB and HMVEC-d cells (**Fig. 2C, D**). Transfection of cells with miR-36 inhibitor reversed the effects of miR-36 mimic on KSHV infection of cells (**Fig. 2E**). The effects of miR-36 mimic and inhibitor was specific as the scramble negative control (miR-NC) and non-specific inhibitor (miR-NS) did not significantly alter KSHV infection of cells (**Fig. 2C, D, E**). It was concluded that the effects of

miR-36 mimic and inhibitor on KSHV infection was at a post attachment stage of internalization as they did not adversely affect virus binding to cells (**Fig. 2F**).

In this study, we originally wanted to use two relevant viruses as negative controls to better understand the specificity of miR-36 on KSHV infection of cells. EBV and HSV-2 were selected as controls: EBV, like KSHV, belongs to γ-herpesvirinae while HSV-2 belongs to *α-herpesvirinae*. Interestingly, we observed a similar effect of miR-36 mimic and inhibitor on EBV and HSV-2 infection of cells (**Fig. 2F**). This could be due to the fact that *α, β, and γ-herpesviruses* exhibit and share a common three-dimensional capsid structure along with the fact that there is quite a bit of homology in the glycoproteins being expressed on the viral envelope(Liu and Zhou, 2007).

One miRNA may regulate many genes as its targets, while one gene may also be targeted by many miRNAs(Hashimoto et al., 2013). Accordingly, miR-36 can possibly target several genes (**Supplemental Figure 6**). Using bioinformatics tools, we identified IFITM1 to be the most promising targets to miR-36. IFITM is a member of the interferon-induced 125–133 amino acid protein family including IFITM1, IFITM2, IFITM3, IFITM5 and IFITM10. This family of proteins is located on chromosome 11 of the human genome and originally described as highly inducible genes by α- and γ-interferons (IFNs)(Hickford et al., 2012; Reid et al., 1989). The three members of the IFITM proteins (IFITM1, IFITM2, and IFITM3) have gained prominence as novel antiviral IFN-stimulated genes (ISGs)(Weidner et al., 2010). Hence, we set out to test the effect of transfecting target cells with IFITM1-3 genes on KSHV infection of target cells. Over-expressing IFITM1 significantly enhanced KSHV infection of cells; IFITM3 moderately enhanced KSHV infection while IFITM2 did not alter the viral infection (**Supplemental Figure 7**). Based on these results, we focused our further studies on IFITM1 in terms of miR-36 and early stages of KSHV infection. Using bioinformatic tools it was determined that the miR-36 target IFITM1 expression. Luciferase assay demonstrated the ability of miR-36 to physically interact with IFITM1 (**Fig. 4B**). miR-36 mimic specifically inhibited IFITM1 expression that could be reverted

by transfecting cells with miR-36 inhibitor (**Fig. 4B**). There was an apparent inverse correlation observed between the KSHV-induced IFITM1 expression and miR-36 response (**Fig. 4C, D**). We propose the sharp decline in the expression of IFITM1 30min PI is because of an increase in the expression of miR-36 **(Fig. 4C, D)**. Taken together, our study established a direct association between virus-induced IFITM1 and endogenous miR-36 expression in the biology of KSHV.

IFITM1 is expressed in many cell types including leukocytes and endothelial cells(Hickford et al., 2012; Lewin et al., 1991). IFITM1 modulates cell functions including immunological responses, cell proliferation, cell adhesion, and germ cell maturation(Bailey et al., 2014). As other IFITM proteins, IFITM1 is significantly upregulated by interferons type I and II and is critical for anti-virus response of innate immunity(Brass et al., 2009). Recent reports indicate IFITM1 to play a significant role in virus entry. IFITM1 inhibits entry of many RNA viruses including influenza A H1N1 Virus, West Nile Virus, Dengue Virus, HIV, and HCV(Brass et al., 2009; Narayana et al., 2015; Yu et al., 2015a). The suggested mechanisms by which IFITM proteins restrict the above virus infections include inhibition of virus binding to corresponding cellular receptors, inhibition of endocytosis, and acting as pattern recognition receptors by sensing virus infection and activation of downstream cellular signaling pathways(Brass et al., 2009). These proteins inhibit fusion of viral membranes with cellular endosomal vesicular membranes by blocking the creation of hemifusion, reducing membrane fluidity and curvature, and by possibly disrupting intracellular cholesterol homeostasis(Amini-Bavil-Olyaee et al., 2013; Li et al., 2013a). However, IFITMs can also enhance viral infection of cells: (i) both IFITM1 and IFITM3 modestly enhanced human papillomavirus 16 (HPV-16) infection of a variety of cells(Warren et al., 2014); and (ii) Zhao et al have shown type I IFN-α, IFN-γ, and type II IFN-λ to significantly promote infection of human coronavirus, HCoV-OC43 by the induction of IFITM proteins. The authors reported that the over-expression of IFITM3

significantly increased susceptibility of Huh7.5 cells to HCoV-OC43 infection(Zhao et al., 2014). In general, the IFITM family of proteins affects virus entry of cells. Over-expression of IFITM1 significantly enhanced KSHV infection of target cells (**Fig. 5C, D**) while silencing expression of IFITM1 had the opposite effect (**Fig. 6**). More interestingly, we observed identical effects of IFITM1 in enhancing EBV and HSV-2 infection of cells (**Fig. 6C**).

IFNs are generally considered to be antiviral cytokines that inhibit virus infection of cells by stimulating ISGs(Samuel, 2001). In fact, we observed a significant increase in the expression of IFN-α and -γ during the early stages of KSHV infection of BJAB and HMVEC-d cells (**Supplemental Figure 8**). If that is the case, how can IFITM1 enhance infection of not just KSHV; but also of EBV and HSV-2? Such a scenario can be possible only if the virus infection is not altered by IFNs and associated proteins(Zhao et al., 2014). Interestingly enough, herpesviruses as a group (including KSHV) is considered to be relatively insensitive to the antiviral effects of IFNs in a variety of different cell systems(Adams et al., 1975; Flowers et al., 1998). In a way, our results demonstrate for the first time that herpesviruses, KSHV, EBV, and HSV-2, not only hijack IFITM1 to their benefit in facilitating virus entry into cells but also evade the IFN-induced antiviral effects.

This study provides a new insight to virus infection. KSHV (including EBV and HSV-2) interactions with target cells induce IFITM1 within minutes, which facilitate virus entry into cells. KSHV-induced IFITM1 is part of the innate immune activation system that occurs in an antigen-independent fashion(Schoggins and Rice, 2011) and relies on the ability of the host to recognize virus via specific pattern recognition receptors(Takeuchi and Akira, 2010). To counter the effects of KSHV-induced IFITM1, infected cells respond within a short period of time by inducing expression of miR-36. Cellular miR-36 in turn inhibits expression of IFITM1 and thus limit virus infection of cells. Perhaps, this could be a mechanism of superinfection resistance (SIR)(Nethe et al., 2005) developed by cells towards KSHV and other related viral

pathogens. IFITM1 suppression by miR-36 may have direct and indirect effects of KSHV pathobiology: (i) directly limit KSHV infection of cells; (ii) block cell proliferation/division(Jin et al., 2017) and thereby promote KSHV latency(Zhi et al., 2015); and (iii) reduce virus-induced inflammation. Such effects of IFITM1 on the biology of KSHV will be better understood by employing the three-dimensional (3-D) cell culture models as they mimic certain aspects of the tissue environment(Cheng et al., 2011; El Assal et al., 2016). For all this time, studies on virus entry have always focused primarily on the roles of virus encoded glycoproteins and their cognate host cell receptors. To our knowledge, this is the first report of a miRNA influencing KSHV infection of cells and this, we hope, will open doors to a further understanding of virus entry; after all, it is the miRNAs that regulate the gene function.

Of late, miRNA-based therapeutics have been used to effectively treat autoimmune diseases(Wang et al., 2015), and cancers including prostate cancer, and leukemia(Braicu et al., 2013) in animal models. The fact that miRNAs can influence virus entry is fascinating as miRNA-based therapeutics like the use of miR-mimics can effectively be used to treat virus entry including pathogenesis. There are several questions that need to be answered and they are as follows: (i) How does IFITM1 enhance KSHV infection of cells? Does it physically bind KSHV envelope-associated protein and facilitate endocytosis? (ii) What is the role of host cell receptors in the IFITM1-facilitated virus entry? (iii) What is the dynamics between the expression pattern of IFITM1 and 3 in regulating KSHV infection of cells? And (iv) Can induction of miR-36 by KSHV infection prevent infected cells from being superinfected with KSHV and other related herpesviruses, *in vivo*? Current studies in our lab are dedicated to answer these questions.

MATERIALS AND METHODS

Cells

Human Burkitt lymphoma B cell line (BJAB), human foreskin fibroblasts (HFFs; Clonetics,Walkersville, MD), HEK-293 (293), and dermal microvascular endothelial cells (HMVEC-ds; CC-2543; Clonetics) were used in this study. BJAB cells were propagated in phenol red–free RPMI medium (Invitrogen, Carlsbad, CA) while HFF and 293 cells were cultured in Dulbecco modified Eagle medium (DMEM) containing 10% charcoal-stripped fetal bovine serum (FBS; Atlanta Biologicals, Lawrenceville, GA), L-glutamine, and antibiotics(Akula et al., 2005). HMVEC-d cells were propagated in EGM MV-microvascular endothelial cell medium (Clonetics) as per standard protocols. The passage numbers for HFFs and HMVEC-ds used in this study ranged between 6 - 10, and 5 - 9, respectively. All the cells used in this study were negative for mycoplasma as tested by *Mycoplasma* PCR ELISA, Roche Life Science. For culture conditions, refer to supplemental data.

Virus

The viruses used in this study were wild-type KSHV(Dyson et al., 2010), herpes simplexvirus-2 (HSV-2)(Akula et al., 2003), and Epstein-Barr virus (EBV)(Bentz et al., 2010). We generated ultraviolet (UV) inactivated KSHV (UV.KSHV) as per early studies(Hussein and Akula, 2017c).

Cytotoxicity assay

The LDH assay was performed using the CytoTox 96 non-radioactive kit (Promega) as per earlier studies(Dyson et al., 2010). Target cells were treated with different concentrations of miR-36 mimic and inhibitor at 37°C in a V-bottom 96-well plate. After a 24h incubation, the cells were analyzed for the expression of LDH, as an indicator of cell death. The LDH assay was performed using the CytoTox 96 non-radioactive kit (Promega) as per earlier studies(Dyson et

al., 2010). G418 (Sigma-Aldridge, St. Louis, MO) and cytochalasin D (Sigma-Aldridge) were used as known cell death inducers.

Virus infection of cells, RNA extraction, and monitoring virus infection

BJAB, HFF, and HMVEC-d cells were infected with 10 multiplicity of infection (MOI)(Walker et al., 2014) of KSHV, EBV, and HSV-2. The cells were left uninfected or infected for 5, 10, 15, and 30min prior to washing the cells twice in PBS and processed appropriately for RNA extraction. Total RNA was extracted using TRIzol (Invitrogen, Carlsbad, CA). The RNA concentration was measured with a NanoDrop ND-2000 spectrophotometer (Thermo Fisher Scientific, Waltham, MA), and then verified for quality using an Agilent 2100 Bioanalyzer (Agilent Technologies, Santa Clara, CA). Only the RNA samples with 260/280 ratios of 1.8 to 2.0 were used in the study.

Extracted RNA was used to synthesize cDNA and the expression of *ORF50* was monitored by qRT-PCR using specific primers as per earlier studies(Dyson et al., 2010) Expression of *ORF50* was used as a scale to measure KSHV infection of cells. As reported earlier(Walker et al., 2014), the lowest limit of detection in the standard samples was 6–60 copies for the *ORF50* gene. The results from the use of *ORF50* primers were consistently confirmed by monitoring the expression of another viral immediate early (IE) gene, vGPCR (data not shown). EBV and HSV-2 infection was monitored using specific primers to BRLF1 (homolog of KSHV *ORF50*)(Robinson et al., 2011) and HSV-2 IE gene, US1(Kaneko et al., 2008).

Transfections of cDNA and miRNA

Target cells were transiently transfected with plasmid DNA using FuGene HD (Promega, Madison, WI) as per manufacturer's recommendations. The plasmid, pQCXIP encoding IFITM1, used in this study was kindly gifted to us by Dr. Michael Farzan (The Scripps Research

Institute, Jupiter, USA). FuGene HD/DNA ratios of 3:1 for adherent cell lines and 6:1 for suspension cell lines were used. Transfection of target cells with different concentrations of miR-36 mimic, or scramble control (miR-NC); miRNA inhibitor to miR-36 and non-specific (NS) inhibitor (Sigma-Aldridge) was achieved using FuGene HD reagent as per standard laboratory procedures. These were transient transfections and experiments using these cells were conducted 48h post transfection.

Binding assay

The effect of miR-mimic and inhibitor on KSHV binding to target cells was assessed by PCR detecting the cell-bound KSHV DNA. Briefly, untransfected cells or cells transfected with miR-mimic or inhibitor were infected with 10MOI of KSHV at +4°C. After 60min of incubation with virus, cells were washed three times with PBS to remove the unbound virus. Cells were pelleted, and total DNA including those representing the cell bound KSHV was isolated using DNeasy kit (Qiagen, Valencia, CA) and subjected to qPCR analysis monitoring *ORF50* according to recently published work(Walker et al., 2014). Incubating KSHV with 100µg/ml of heparin and chondroitin sulfate A (CSA; Sigma-Aldridge) for 1h at 37°C were used as known positive and negative controls.

Flow cytometry

Flow cytometry was used to monitor expression of IFITM1 in the cells as per earlier protocols(Walker et al., 2014). Briefly, target cells were fixed in 10ml of ice-cold acetone for 20min, washed thrice in PBS prior to incubating cells in 25µg/ml of rabbit polyclonal antibody to IFITM1 (EMD Millipore, Billerica, MA) for 60min at 4°C. The cells were washed thrice in PBS and further incubated with FITC conjugated appropriate secondary IgG at 4°C for 30 min,

washed and analyzed in a FACScan flow cytometer (Becton Dickinson) with appropriate gating parameters.

Western blotting

All the buffers used in this project were made with water that was endotoxin and pyrogen free. Western blotting was conducted as per earlier studies(Walker et al., 2014) using the following primary antibodies: rabbit anti-IFITM1 polyclonal antibody (EMD Millipore) and mouse anti-actin antibodies (Clone AC-74; Sigma-Aldridge).

Real-time *qRT-PCR* analysis of the expression of miRNAs and IFNs

The quality of RNA was tested using a spectrophotometer. Only the RNA samples with 260/280 ratios of 1.8 to 2.0 were used in the study. Approximately 500ng of RNA was reverse transcribed in a 25µl reaction volume using the All-in-one^{TM} miRNA qRT-PCR detection kit (GeneCopoeia, Rockville, MD). Briefly, the cDNA was synthesized in a 25µl reaction mix containing 5µl of 5x reaction buffer, 2.5U/µl Poly A Polymerase, 10ng/µl MS2 RNA, and 1µl RTase Mix. The reaction was performed at 37°C for 60 min and terminated at 85°C for 5 min. cDNA that was produced in the RT reaction was diluted ten-fold and was used as the template for the PCR reaction in an Applied Biosystems ViiA 7 Real-Time PCR System (Life Technologies, USA). In this system, MS2 RNA was used as an external reference for the quality of the extracted miRNAs, and RNU6B, RNU44, RNU48, and RNU49 were used for normalization. The expression levels of miRNAs were measured employing qRT-PCR with the SYBR green detection and specific forward primer for the mature miRNA sequence and the universal adaptor reverse primer (GeneCopoeia, USA). Expression of IFN-α, -β, and -γ by qRT-PCR was conducted as per earlier protocols(Dyson et al., 2010) using appropriate primers(Colantonio et al., 2011; Padua et al., 2016; Wu et al., 2017).

Dual-luciferase reporter assay

Luciferase reporter plasmids with wild-type IFITM1 3′-UTR were purchased from GeneCopoeia (Rockville, MD). 293 cells were plated onto 6-well plates. At 24h post-plating, 293 cells were co-transfected with IFITM1 3′-UTR luciferase reporter plasmid and miR-36 mimic or miR-NCNA scramble control (miR-NC) using FuGene HD (Promega). At 12, 24, 48h post transfection, supernatants were collected from each treatment and the luciferase activity measured using the Secrete-Pair Dual Luminescence Assay Kit (GeneCopoeia) as per the manufacturers' recommendations.

Northern blotting

Northern blotting to monitor IFITM1 and β-actin expression was performed using a DIG Luminescent Detection Kit (Roche, Indianapolis, IN) as per the manufacturer's recommendations(Dyson et al., 2010).

Silencing IFITM1 using siRNA

Expression of IFITM1 was inhibited by the transfection of double-stranded (ds) RNA oligos as per standard protocols(Dyson et al., 2010). IFITM1 siRNA was purchased from Dharmacon RNA Technologies (Lafayette, CO). Briefly, 1 x 10^6 cells were washed twice in RPMI and incubated in phenol red–free RPMI supplemented with 5% FBS at 37°C. After 24 hours incubation (considered as 0h for experiments in **Fig. 6A**), the target cells were transfected with either ds short interfering RNAs (siRNAs) or the nonspecific (NS) controls using Fugene HD as per manufacturer's recommendations (Promega). At 0, 12, 24, and 48 hours after transfection, total RNA was isolated from the cells and subjected to Northern blotting to monitor the expression of IFITM1 and β-actin mRNA as per the protocol mentioned in the "Materials and methods" section describing Northern blotting. In another set of experiments, untransfected cells and cells transfected with siRNA or (NS)siRNA for 12h were infected with 10 MOI of KSHV. At

the end of 30min PI, KSHV infection was assessed by monitoring ORF50 expression by qRT-PCR.

ACKNOWLEDGMENTS

We sincerely thank Ikenna Okafor and Frank Williams to have conducted the double-blinded qRT-PCR experiments. We thank Dr. Michael Farzan (The Scripps Research Institute, Jupiter, USA) for kindly providing the plasmid, pQCXIP encoding IFITM1. Technical help by Dr. Douglas Weidner with the use of flow cytometer is highly appreciated. We thank Dr. Joseph Pagano (UNC-Chapel Hill, NC) to have provided us with the EBV stock virus. We thank Dr. Blossom Damania (University of North Carolina at Chapel Hill) to have kindly provided us with the BJAB cells. We thank Dr. Adrian Reber, Centers for Disease Control and Prevention, to have read and critiqued this report.

COMPETING FINANCIAL INTERESTS

The authors declare no competing financial interests: details are available in the online version of the paper.

DATA AVAILABILITY STATEMENT

All data generated or analyzed during this study are included in this published article (and its Supplementary Information files).

Figure legends.

Figure 1. KSHV induces the expression of miR-36 at an early stage of infection. Expression of miR-36, has-let-7c, and has-miR-3130-5p were detected by qRT-PCR at different time points post-infection in cells infected with 10 MOI of KSHV compared to uninfected cells. The qRT-PCR data was plotted for fold changes in the expression of miR-36, has-let-7c and has-miR-3130-5p in (**A**) BJAB cells, and (**B**) HMVEC-d. BJAB (**C**) and HMVEC-d (**D**) cells were either untreated or treated with heparinase I/III prior to performing the infection assay followed by monitoring the expression of miR-36. UV.KSHV was used in this study as a control to understand the importance of an intact virus envelope and associated proteins in inducing miR-36. The relative expression of miRNAs was measured in terms of cycle threshold value (Ct) and normalized to snRNA RNU6B. The *x-axis* indicates the time points post KSHV infection in minutes and *y-axis* indicates fold change in the expression of miR-36. Bars (panels **A**, **B, C, D**) represent average ± s.d. of five individual experiments. (**A, B**) Student *t* test was performed to compare expression of miR-36 in uninfected cells versus 5, 10, 15, and 30min PI. In panels '**C** and **D**', Student *t* test was performed to study the effect of HS and compare infection of cells with KSHV versus UV.KSHV on miR-36 expression at 5, 10, 15, and 30min PI. Two-tailed P value of 0.05 or less was considered statistically significant. *p<0.05; **p,0.01; ***p<0.001; NS-not significant.

Figure 2. miR-36 overexpression inhibits KSHV infection of cells. To determine the cytotoxic effect of miR-36 mimic and inhibitor, cells were transfected with different concentrations of miR-36 mimic and inhibitor. At 24h post transfection, lactate dehydrogenase release as an indicator of percentage of cell death was monitored for miR-36 mimic (miR-mimic) (**A**) and miR-inhibitor (**B**). Known inducers of cell death, 1 mg/ml G418 in the case of BJAB cells and 2.5 µg/ml Cytochalasin D for HMVEC-d, were used as positive controls in this study. (**C-D**) **Transfection of cells with miR-36 mimic specifically inhibit KSHV infection of cells.** (**C**)

BJAB and (**D**) HMVEC-d cells were either untransfected, mock transfected, or transiently transfected with different concentrations of miR-36 mimic or control mimic (miR-NC) before infection with 10 MOI of KSHV. Data was plotted to represent the percentage of KSHV infection as determined by monitoring the change in KSHV-*ORF50* RNA copy numbers that were detected in transfected cells compared to that detected in untransfected cells (1905 KSHV-*ORF50* RNA copies). Expression of *ORF50* was used as a scale to measure KSHV infection of cells. As reported earlier(Walker et al., 2014), the lowest limit of detection in the standard samples was 6–60 copies for the *ORF50* gene. (**E**) **Transfection of cells with miR-36 inhibitor opposes the effects of miR-36 mimic on KSHV infection of cells.** BJAB and HMVEC-d were either untransfected, mock transfected, transiently transfected with miR-36 mimic, co-transfected with miR-36 mimic and miR-36 inhibitor (miR-mimic+mir-inhib), or co-transfected with miR-36 mimic and nonspecific inhibitor (miR-mimic+mir-NS) before infection with KSHV. Data was plotted to represent the percentage of KSHV infection in transfected cells compared to untransfected cells. The *x-axis* indicates the transfection and *y-axis* indicates the percentage of KSHV infection. (**F**) **miR-36 mimic inhibition of KSHV infection of cells is at a post-attachment stage of virus entry.** KSHV binding to BJAB and HMVEC-d that were untransfected, mock transfected, transiently transfected with miR-36 mimic, co-transfected with miR-36 mimic and miR-36 inhibitor(miR-mimic+mir-inhib), co-transfected with miR-36 mimic and nonspecific inhibitor (miR-mimic+mir-NS), or untransfected and treated with Heparin or CSA. Data was plotted to represent the percentage of KSHV binding to target cells treated differently compared to the untransfected cells. Bars (panels **A-F**) represent average ± s.d. of five individual experiments. Student t test was performed to compare groups. Two-tailed P value of 0.05 or less was considered statistically significant. *p<0.05; **p,0.01; ***p<0.001; NS-not significant.

Figure 3. miR-36 overexpression inhibits EBV and HSV-2 infection of BJAB cells. BJAB was either untransfected, mock transfected, transiently transfected with miR-36 mimic (miR-mimic), co-transfected with miR-36 mimic and miR-36 inhibitor (miR-mimic+mir-inhib), or co-transfected with miR-36 mimic and nonspecific inhibitor (miR-mimic+mir-NS) prior to infecting the cells with 10 MOI of EBV or HSV-2. Data was plotted to represent the percentage of virus infection as determined by monitoring the change in RNA copy numbers of EBV-BRLF1 or HSV-2 US1 as detected in transfected cells compared to that detected in untransfected cells (1750 copies of EBV BRLF-1 and 2678 copies of HSV-2 US1). Bars represent average ± s.d. of five individual experiments. Student *t* test was performed to compare viral infection of untransfected cells versus cells transfected with miR-36 mimic, inhibitor, miR-NS, or mock transfected cells. Two-tailed P value of 0.05 or less was considered statistically significant. ***p<0.001; NS-not significant.

Figure 4. miR-36 targets IFITM1. (**A**) **miR-36 mimic lowers KSHV-induced IFITM1 expression.** Western blotting analysis demonstrate a decrease in IFITM1 protein levels upon over-expression of miR-36 mimic. BJAB and HMVEC-d cells were either untransfected, transiently transfected with miR-36 mimic, or transfected with control mimic (miR-NC) prior to infecting cells with 10 MOI of KSHV. Monitoring IFITM1 protein levels was performed 15 minutes post KSHV infection and normalized to β-actin protein levels. Data representing the IFITM1 protein expression levels are presented as fold increase (average±s.d. from three experiments) in the boxes below the panels. The results presented are a representative data and the original full-length blots of the cropped images is provided in **Supplemental Figure 3**. (**B**) **miR-36 specifically binds and interact with IFITM1.** Luciferase activity in 293 cells transfected with Dual-luciferase vector encoding Gaussia Luciferase (GLuc) and secreted alkaline phosphatase (SEAP) with 3'UR of IFITM placed downstream of Glu luciferase reporter (IFITM1 3'UTR). 293 cells were either transfected with IFITM1 3'UTR, co-transfected with

IFITM1 3'UTR and miR-36 mimic, co-transfected with IFITM1 3'UTR and control mimic (miR-NC), or co-transfected with IFITM1 3'UTR, miR-36 mimic and miR-36 inhibitor. GLuc activity was monitored at 18h, 24h, 36h, 84, and 72h post-transfection and was normalized to SEAP. Data is plotted as GLuc/SEAP ratio where the *x-axis* indicates the transfection and time points, and *y-axis* indicates the relative luciferase activity. The relative expression of IFITM1 and miR-36 in KSHV-infected BJAB (**C**) and HMVEC-d (**D**) cells was monitored by qRT-PCR. The expression was measured in terms of cycle threshold value (Ct) and normalized to expression of β-actin and snRNA RNU6B, respectively. The *x-axis* denotes the time point post KSHV infection in minutes and *y-axis* denotes fold change in expression of IFITM1 and miR-36. The R2 values for the miRNA expression during the early course of KSHV infection is provided. Bars (**B-D**) represent average ± s.d. of five individual experiments. Student *t* test was performed to compare groups. Two-tailed P value of 0.05 or less was considered statistically significant. *p<0.05; **p,0.01; ***p<0.001; NS-not significant.

Figure 5. IFITM1 overexpression enhances KSHV infection of cells. (**A**) **KSHV infection of cells induce IFITM1 expression.** Western blotting analysis demonstrate KSHV infection of target cells to increase IFITM1 protein levels. Expression of IFITM1 levels was normalized to β-actin protein levels. Data representing the IFITM1 protein expression levels are presented as fold increase (average±s.d. from three experiments) in the boxes below the panels. The results presented are a representative data and the original full-length blots of the cropped images is provided in **Supplemental Figure 4**. (**B**) Flow cytometry data confirming the expression of IFITM1 protein in transfected cells. BJAB and HMVEC-d cells transiently transfected with pQCXIP/IFITM1 vector were analyzed for the expression of IFITM1 protein. This was performed by staining untransfected cells (red line) and transfected cells (green line) with rabbit polyclonal anti-IFITM1 antibodies followed by incubation with goat anti-rabbit FITC, before examining by FACS. As a control for the antibodies, transfected cells stained only with polyclonal anti-IFITM1

antibodies (purple dark line) were used. (**C-D**) **IFITM1 enhances KSHV infection of cells.** (**C**) BJAB and (**D**) HMVEC-d cells were untransfected, mock transfected, transiently transfected with pQCXIP/IFITM1, pQCXIP, co-transfected with pQCXIP/IFITM1 and miR-36 mimic, or co-transfected with pQCXIP/IFITM1 and control mimic (miR-NC) prior to infecting with 10 MOI of KSHV, EBV or HSV-2. Data was plotted to represent the percentage of virus infection as determined by monitoring the change in RNA copy numbers of KSHV-*ORF50*, EBV-BRLF1 or HSV-2 US1, respectively. Bars (**C-D**) represent average ± s.d. of five individual experiments. Student *t* test was performed to compare the effects of IFITM1 and miR-36 mimic on virus infection of cells compared to appropriate control groups. Two-tailed P value of 0.05 or less was considered statistically significant. **p,0.01; ***p<0.001; NS-not significant.

Figure 6. Knock-down of IFITM1 by siRNA decreases KSHV, EBV and HSV-2 infection of cells. (**A**) **Northern blotting to monitor the effect of transfecting cells with siRNA specific to IFITM1.** Target cells were untransfected or transfected either with ds siRNA or (NS)siRNA controls. After 0, 12, 24, and 48 hours after transfection, total RNAwas isolated from the cells and subjected to Northern blotting as per standard protocols to monitor IFITM1and β-actin mRNA. Data representing the IFITM1 mRNA expression levels are presented as fold increase (average±s.d. from three experiments) in the boxes below the panels. The results presented are a representative data and the original full-length blots of the cropped images is provided in **Supplemental Figure 5**. (**B**) BJAB and HMVEC-d cells were un-transfected, transfected with IFITM1-specific siRNA, or NS- siRNA prior to infecting cells with 10 MOI of KSHV. IFITM1 mRNA levels was monitored at 15min PI by Northern blotting and normalized to β-actin levels. (**C**) **KSHV, EBV, and HSV-2 infection significantly lowered in cells silenced for IFITM1 expression.** BJAB and HMVEC-d were either un-transfected, transfected with IFITM1-specific siRNA, or transfected with (NS)siRNA before infecting with KSHV, EBV or HSV-2. Data was plotted to represent the percentage of virus infection as determined by monitoring the change in

RNA copy numbers of KSHV-*ORF50*, EBV-BRLF1, or HSV-2 US1. Bars represent average ± s.d. of five individual experiments. Student t test was performed to compare groups. Two-tailed P value of 0.05 or less was considered statistically significant. ***p<0.001.

Table 1. Characteristics of miR-36:

Name	hsa-miR36
Sequence	CGCAGGAGCCGCGGAGGGCCGGA
Pre-miR36	CGGACTGGCTGGCCGCGCTCTTCGCACGGGGCGCTTTTGCGTGGGGTCGCGCAGGAGCCGCGGA GGGCCGGATCGCT
Chromosome	Chr5
ChromStart	127419226
ChromEnd	127419302
Strand	+
5p Seq	TGGCTGGCCGCGCTCTTCGCAC
3p Seq	CGCAGGAGCCGCGGAGGGCCGGA
Type	Duplex
Hairpin	True

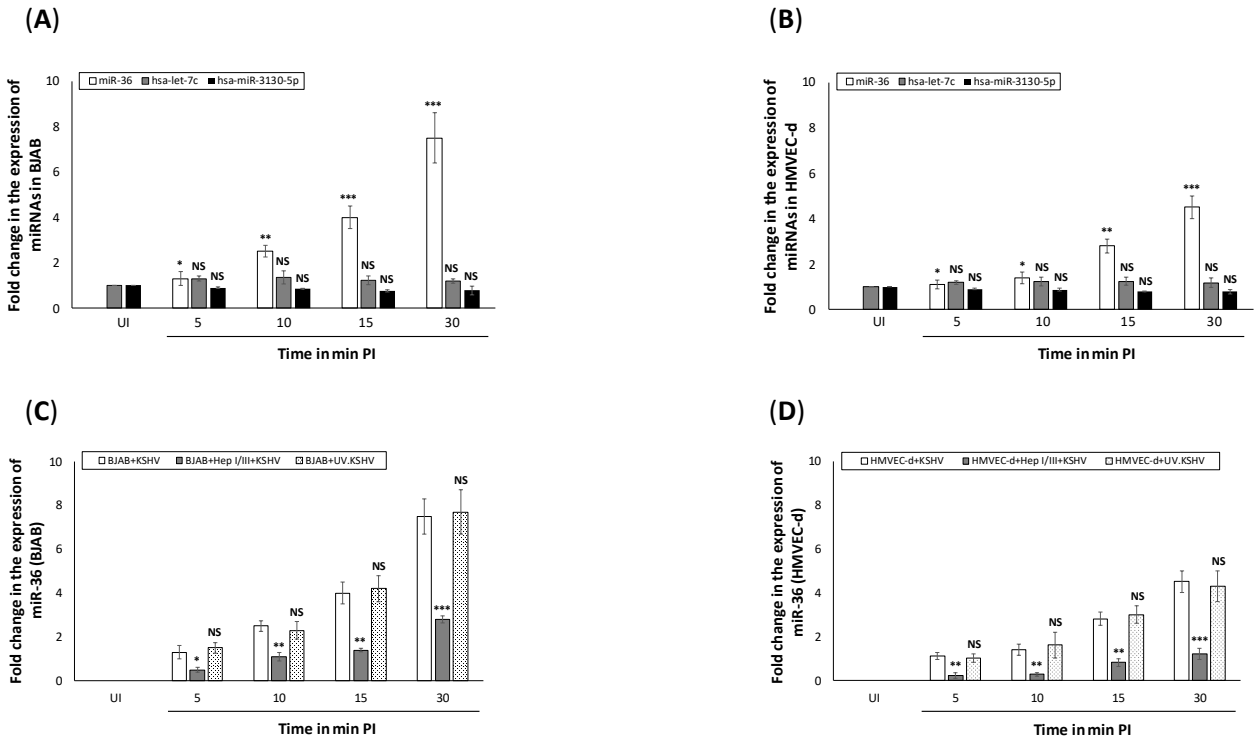
(A)
miR-36
hsa-let-7c
hsa-miR-3130-5p
Fold change in the expression of miRNAs in BJAB
Time in min PI
(B)
Fold change in the expression of miRNAs in HMVEC-d
(C)
BJAB+KSHV
BJAB+Hep I/III+KSHV
BJAB+UV.KSHV
Fold change in the expression of miR-36 (BJAB)
(D)
HMVEC-d+KSHV
HMVEC-d+Hep I/III+KSHV
HMVEC-d+UV.KSHV
Fold change in the expression of miR-36 (HMVEC-d)
UI
5
10
15
30
NS

Figure 1

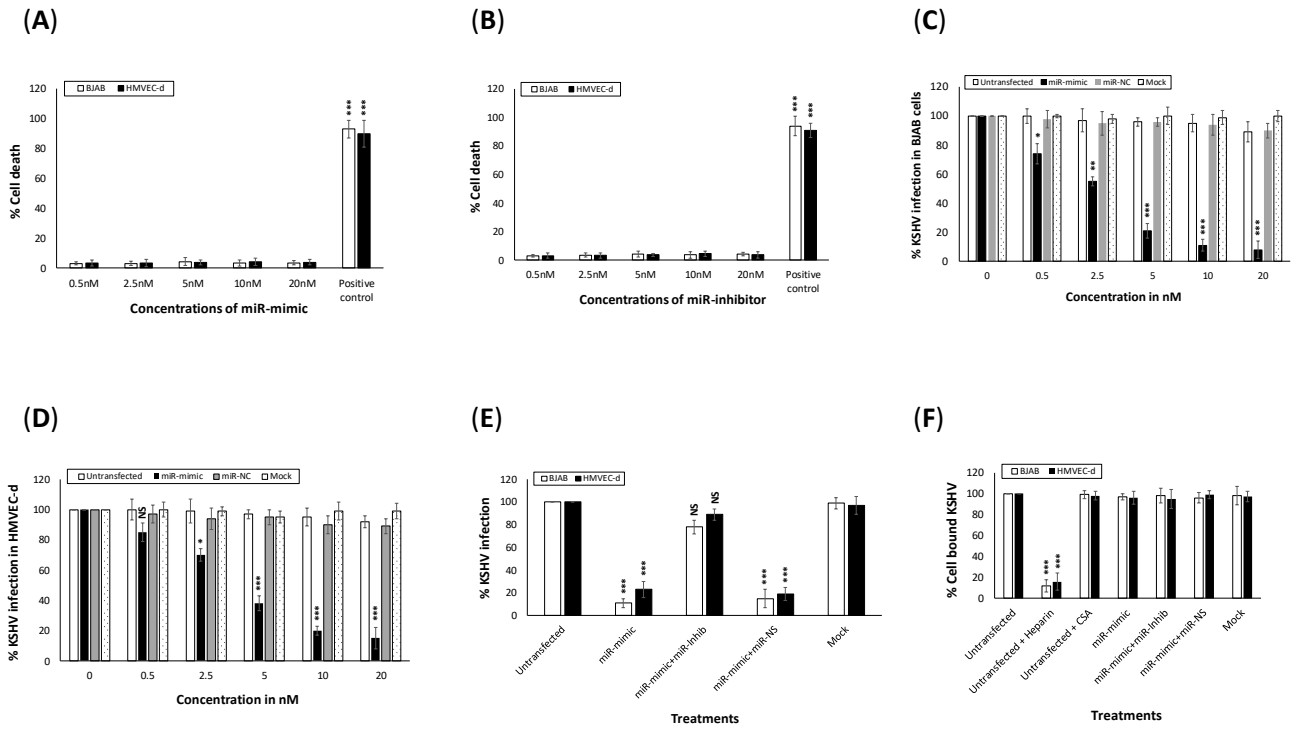
(A)
BJAB
HMVEC-d
% Cell death
0.5nM
2.5nM
5nM
10nM
20nM
Positive control
Concentrations of miR-mimic
(B)
BJAB
HMVEC-d
% Cell death
0.5nM
2.5nM
5nM
10nM
20nM
Positive control
Concentrations of miR-inhibitor
(C)
Untransfected
miR-mimic
miR-NC
Mock
% KSHV infection in BJAB cells
0
0.5
2.5
5
10
20
Concentration in nM
(D)
Untransfected
miR-mimic
miR-NC
Mock
% KSHV infection in HMVEC-d
NS
0
0.5
2.5
5
10
20
Concentration in nM
(E)
BJAB
HMVEC-d
% KSHV infection
NS
NS
Untransfected
miR-mimic
miR-mimic+miR-Inhib
miR-mimic+miR-NS
Mock
Treatments
(F)
BJAB
HMVEC-d
% Cell bound KSHV
Untransfected
Untransfected + Heparin
Untransfected + CSA
miR-mimic
miR-mimic+miR-Inhib
miR-mimic+miR-NS
Mock
Treatments

Figure 2

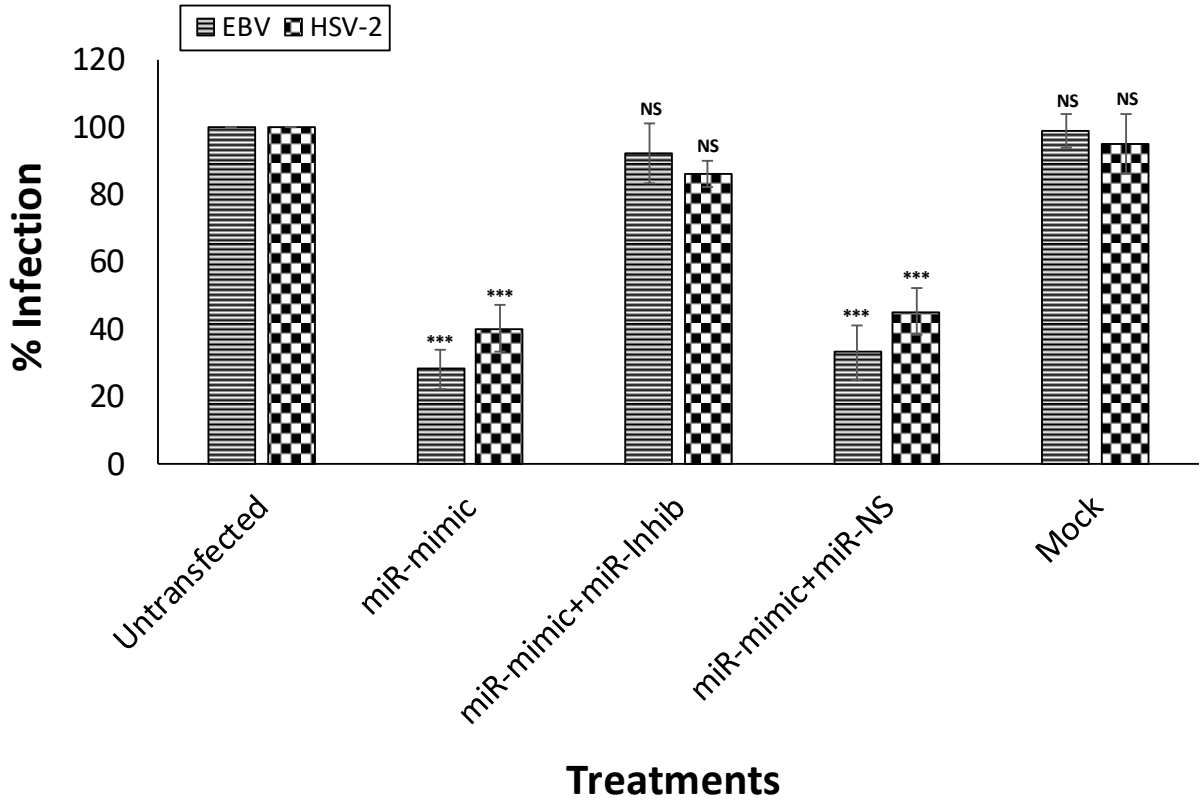
EBV
HSV-2
120
100
80
60
40
20
0
% Infection
NS
NS
NS
NS
***
***
***
***
Untransfected
miR-mimic
miR-mimic+miR-Inhib
miR-mimic+miR-NS
Mock
Treatments

Figure 3

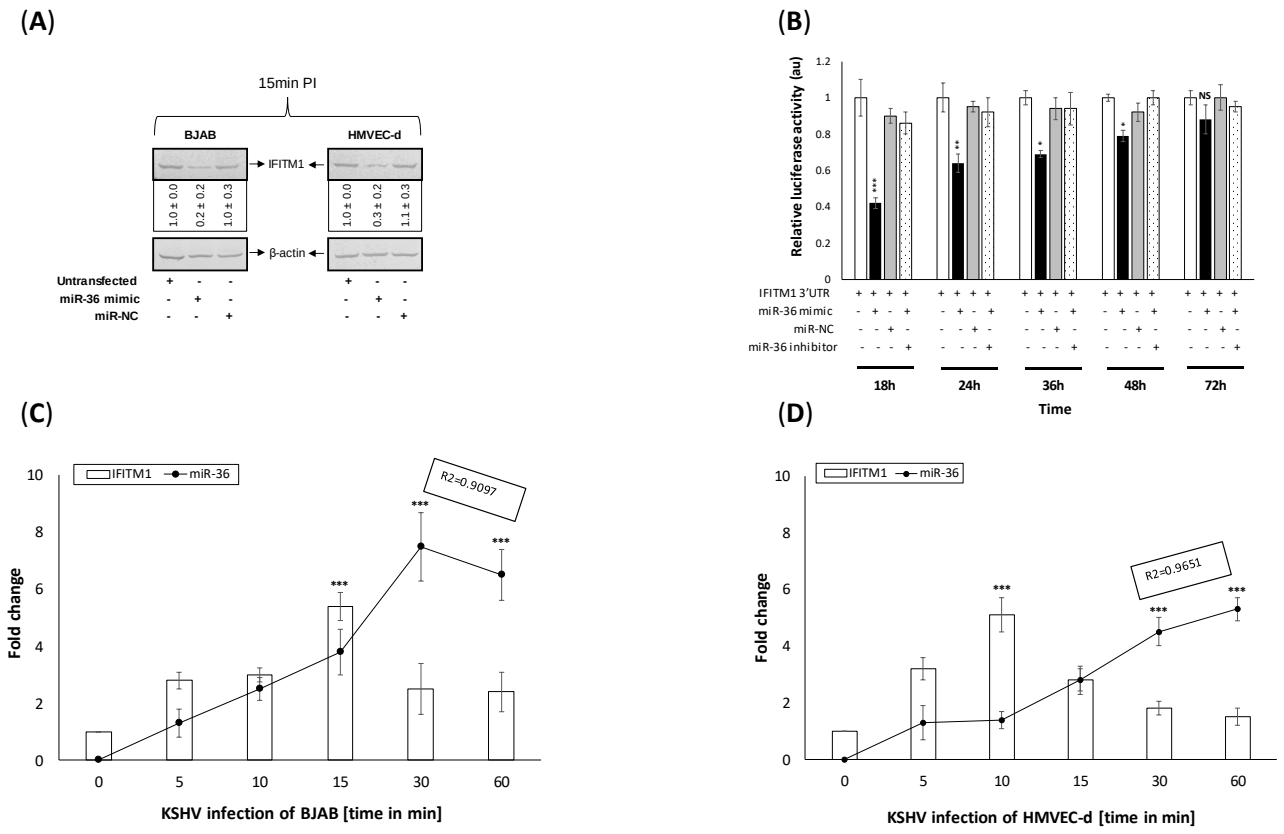
(A)
15min PI
BJAB
HMVEC-d
IFITM1
β-actin
1.0 ± 0.0
0.2 ± 0.2
1.0 ± 0.3
1.0 ± 0.0
0.3 ± 0.2
1.1 ± 0.3
Untransfected
miR-36 mimic
miR-NC
(B)
Relative luciferase activity (au)
IFITM1 3'UTR
miR-36 mimic
miR-NC
miR-36 inhibitor
NS
18h
24h
36h
48h
72h
Time
(C)
IFITM1
miR-36
R2=0.9097
Fold change
KSHV infection of BJAB [time in min]
(D)
IFITM1
miR-36
R2=0.9651
Fold change
KSHV infection of HMVEC-d [time in min]

Figure 4

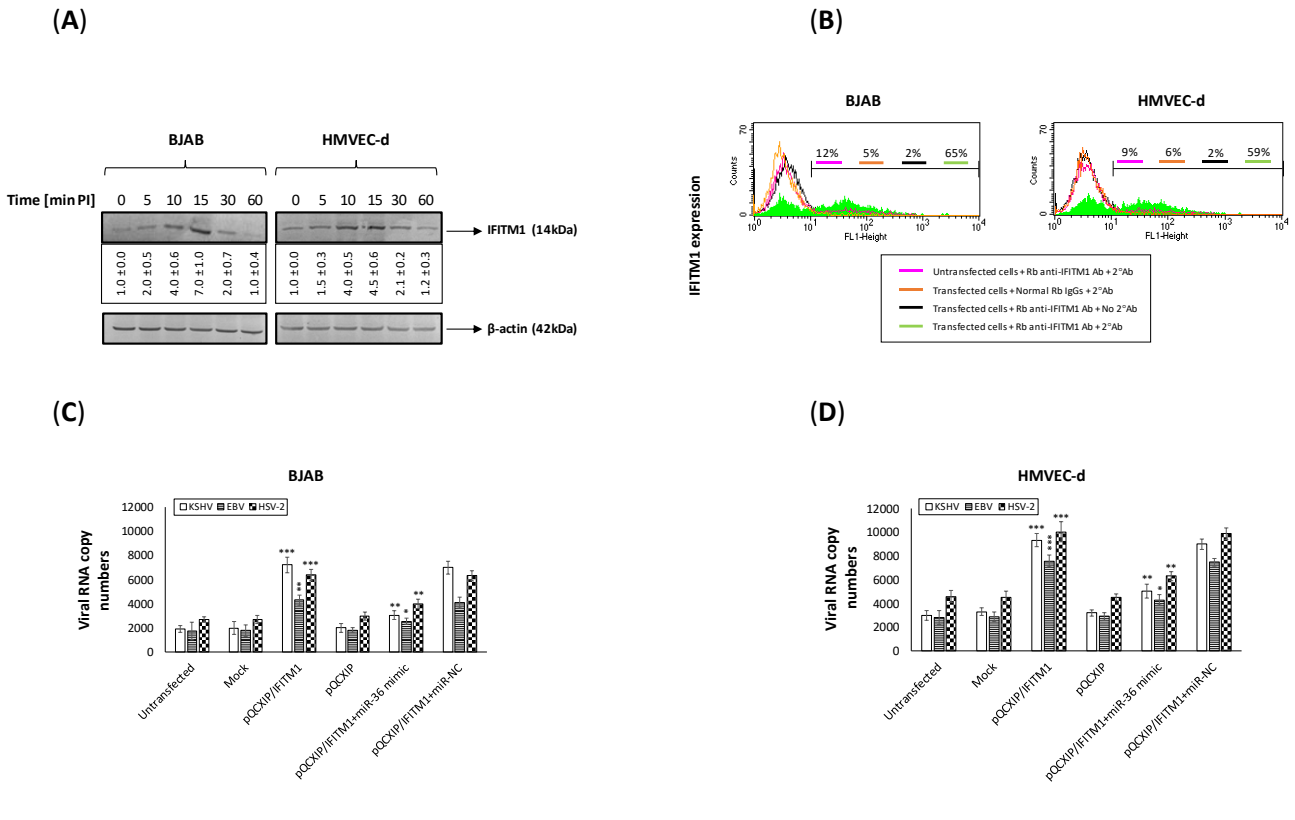
(A)
BJAB
HMVEC-d
Time [min PI]
0 5 10 15 30 60
0 5 10 15 30 60
IFITM1 (14kDa)
β-actin (42kDa)
1.0 ±0.0
2.0 ±0.5
4.0 ±0.6
7.0 ±1.0
2.0 ±0.7
1.0 ±0.4
1.0 ±0.0
1.5 ±0.3
4.0 ±0.5
4.5 ±0.6
2.1 ±0.2
1.2 ±0.3
(B)
BJAB
HMVEC-d
IFITM1 expression
Counts
FL1-Height
12%
5%
2%
65%
9%
6%
2%
59%
Untransfected cells + Rb anti-IFITM1 Ab + 2°Ab
Transfected cells + Normal Rb IgGs + 2°Ab
Transfected cells + Rb anti-IFITM1 Ab + No 2°Ab
Transfected cells + Rb anti-IFITM1 Ab + 2°Ab
(C)
BJAB
KSHV EBV HSV-2
Viral RNA copy numbers
Untransfected
Mock
pQCXIP/IFITM1
pQCXIP
pQCXIP/IFITM1+miR-36 mimic
pQCXIP/IFITM1+miR-NC
(D)
HMVEC-d
KSHV EBV HSV-2
Viral RNA copy numbers
Untransfected
Mock
pQCXIP/IFITM1
pQCXIP
pQCXIP/IFITM1+miR-36 mimic
pQCXIP/IFITM1+miR-NC

Figure 5

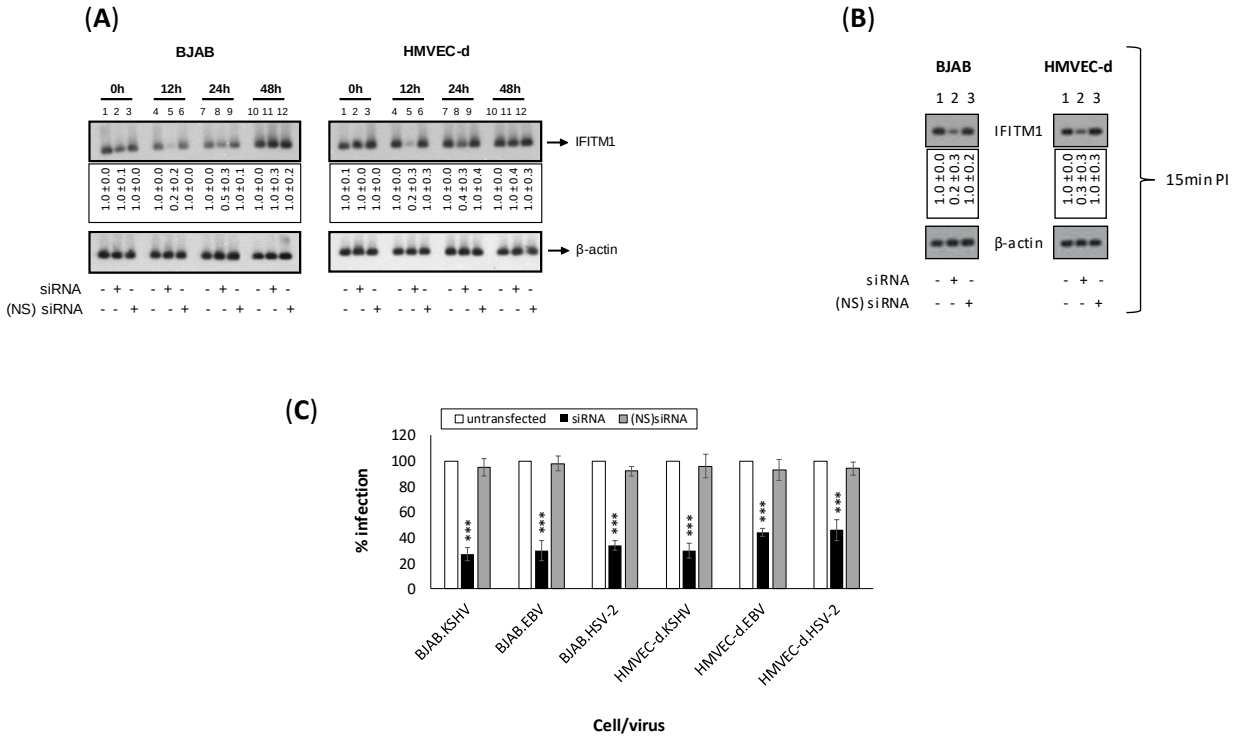
(A)
BJAB
HMVEC-d
0h
12h
24h
48h
IFITM1
β-actin
siRNA
(NS) siRNA
(B)
BJAB
HMVEC-d
IFITM1
β-actin
15min PI
siRNA
(NS) siRNA
(C)
untransfected
siRNA
(NS)siRNA
% infection
BJAB.KSHV
BJAB.EBV
BJAB.HSV-2
HMVEC-d.KSHV
HMVEC-d.EBV
HMVEC-d.HSV-2
Cell/virus

Figure 6

SUPPLEMENTAL DATA:

The supplementary data for this manuscript includes the following and they can be downloaded at the following link:

https://static-content.springer.com/esm/art%3A10.1038%2Fs41598-017-18225-w/MediaObjects/41598_2017_18225_MOESM1_ESM.pdf

SUPPLEMENTAL DATA

1. MATERIALS AND METHODS

Cell culture: BJAB cells were propagated in phenol red–free RPMI medium (Invitrogen, Carlsbad, CA) while HFF and 293 cells were cultured in Dulbecco modified Eagle medium (DMEM) containing 10% charcoal-stripped fetal bovine serum (FBS; Atlanta Biologicals, Lawrenceville, GA), L-glutamine, and antibiotics[80]. HMVEC-d cells were propagated in EGM MV-microvascular endothelial cell medium (Clonetics) as per standard protocols. The passage numbers for HFFs and HMVEC-ds used in this study ranged between 6 - 10, and 5 - 9, respectively (Akula et al., 2005).

Cytotoxicity assay

Target cells were treated with different concentrations of miR-36 mimic and inhibitor at 37°C in a V-bottom 96-well plate. After a 24h incubation, the cells were analyzed for the expression of LDH, as an indicator of cell death. The LDH assay was performed using the CytoTox 96 non-radioactive kit (Promega) as per earlier studies(Dyson et al., 2010). G418 (Sigma-Aldridge, St. Louis, MO) and cytochalasin D (Sigma-Aldridge) were used as known cell death inducers.

Virus infection of cells, RNA extraction, and monitoring virus infection

BJAB, HFF, and HMVEC-d cells were infected with 10 multiplicity of infection (MOI)(Hamden et al., 2004; Walker et al., 2014) of KSHV, EBV, and HSV-2. The cells were left uninfected or infected for 5, 10, 15, and 30min prior to washing the cells twice in PBS and processed appropriately for RNA extraction. Total RNA was extracted using TRIzol (Invitrogen, Carlsbad, CA). The RNA concentration was measured with a NanoDrop ND-2000 spectrophotometer (Thermo Fisher Scientific, Waltham, MA), and then verified for quality using an Agilent 2100 Bioanalyzer (Agilent Technologies, Santa Clara, CA). Only the RNA samples with 260/280 ratios of 1.8 to 2.0 were used in the study.

Extracted RNA was used to synthesize cDNA and the expression of *ORF50* was monitored by qRT-PCR using specific primers as per earlier studies(Dyson et al., 2010). Expression of *ORF50* was used as a scale to measure KSHV infection of cells. As reported earlier(Walker et al., 2014), the lowest limit of detection in the standard samples was 6–60 copies for the *ORF50* gene. The results from the use of *ORF50* primers were consistently confirmed by monitoring the expression of another viral immediate early (IE) gene, vGPCR (data not shown). EBV and HSV-2 infection was monitored using primers to BRLF1 (homolog of KSHV *ORF50*)(Robinson et al., 2011) and HSV-2 IE gene, US1(Kaneko et al., 2008).

Flow cytometry

Flow cytometry was used to monitor expression of IFITM1 in the cells. Briefly, target cells were fixed in 10ml of ice-cold acetone for 20min, washed thrice in PBS prior to incubating cells in 25µg/ml of rabbit polyclonal antibody to IFITM1 (EMD Millipore, Billerica, MA) for 60min at 4°C. The cells were washed thrice in PBS and further incubated with FITC conjugated appropriate secondary IgG at 4°C for 30 min, washed and analyzed in a FACScan flow cytometer (Becton Dickinson) with appropriate gating parameters.

Real-time *qRT-PCR* analysis of the expression of miRNAs

The quality of RNA was tested using a spectrophotometer. Only the RNA samples with 260/280 ratios of 1.8 to 2.0 were used in the study. Approximately 500ng of RNA was reverse transcribed in a 25µl reaction volume using the All-in-one^{TM} miRNA qRT-PCR detection kit (GeneCopoeia, Rockville, MD). Briefly, the cDNA was synthesized in a 25µl reaction mix containing 5µl of 5x reaction buffer, 2.5U/µl Poly A Polymerase, 10ng/µl MS2 RNA, and 1µl RTase Mix. The reaction was performed at 37°C for 60 min and terminated at 85°C for 5 min. cDNA that was produced in the RT reaction was diluted ten-fold and was used as the template for the PCR reaction in an Applied Biosystems ViiA 7 Real-Time PCR System (Life Technologies, USA). In this system, MS2 RNA was used as an external reference for the quality of the extracted miRNAs, and RNU6B, RNU44, RNU48, and RNU49 were used for normalization. The expression levels of miRNAs were measured employing qRT-PCR with the SYBR green detection and specific forward primer for the mature miRNA sequence and the universal adaptor reverse primer (GeneCopoeia, USA).

Silencing IFITM1 using siRNA

Expression of IFITM1 was inhibited by the transfection of double-stranded (ds) RNA oligos as per standard protocols(Akula et al., 2005). IFITM1 siRNA was purchased from Dharmacon RNA Technologies (Lafayette, CO). Briefly, 1 x 10^6 cells were washed twice in RPMI and incubated in phenol red–free RPMI supplemented with 5% FBS at 37°C. After 24 hours incubation (considered as 0h for experiments in **Fig. 6A**), the target cells were transfected with either ds short interfering RNAs (siRNAs) or the nonspecific (NS) controls using Fugene HD as per manufacturer's recommendations (Promega). At 0, 12, 24, and 48 hours after transfection, total RNA was isolated from the cells and subjected to Northern blotting to monitor the expression of IFITM1 and β-actin mRNA as per the protocol mentioned in the "Materials and methods" section describing Northern blotting. In another set of experiments, untransfected cells and cells

transfected with siRNA or (NS)siRNA for 12h were infected with 10 MOI of KSHV. At the end of 30min PI, KSHV infection was assessed by monitoring ORF50 expression by qRT-PCR.

2. SUPPLEMENTAL FIGURES:

Supplemental Figure 1. Secondary structures of Pre-mir-36. Structure was predicted using the RNAstructure software and base-pairing probability depicted in colors. miR-36 is located at 3p of the duplex (Reuter and Mathews, 2010).

Supplemental Figure 2. RNA hybrid analysis shows the miR-36 binding site located in 3'UTR of IFITM1 mRNA. This is predicted using DIANA and MiRmap algorithms (Paraskevopoulou et al., 2013; Vejnar and Zdobnov, 2012).

Supplemental Figure 3. Original Western blots of the data presented in Figure 4a.

Supplemental Figure 4. Original Western blots of the data presented in Figure 5a.

Supplemental Figure 5. Original Northern blots of the data presented in Figure 6a, b.

Supplemental Figure 6. Putative target genes for miR-36. miR-36 has been predicted to modulate expression of 25 target genes with confirmed roles during early stages of virus infection. DIANA and MiRamp tools was used for prediction of miR-36 target genes.

Supplemental Figure 7. IFITM1 and IFITM3 but not IFITM2 enhance KSHV infection of cells. BJAB, HMVEC-d, HFF and 293 cells were either untransfected, mock transfected, transiently transfected with pQCXIP/IFITM1, pQCXIP/IFITM2, pQCXIP/IFITM3, or pQCXIP prior to infecting with 10 MOI of KSHV. Data was plotted to represent the changes in KSHV-*ORF50*

RNA copy numbers at 30min PI. Bars represent average ± s.d. of five individual experiments. Student *t* test was performed to compare groups. Two-tailed P value of 0.05 or less was considered statistically significant. *p<0.05; **p,0.01; ***p<0.001; NS-not significant.

Supplemental Figure 8. KSHV infection of cells induce expression of IFNs in target cells. Expression of IFNs were detected by qRT-PCR at different time points post-infection in BJAB (**A**) and HMVEC-d (**B**) cells infected with 10 MOI of KSHV compared to uninfected cells. The qRT-PCR data was plotted for fold changes in the expression of IFNs in cells during the course of infection when compared to the uninfected cells. Bars represent average ± s.d. of five individual experiments. Student *t* test was performed to compare expression of IFNs in uninfected cells versus 15, and 30min PI. Two-tailed P value of 0.05 or less was considered statistically significant. **p,0.01; ***p<0.001.

CHAPTER 4: IFITM1 EXPRESSION IS CRUCIAL TO GAMMAHERPESVIRUS INFECTION, *IN VIVO*

Hosni A.M. Hussein[1€], Katarina Briestenska2[€], Jela Mistrikova[2], Shaw M. Akula[1*]

[1]Department of Microbiology & Immunology, Brody School of Medicine at East Carolina University, Greenville, NC 27834; [2]Department of Microbiology and Virology, Faculty of Natural Sciences, Comenius University in Bratislava, Mlynská dolina, SK-842 15 Bratislava, Slovak Republic.

This manuscript has been submitted:

Address correspondence to: Shaw M. Akula, Department of Microbiology & Immunology, Brody School of Medicine, East Carolina University, Greenville, North Carolina, USA 27834. Phone: (252)744-2702; Fax: (252) 744-3104; Email: akulas@ecu.edu

ABSTRACT

The oncogenic *gammaherpesviruses,* Epstein–Barr virus (EBV) and Kaposi's sarcoma herpesvirus (KSHV), are etiologically associated with a variety of human cancers, including Burkitt's lymphoma (BL), Hodgkin lymphoma (HL), Kaposi's sarcoma (KS), and primary effusion lymphoma (PEL). Recently, we demonstrated KSHV infection of B- and endothelial cells to significantly upregulate the expression of interferon induced transmembrane protein 1 (IFITM1) which in turn enhances virus entry [*Hussein and Akula, 2017*]. In this study, we determined EBV infection of cells to trigger IFITM1 expression, *in vitro*. Silencing IFITM1 expression using siRNA specifically lowered *gammaherpesvirus* infection of cells at a post binding stage of entry. A natural model system to explore the effect of IFITM1 on *gammaherpesvirus* infection *in vivo* is infection of BALB/c mice with murine gammaherpesvirus 68 (MHV-68). Priming mice with siRNA specific to IFITM1 significantly lowered MHV-68 titers in the lung specimens compared to priming with (NS)siRNA or PBS. MHV-68 titers were monitored by plaque assay and qPCR. Taken together, for the first time, this study provides insight into the critical role of IFITM1 to promoting *in vitro* and *in vivo* infection of EBV and KSHV.

INTRODUCTION

Kaposi's sarcoma-associated herpesvirus (KSHV) is the etiological agent of Kaposi's sarcoma (KS), the most common cancer afflicting HIV-infected individuals (Chang et al., 1994). KSHV is also associated with two other B cell lymphoproliferative disorders: primary effusion lymphoma (PEL) and multicentric Castlesman disease (MCD) (Hamden et al., 2005). KSHV belongs to the *γ-herpesvirinae* subfamily (genus *Rhadinovirus*) and was first described in 1994 (Chang and Moore, 2014; Neipel and Fleckenstein, 1999). KSHV is among the list of viral pathogens estimated to cause 12-25% of human cancers worldwide (La Ferla et al., 2013; Morrison et al., 2015).

KSHV internalization is a highly orchestrated but complicated event yet to be thoroughly understood. The initial step in the virus entry process is the reversible step of binding or attachment to the target cells (Akula et al., 2001b). This step is primarily achieved by KSHV interacting with the ubiquitously expressed cell surface receptor, heparan sulfate (HS) (Akula et al., 2001a; Akula et al., 2001b). The attachment to cells enables KSHV to interact with entry promoting receptors allowing the virus to eventually enter the cell (Akula et al., 2002; Hahn et al., 2012). In a recent study, we determined that interferon (IFN)-induced transmembrane-1 (IFITM1) expression to significantly enhance KSHV infection of human B and endothelial cells (Hussein and Akula, 2017a). In opposition to this process, over-expression of microRNA (miRNA)-36 (miR-36) significantly lowered expression of IFITM1 and thus the virus entry. We concluded IFITM1 to play a role in promoting early stages of KSHV infection of cells, *in vitro*.

Over the past few years, several novel genes downstream of type I IFN signaling that inhibit infection by individual or multiple families of viruses have been described. There are two genetically and functionally distinct families of interferon stimulated genes (ISGs) that have antiviral properties, they are IFN-induced proteins with tetratricopeptide repeats (IFIT) and IFITMs. IFITs contribute to an antiviral state against some viruses by binding components of the eIF3 translation initiation complex and inhibiting protein translation (Guo et al., 2000). In

contrast, IFITMs block viral infection at the entry stage (Lu et al., 2011). IFITMs are a double-edged sword when it comes to influencing viral entry; they can also enhance viral entry (Hussein and Akula, 2017a; Warren et al., 2014; Zhao et al., 2014). Interestingly, IFITM1 expression not only enhanced KSHV infection of cells, but also infection of cells with a closely related herpesvirus belonging to the *γ-herpesvirinae* subfamily, Epstein-Barr virus (EBV) (Hussein and Akula, 2017a).

Both KSHV and EBV are the most relevant human *γ-herpesviruses*. Therefore, we conducted further studies to confirm the role of IFITM1 in KSHV and EBV infections, *in vitro* and *in vivo*. For *in vivo* studies, we used murine γ-herpesvirus 68 (MHV-68), that serves as a good model to understand *γ-herpesvirus* (KSHV and EBV) pathogenesis (Leang et al., 2011; Steer et al., 2010). Herein, we provide pioneering evidence to demonstrate a key role for IFITM1 in the *in vitro* and *in vivo* infection of *γ-herpesviruses*.

MATERIALS AND METHODS

Cells

Human Burkitt lymphoma B cell line (BJAB) was used in this study. BJAB cells were propagated in phenol red–free RPMI medium (Invitrogen, Carlsbad, CA) containing 10% charcoal-stripped fetal bovine serum (FBS; Atlanta Biologicals, Lawrenceville, GA), L-glutamine, and antibiotics (Akula et al., 2005). The cells used in this study were negative for mycoplasma as tested by *Mycoplasma* PCR ELISA (Roche Life Science, Indianapolis, IN).

Virus and mice

The viruses used in this study were wild-type KSHV (Dyson et al., 2010), EBV (Bentz et al., 2010), and MHV-68 (Ancicova et al., 2015). Female 6-week-old inbred BALB/c mice supplied by the Faculty of Veterinary Medicine, Brno, Czech Republic were used in this study.

Virus infection of cells, RNA and DNA extraction, and monitoring virus infection

BJAB cells were infected with 10 multiplicity of infection (MOI) of KSHV and EBV. The cells were left uninfected or infected for 5, 10, 15, and 30min prior to washing the cells twice in PBS and processed appropriately for RNA and DNA extraction. Total RNA was extracted using TRIzol (Invitrogen, Carlsbad, CA). The RNA concentration was measured with a NanoDrop ND-2000 spectrophotometer (Thermo Fisher Scientific, Waltham, MA), and then verified for quality using an Agilent 2100 Bioanalyzer (Agilent Technologies, Santa Clara, CA). Only the RNA samples with 260/280 ratios of 1.8 to 2.0 were used in the study. Viral DNA was extracted by isolating total genomic DNA and determining the internalized virus particles by qPCR (Walker et al., 2016).

Extracted RNA was used to synthesize cDNA and the expression of *ORF50* was monitored by qRT-PCR using specific primers as per earlier studies (Dyson et al., 2010). Expression of *ORF50* was used as a scale to measure KSHV infection of cells. As reported earlier (Walker et al., 2014), the lowest limit of detection in the standard samples was 6–60 copies of the *ORF50* gene. The results from the use of *ORF50* primers were consistently confirmed by monitoring the expression of another viral immediate early (IE) gene, vGPCR (data not shown). EBV infection was monitored using specific primers to *BRLF1* (homolog of KSHV *ORF50*) (Robinson et al., 2011).

Transfection of cDNA

Target cells were transiently transfected with plasmid DNA using FuGene HD (Promega, Madison, WI) as per manufacturer's recommendations. The plasmid, pQCXIP encoding IFITM1, used in this study was kindly gifted to us by Dr. Michael Farzan (The Scripps Research Institute, Jupiter, USA). FuGene HD/DNA ratios of 3:1 for adherent cell lines and 6:1 for suspension cell lines were used. These were transient transfections and experiments using these cells were conducted 48h post transfection.

In vitro silencing IFITM1 using siRNA

Expression of IFITM1 was inhibited by the transfection of double-stranded (ds) RNA oligos as per standard protocols (Hussein and Akula, 2017a). IFITM1 siRNA was purchased from Dharmacon RNA Technologies (Lafayette, CO). Briefly, untransfected cells and cells transfected with siRNA or (NS)siRNA for 12h were infected with 10 MOI of KSHV. At the end of 30min PI, KSHV infection was assessed by monitoring *ORF50* expression by qRT-PCR.

Binding assay

The effect of IFITM1 on KSHV binding to target cells was assessed by PCR detecting the cell-bound KSHV DNA. Briefly, untransfected cells or cells transfected with (NS)siRNA, or siRNA specific to IFITM1 were infected with 10MOI of KSHV at +4°C. After 60min of incubation with virus, cells were washed three times with PBS to remove the unbound virus. Cells were pelleted, and total DNA including those representing the cell bound KSHV was isolated using DNeasy kit (Qiagen, Valencia, CA) and subjected to qPCR analysis monitoring *ORF50* according to recently published work (Walker et al., 2014). Incubating KSHV with 100µg/ml of heparin and chondroitin sulfate A (CSA; Sigma-Aldridge) for 1h at 37°C were used as known positive and negative controls.

Animal studies

Animal studies using BALB/c mice was performed to understand the effects of IFITM1 on γ-herpesviruses, *in vivo*. Briefly, five groups of mice (n=5/group) used in this study were (i) virus free or uninfected; (ii) MHV-68 infected; (iii) IFITM1 siRNA primed + MHV-68 infected; (iv) (NS)siRNA primed + MHV-68 infected; and (v) PBS primed + MHV-68 infected. The experimental design is detailed in the schematic (**Fig. 1**). Mice were primed with PBS, 20µg/mouse of IFITM1-siRNA, or (NS)siRNA on day 0 by tail vein injection. The uninfected and

the MHV-68 infected groups were left untreated. On day 02, only groups (iii), (iv), and (v) were tail vein-injected with IFITM1 siRNA, (NS)siRNA, and PBS, respectively. After this step, animals in groups (ii), (iii), (iv), and (v) were intranasally (i.n) infected with 2 x 10^4 PFU (20µl) of MHV-68. On day 04, the animals in groups (iii), (iv), and (v) received tail vein injections of IFITM1 siRNA, (NS)siRNA, and PBS, respectively; while animals in groups (i) and (ii) were left undisturbed. On day 06, mice were sacrificed and lungs were collected. Relative IFITM1 gene expression was calculated using the $2^{-\Delta\Delta C_T}$ method (Schmittgen and Livak, 2008), using β-actin mRNA expression as reference gene and the virus free group as the calibrator. Plaque assay (Stiglincova et al., 2011) and qPCR (Hajnicka et al., 2017) was conducted to determine MHV-68 infection of lungs.

All animal experiments were performed according to the European Union standards, and fundamental ethical principles including animal welfare requirements were respected. All experiments were done with the approval of State Veterinary and Food Administration of the Slovak Republic (2937/10221).

RESULTS

Infection of BJAB cells with *γ-herpesviruses* induce expression of IFITM1.

In a recently concluded study, we demonstrated the ability of KSHV to induce IFITM1 expression during early stages of infection (Hussein and Akula, 2017a). In the present study, we analyzed the effect of another closely related *γ-herpesvirus*, EBV, on IFITM1 expression. IFITM1 transcript (**Fig. 2A**) and protein expression (**Fig. 2B**) levels were significantly elevated with EBV and KSHV infection of BJAB cells. The expression of IFITM1 increased in virus infected cells as early as 5min PI which was elevated by 10min and 15min PI in BJAB, but significantly declined by 30 min PI (**Fig. 2**).

IFITM1 expression is a necessity for *γ-herpesvirus* infection of cells.

In a recently concluded study, we demonstrated a crucial role for IFITM1 expression in KSHV infection of cells. This was possible by monitoring the expression of *ORF50* transcript as a measure of infection. In the current study, we analyzed internalization of the *γ-herpesviruses* by monitoring the internalized viral DNA compared to the expression of *ORF50* and *BRLF-1* transcripts. BJAB cells (**Fig. 3A**) expressing IFITM1 supported a significantly enhanced KSHV infection compared to those cells that were left untransfected, mock transfected, or transfected with the empty vector. To authenticate the role for IFITM1 in enhancing infection of *γ-herpesviruses*, we tested the effect of silencing IFITM1 on the internalization of the viruses. Briefly, we first transfected cells with siRNA specific for IFITM1. Northern blotting was performed at 0, 12, 24, and 48 hours after transfection as per the standard protocols to monitor IFITM1 mRNA expression. A maximum IFITM1 mRNA inhibition was observed in cells transfected with siRNA specific to IFITM1 at 12h post transfection (Hussein and Akula, 2017a). On the same lines, internalized *γ-herpesviruses* in cells silenced for the expression of IFITM1 was significantly lower compared to cells that were untransfected or transfected with (NS)siRNA (**Fig. 3B**). The expression of viral transcripts *BRLF-1* and *ORF50* for EBV and KSHV, respectively, was also decreased in cells transfected with siRNA specific to IFITM1 compared to (NS)siRNA. Taken together, the results clearly implicate a role for IFITM1 in enhancing KSHV, and EBV infection of cells.

IFITM1 enhances virus infection at a post-attachment stage.

To enumerate the role of IFITM1 on binding of viruses to target cells, we used untransfected or BJAB cells transfected with siRNA to IFITM1, or (NS)siRNA. These cells were used in binding assays. The binding assay performed on BJAB cells demonstrated that the transfection of cells with (NS)siRNA or siRNA specific to IFITM1 did not block KSHV and EBV from binding the

target cells (**Fig. 4A**). Incubating KSHV with heparin but not CSA significantly blocked KSHV and EBV from binding cells (**Fig. 4A**). This data was confirmed by electron microscopy by monitoring KSHV **(Fig. 4B)** and EBV (data not shown) binding to BJAB cells. Based on these results, we concluded IFITM1 to alter virus infection at a post-attachment stage of entry.

Silencing IFITM1 expression in BALB/c mice lowered MHV-68 infection.

MHV-68 is regarded as a substitute for human *γ-herpesvirus* and has been widely used in *in vivo* studies [46, 72, 77]. We used mouse siRNA specific to IFITM1 to appreciate the effect of IFITM1 on MHV-68 infection, *in vivo*, using BALB/c mice. Priming mice with siRNA specific to IFITM1 significantly lowered expression of IFITM1 in the lungs of the mice compared to (NS)siRNA (**Fig. 5A**). Our data demonstrates a significant increase in the leukocyte count in mice that were infected with MHV-68 compared to the uninfected mice (**Table 1**). The leukocyte count in infected mice that were primed with siRNA specific to IFITM1 was significantly lower compared to those that were primed with PBS or (NS)siRNA. We did not notice atypical lymphoid monocytes in these animals.

MHV-68 infection of mice was monitored by the traditional plaque assay. Plaque assay could detect MHV-68 in lungs of the infected mice (**Fig. 5B**). MHV-68 infection was significantly inhibited in the mice that were primed with siRNA specific to IFITM1 compared to those that were primed with (NS)siRNA or PBS (**Fig. 5B**). The results were confirmed by performing qRT-PCR (**Fig. 5C**). Taken together, silencing the expression of IFITM1 significantly hampered MHV-68 infection of mice.

DISCUSSION

Many different types of cellular sensors can detect viruses and induce the expression of the type I interferons (IFNs)—IFN-α and IFN-β. Type I IFNs bind to the ubiquitously expressed IFNAR (IFN-α/β receptor), activating the JAK/STAT pathway (Donlin et al., 2014; Ivashkiv and

Donlin, 2014). The type I IFN response can induce the expression of hundreds of interferon stimulated genes (ISGs) which primarily serve to limit further virus spread and infection (Schneider et al., 2014). IFITMs are a family of proteins that have gained popularity as novel antiviral ISGs (Weidner et al., 2010). IFITMs are a member of the interferon-induced 125–133 aa protein family including IFITM1, IFITM2, IFITM3, IFITM5 and IFITM10. This family of proteins is located on chromosome 11 of the human genome and originally described as highly inducible genes by α- and γ-interferons (IFNs) (Friedman et al., 1984; Hickford et al., 2012; Reid et al., 1989). IFITM proteins are significantly upregulated by type I and II IFNs and are critical for anti-viral innate immune responses (Brass et al., 2009; Deblandre et al., 1995; Evans et al., 1990; Smith et al., 2006). Recent reports indicate IFITMs play a significant role in virus entry. IFITMs inhibits entry of many RNA viruses including influenza A H1N1 Virus, West Nile Virus, Dengue Virus, HIV, and HCV (Brass et al., 2009; Narayana et al., 2015; Yu et al., 2015a). However, IFITMs can also enhance viral infection of cells: (i) both IFITM1 and IFITM3 modestly enhance human papillomavirus 16 (HPV-16) infection of a variety of cells (Warren et al., 2014); (ii) Zhao et al have shown type I IFN-α, IFN-γ, and type II IFN-λ to significantly promote infection of human coronavirus, HCoV-OC43 by the induction of IFITM proteins. The authors reported that the over-expression of IFITM3 significantly increased susceptibility of Huh7.5 cells to HCoV-OC43 infection (Zhao et al., 2014); and (iii) Inhibition of IFITM1 expression by specific miR-36 mimic significantly inhibited early stages of KSHV infection of human B and endothelial cells (Hussein and Akula, 2017a). In general, the IFITM family of proteins affects virus entry of cells.

In the current study, we demonstrated that EBV, another *γ-herpesvirus*, induces IFITM1 expression during the early stages of infection and it followed an identical pattern as that of KSHV (**Fig. 2**). We went one step further in demonstrating that either over-expressing or silencing the expression of IFITM1 significantly alter not only the internalization of the *γ-herpesviruses* (**Fig. 3A**) but also the ability to establish infection as monitored by the expression

of the respective viral transcripts (**Fig. 3B**). IFITM1 promotes *γ-herpesvirus* infections at a post-binding stage of entry as silencing IFITM1 did not alter the KSHV and EBV binding to the cell surfaces (**Fig. 4**).

A natural model system to investigate *γ-herpesvirus*-host interactions is the infection of mice with MHV-68, a natural pathogen of wild rodents (Barton et al., 2011; Cipkova-Jarcuskova et al., 2013). Therefore, to understand the *in vivo* effects of IFITM1 on *γ-herpesviruses*, we used MHV-68 as a model virus. Leukocyte counts were increased in response to MHV-68 infection of mice (**Table 1**). This increase in the leukocyte count was significantly lowered when the mice were primed with siRNA compared to (NS)siRNA and PBS. We did not observe atypical lymphoid monocytes in the mice from all the groups used as it was too early to observe any such changes. Priming mice with siRNA specific to IFITM1 significantly lowered expression of IFITM1 in lungs compared to PBS, (NS)siRNA (**Fig. 5A**). It was determined by plaque assay and qPCR that a decrease in the expression of IFITM1 resulted in a significant decrease in MHV-68 infection of lungs obtained from the mice (**Fig. 5B, C**). This study focused primarily in monitoring infection of lungs because intranasal MHV-68 infection of mice results in acute lytic infection of lungs followed by the establishment of lifelong latency (Flano et al., 2000). Taken together, we demonstrate for the first time a crucial role for IFITM1 in the *in vivo* infection of *γ-herpesviruses.*

The results from this study puts forth crucial questions in terms of better understanding the role of IFITM1 in altering entry of *γ-herpesviruses.* Numerous mechanisms by which IFITM proteins alter virus entry have been proposed and it is not limited to the following: (i) acting as pattern recognition receptors by sensing virus infection and activation of downstream cellular signaling pathways (Brass et al., 2009); and (ii) reducing membrane fluidity and curvature, and by possibly disrupting intracellular cholesterol homeostasis (Amini-Bavil-Olyaee et al., 2013; Li et al., 2013a). Albeit, none of the mechanisms have been confirmed. Future studies will be

aimed at delineating that eluding mechanism by which IFITM1 enhance the internalization of the *γ-herpesviruses.* These studies are crucial because they help us understand the role of ISGs in modulating *γ-herpesvirus* infection of cells. In addition, the results from this study will benefit in designing IFITM1 targeted therapies to treat cancers (Borg et al., 2016; Lui et al., 2017), and *γ-herpesvirus* infections including that of HIV (Raposo et al., 2017) and HCV (Wilkins et al., 2013).

Conflict of interest

The authors declare no conflict of interest.

Ethical approval

This article does not contain any studies with human participants.

All animal experiments were performed according to the European Union standards, and fundamental ethical principles including animal welfare requirements were respected. All experiments were done with the approval of State Veterinary and Food Administration of the Slovak Republic (2937/10221).

FIGURE LEGENDS:

Figure 1. Schematic depicting the animal study design. The study was approved by the State Veterinary and Food Administration of the Slovak Republic (2937/10221) and strictly followed the European Union standards.

Figure 2. Infection of BJAB cells with EBV and KSHV induce expression of IFITM1. (**A**) The relative expression of IFITM1 in EBV or KSHV infected BJAB cell was monitored by qRT-PCR. The expression was measured in terms of cycle threshold value (Ct) and normalized to expression of β-actin. The *x-axis* denotes the time point post virus infection in minutes and the *y-axis* denotes fold change in expression of IFITM1. (**B**) Western blotting analysis demonstrates EBV or KSHV infection of BJAB cells to increase IFITM1 protein levels. Expression of IFITM1 levels was normalized to β-actin protein levels. Data representing the IFITM1 protein expression levels are presented as fold increase (average ± s.d. from three experiments) in the boxes below the panels. Bars **(A)** represent average ± s.d. of five individual experiments. Columns with different alphabets indicate the values to be statistically significant ($p < 0.05$) by least significance difference (LSD).

Figure 3. IFITM1 expression is a necessity for EBV and KSHV infection of cells. (A) Overexpression of IFITM1 enhances EBV and KSHV infection of cells. BJAB cells were untransfected, mock transfected, transiently transfected with pQCXIP/IFITM1, or pQCXIP prior to infecting with 10 MOI of EBV or KSHV. **(B)** Silencing the expression of IFITM1 by siRNA significantly decreased EBV and KSHV infection of cells. BJAB cells were either un-transfected, transfected with IFITM1-specific siRNA, or transfected with non-specific (NS) siRNA before infecting with KSHV, or EBV. Data was plotted **(A, B)** to represent the percentage of virus infection as determined by monitoring the change in copy numbers of viral DNA or RNA copy numbers of *BRLF1* and *ORF50* of EBV and KSHV respectively. Bars represent average ± s.d.

of five individual experiments. Columns with different alphabets indicate the values to be statistically significant ($p < 0.05$) by LSD.

Figure 4. IFITM1 enhancement of EBV and KSHV infection of cells is at a post-attachment stage of virus entry. (A) EBV and KSHV binding to BJAB cells were monitored in cells that were untransfected, untransfected and treated with heparin or CSA, or transiently transfected with IFITM1-specific siRNA, or transfected with non-specific (NS) siRNA. Data was plotted to represent the percentage of EBV or KSHV binding to BJAB cells treated differently compared to the untransfected cells. **(B)** Representative electron micrographs of KSHV binding to BJAB cells is depicted. KSHV allowed to bind at 4°C to BJAB cells that were untransfected, or transiently transfected with IFITM1-specific siRNA, or (NS) siRNA. After 60min cells were fixed with 2% glutaraldehyde. Thin sections were examined by transmission electron microscopy. Enveloped virus particles bound to the BJAB cells surfaces are indicated by the arrows. Magnification: 82,000X (solid bar denotes 500nm). Bars **(A)** represent average ± s.d. of five individual experiments. Columns with different alphabets indicate the values to be statistically significant ($p < 0.05$) by LSD.

Figure 5. Silencing IFITM1 expression in BALB/c mice lowered MHV-68 infection. The four groups of mice (n=5/group) that were used in this study are as follows: (i) uninfected; (ii) MHV-68 infected; (iii) IFITM1 siRNA primed + MHV-68 infected; (iv) (NS)siRNA primed + MHV-68 infected; and (v) PBS primed + MHV-68 infected. On 7dPI, expression of (**A**) IFITM1 or (**B, C**) virus titer by (**B**) plaque assay and (**C**) qPCR was determined. (**B**) Replication of the MHV-68 in the lungs of the Balb/c mice (n=5) was determined by plaque assay on Vero cells. The data represent the mean ± SD of three independent experiments, each performed in duplicates. The results are expressed as relative ratios of plaque numbers in MHV-68 infected mice primed with siRNA, (NS)siRNA, or PBS treated groups to that in the MHV-68 infected group (virus control,

100%). Bars (**A, B, and C**) represent average ± s.d. of five mice. Columns with different alphabets indicate the values to be statistically significant ($p < 0.05$) by LSD.

Table 1: Leukocyte count in the experimental groups:

Groups (n=7)	Number of leukocytes per 1 µl of blood
Uninfected	11633 ± 1500
MHV-68	14480 ± 1943
siRNA + MHV-68	11031 ± 2179
(NS)siRNA + MHV-68	14520 ± 2431
PBS + MHV-68	14729 ± 1735

DESIGN to study the role of IFITM1 on MHV-68 infection of mice

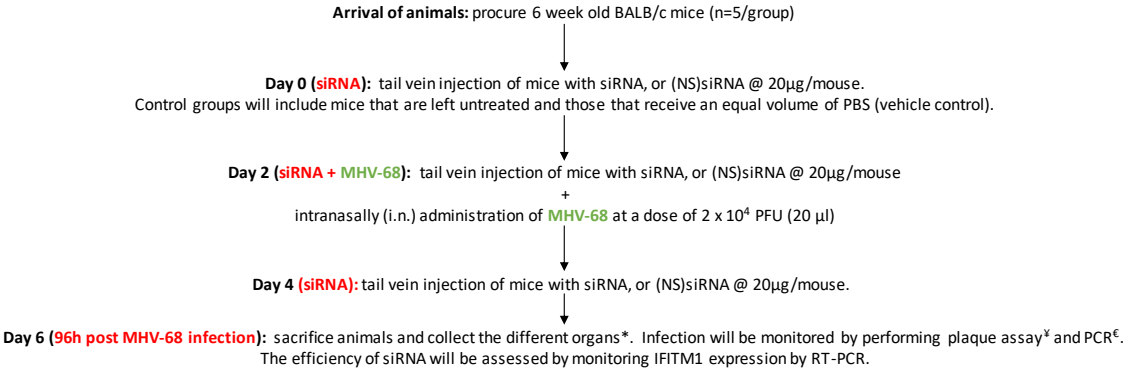

***Organ collected:** lungs.

Groups of mice:
(i) Uninfected
(ii) MHV-68
(iii) siRNA + MHV-68
(iv) (NS)siRNA + MHV-68
(v) PBS + MHV-68

Figure 1

(A)

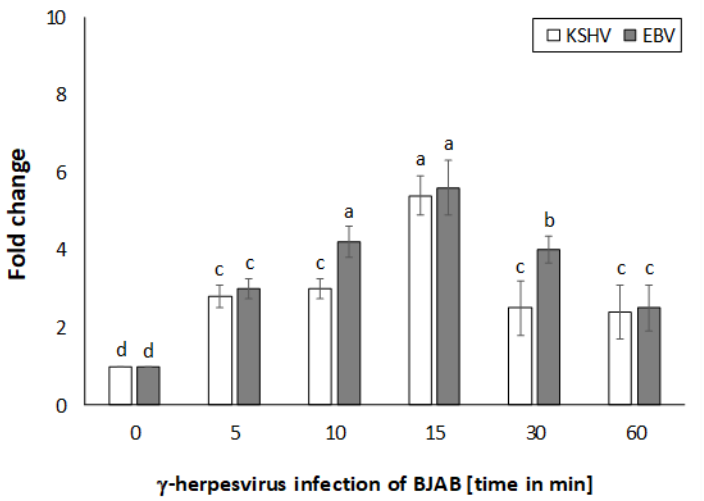
KSHV
EBV
Fold change
10
8
6
4
2
0
d d
c c
c a
a a
c b
c c
0
5
10
15
30
60
γ-herpesvirus infection of BJAB [time in min]

(B)

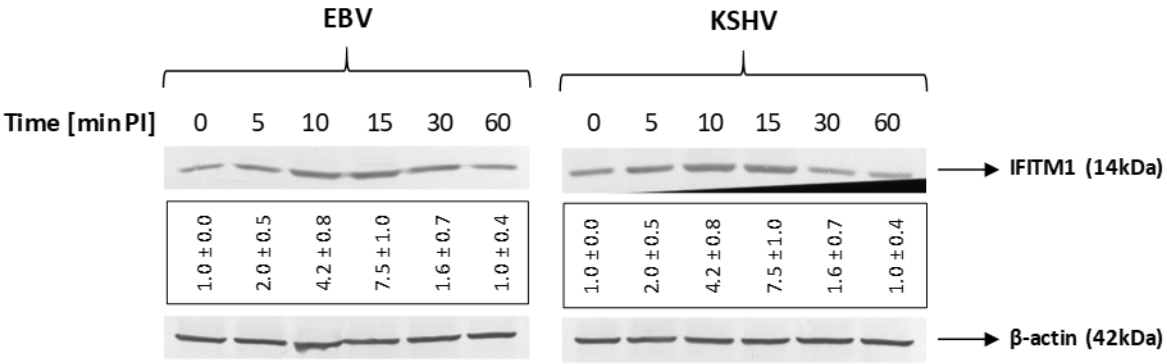
EBV
KSHV
Time [min PI]
0 5 10 15 30 60
0 5 10 15 30 60
IFITM1 (14kDa)
1.0 ± 0.0
2.0 ± 0.5
4.2 ± 0.8
7.5 ± 1.0
1.6 ± 0.7
1.0 ± 0.4
β-actin (42kDa)

Figure 2

(**A**)

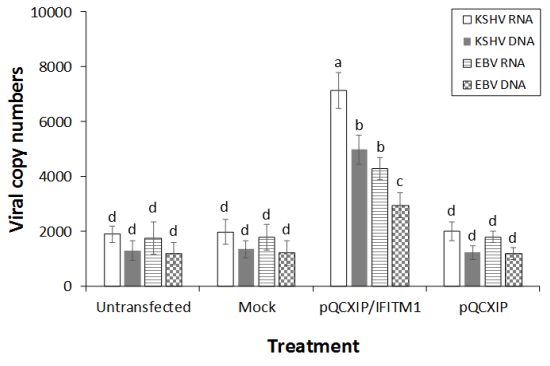
10000
8000
6000
4000
2000
0
Viral copy numbers
KSHV RNA
KSHV DNA
EBV RNA
EBV DNA
Untransfected
Mock
pQCXIP/IFITM1
pQCXIP
Treatment

(**B**)

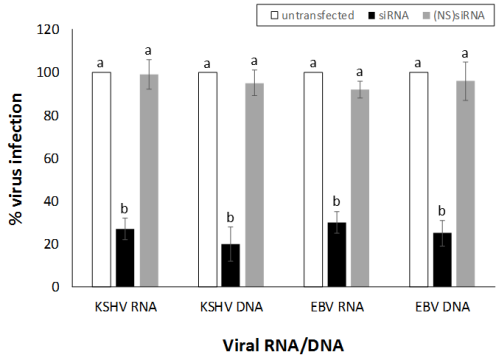
untransfected
siRNA
(NS)siRNA
120
100
80
60
40
20
0
% virus infection
KSHV RNA
KSHV DNA
EBV RNA
EBV DNA
Viral RNA/DNA

Figure 3

(**A**)

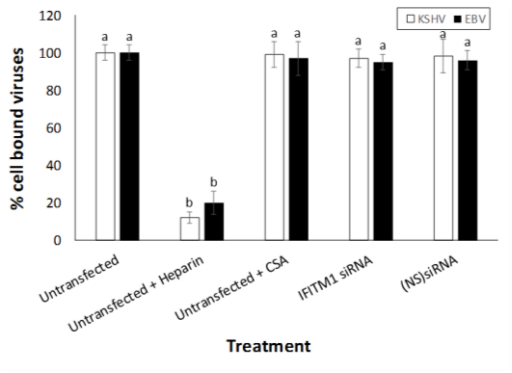
KSHV
EBV
% cell bound viruses
120
100
80
60
40
20
0
a
b
Untransfected
Untransfected + Heparin
Untransfected + CSA
IFITM1 siRNA
(NS)siRNA
Treatment

(**B**)

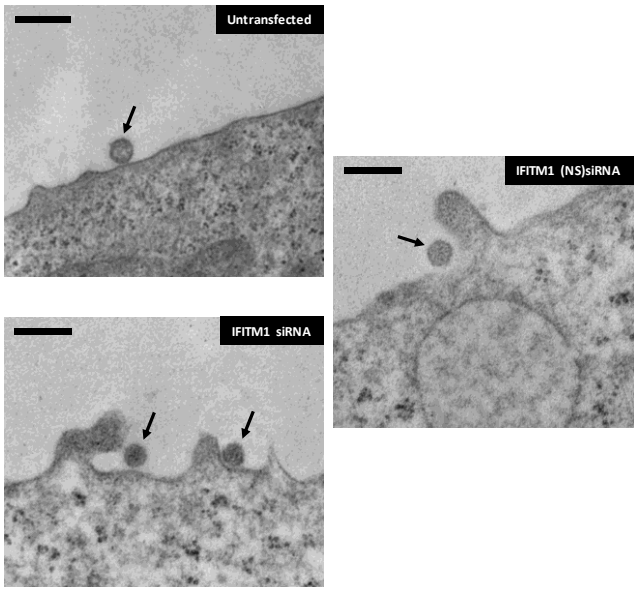
Untransfected
IFITM1 (NS)siRNA
IFITM1 siRNA

Figure 4

(A)

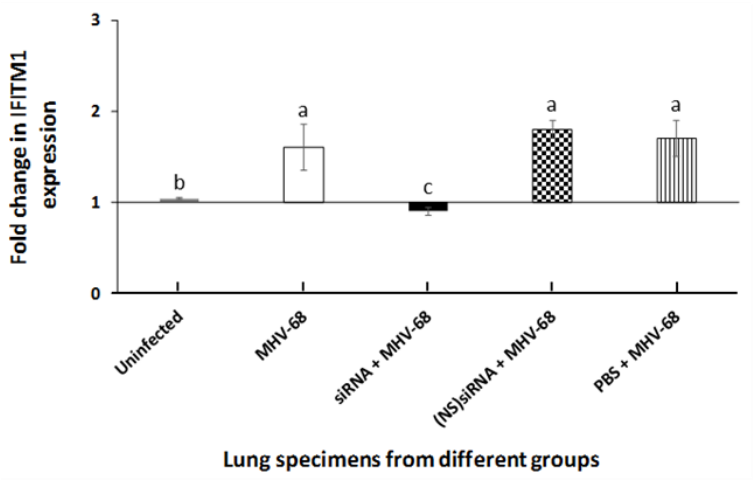
Fold change in IFITM1 expression
3
2
1
0
a
b
c
a
a
Uninfected
MHV-68
siRNA + MHV-68
(NS)siRNA + MHV-68
PBS + MHV-68
Lung specimens from different groups

(B)

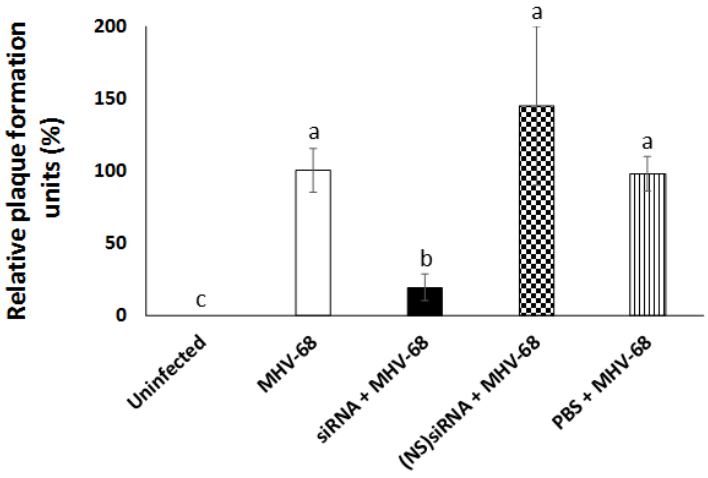
Relative plaque formation units (%)
200
150
100
50
0
c
a
b
a
a
Uninfected
MHV-68
siRNA + MHV-68
(NS)siRNA + MHV-68
PBS + MHV-68

(C)

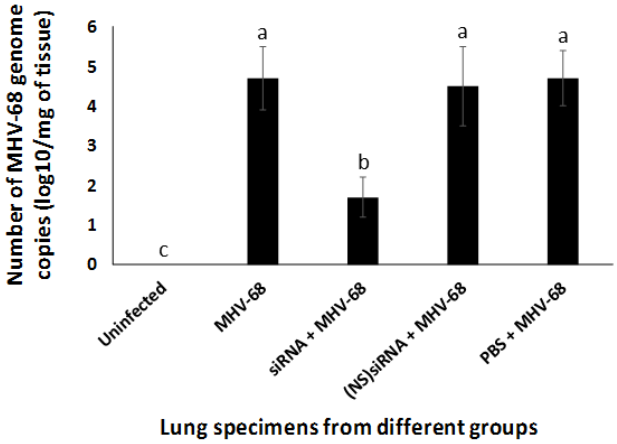
Number of MHV-68 genome copies (log10/mg of tissue)
6
5
4
3
2
1
0
c
a
b
a
a
Uninfected
MHV-68
siRNA + MHV-68
(NS)siRNA + MHV-68
PBS + MHV-68
Lung specimens from different groups

Figure 5

SUMMARY AND FUTURE DIRECTIONS

Cellular and KSHV-encoded miRNAs have been demonstrated to regulate KSHV infection in terms of latency, reactivation, virus replication, and tumor formation. To date, little is known about the role of miRNAs in regulating early stages of virus infection. Our studies, for the first time, demonstrate the ability of KSHV to significantly alter the expression of cellular miRNAs during the initial stages of infection. Several of these miRNAs in turn target cellular genes to inhibit virus entry **(Summary Figure)**.

In the first study (**Chapter 2**), we used deep sequencing to identify and examine the host cell miRNAs expressed by a human B cell line (BJAB) in response to KSHV infection that may regulate virus internalization and immune response. Small-RNA sequencing data demonstrated the significantly altered cellular miRNA expression pattern in response to KSHV infection during the first 15 minutes PI. We identified a total of 32 known and 28 novel cellular miRNAs to be differentially expressed in KSHV-infected compared to uninfected BJAB cells. These miRNAs were further authenticated by qRT-PCR using miRNA-specific primers.

We also tested the ability of UV-inactivated KSHV (UV-KSHV) to alter the expression of cellular miRNAs. Interestingly, profiling of miRNAs expression during the early stages of UV-KSHV infection of BJAB cells yielded comparable levels as the live wild-type KSHV. These data may indicate that the induction of cellular miRNAs by KSHV infection in BJAB cells is purely dependent on the interactions between the virus envelope-associated proteins and cell-surface receptors, and not due to virus replication.

miRNA-target prediction analysis indicated that target genes regulated by KSHV-induced known miRNAs are mainly involved in regulating cell signaling, initiating transcription of KSHV IE genes, promoting virus latency, and modulating the host immune responses. Similarly, novel cellular miRNAs that were up-regulated by KSHV infection in our study primarily target genes that are involved in virus uptake and immune responses. Using qRT-PCR and Western blotting,

we were able to further authenticate some of the target genes that have been shown to be regulated by novel miRNAs. These findings provide clear evidence that KSHV entry induces cellular miRNAs that in turn regulate virus infection and cellular-antiviral defense mechanisms.

One of the KSHV-induced miRNAs, miR-36 was shown to be significantly upregulated by 15min PI. Thus, our next study (**Chapter 3**) was to further investigate the role of miR-36 during virus entry. Initially, we monitored the expression of miR-36 at 5, 10, 15, and 30min PI in BJAB and endothelial (HMVEC-d) cells, both are physiologically relevant cells to KSHV biology. Our results showed that miR-36 triggered by KSHV at as early as 5 min PI and peaked at 30 min PI. Transfection of cells with miR-36 mimic significantly inhibited KSHV infection, while miR-36 specific inhibitor reversed the effects of miR-36 on virus infection of cells. Interestingly, we observed similar effects of miR-36 mimic and inhibitor on EBV and HSV-2 infection of cells.

Using bioinformatics tools, we identified IFITM1 to be one of the most promising targets for miR-36. Luciferase assay demonstrated the ability of miR-36 mimic to physically interact with IFITM1. Hence, we set out to test the function of IFITM1 during the initial stages of KSHV infection. We monitored the expression of IFITM1 at 5, 10, 15, 30 and 60min post-KSHV infection of BJAB and HMVEC-d cell lines. There was an inverse correlation observed between the expression of KSHV-induced IFITM1 and miR-36. This confirms the direct association between virus-induced IFITM1 and endogenous miR-36 expression during KSHV infection. Overexpression of IFITM1 in BJAB and HMVEC-d cells significantly enhanced KSHV infection, while knock-down of IFITM1 expression by specific siRNA had the opposite effects. We observed identical effects of IFITM1 on EBV and HSV-2 infection of cells. These findings indicate cellular miR-36 to regulate the internalization of KSHV, EBV, and HSV-2 by targeting expression of IFITM1 **(Summary Figure)**.

Both KSHV and EBV are the most closely related human *γ-herpesviruses*. Therefore, we analyzed the effect of EBV infection on IFITM1 expression (**Chapter 4**). Similar to KSHV, IFITM1 expression was significantly elevated in BJAB cells infected with EBV. IFITM1 enhances

EBV infection at the post-attachment stage as IFITM1-specific siRNA significantly inhibits virus infection but has no effect on binding of KSHV and EBV to BJAB cells.

Finally, we conducted *in vivo* studies to confirm the role of IFITM1 in KSHV and EBV infections (**Chapter 4**). We used murine γ-herpesvirus 68 (MHV-68), that is commonly used as a model to study *γ-herpesvirus* (KSHV and EBV) pathogenesis. Silencing IFITM1 expression in BALB/c mice using IFITM1-specific *in vivo* siRNA lowered MHV-68 infection. Plaque assay and qPCR indicated a sharp decline in the MHV-68 titers in the lung tissues collected from mice that were primed with siRNA specific to IFITM1 compared to those that were primed with (NS)siRNA or PBS.

Taken together, our results indicate the following: (i) Interactions between KSHV envelope proteins and the host cell receptors trigger the induction of cellular miRNAs; (ii) IFITM1 promotes infection of KSHV, EBV, and HSV2; (iii) miR-36 inhibits *in vitro* KSHV, EBV, and HSV2 infection via targeting IFITM1; and (iv) silencing expression of IFITM1 significantly decrease *γ-herpesvirus* infection of BALB/c mice **(Summary Figure)**. Inhibition of virus entry by cellular miR-36 could be a mechanism of superinfection resistance (SIR) (Nethe et al., 2005) developed by cells towards KSHV and other related viral pathogens. This idea of a miRNA expressed during early stages of infection to actively suppress superinfection is particularly appealing because such a mechanism would help to keep a permanent check in the low number (1-3%) of KSHV infected cells to undrgoing lytic replication, *in vivo*.

Our future studies will be dedicated to answering the following questions:

(**i**) What is the molecular mechanism by which KSHV induces cellular miR-36?

(**ii**) How does IFITM1 enhance virus infection?

(**iii**) What is the role of host cell receptors in the IFITM1-facilitated virus entry?

(**iv**) Can miR-36 be used as a diagnostic biomarker for virus infection?

Summary Figure

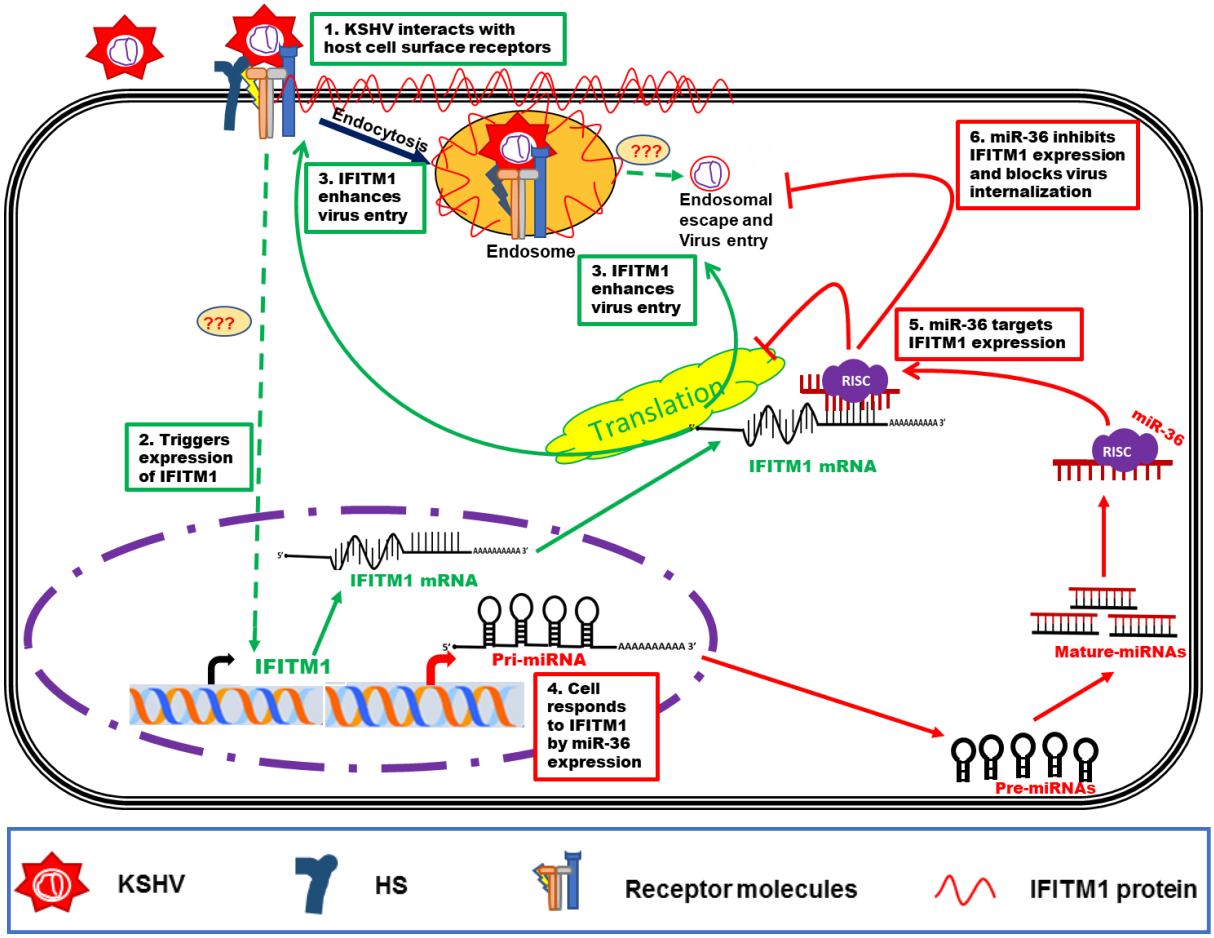

Summary Figure: KSHV-induced miR-36 inhibits KSHV entry by targeting IFITM1. KSHV-interactions with host cell surface molecules trigger the expression of IFITM1 which in turn enhances virus entry. Infected cell responds to IFITM1 expression by upregulation of miR-36 that inhibits the expression of IFITM1 and blocks KSHV entry. A summary of the events from the time of virus binding to the internalization is depicted in a sequentially numbered manner. Green lines indicate events that promote virus entry while the red lines denote those events that block the virus entry. Future studies are indicated by dotted lines.

LITERATURE CITED:

Ablashi, D.V., Chatlynne, L.G., Whitman, J.E., Jr., Cesarman, E., 2002. Spectrum of Kaposi's sarcoma-associated herpesvirus, or human herpesvirus 8, diseases. Clin Microbiol Rev 15, 439-464.

Adams, A., Strander, H., Cantell, K., 1975. Sensitivity of the Epstein-Barr virus transformed human lymphoid cell lines to interferon. J Gen Virol 28, 207-217.

Akula, S.M., Ford, P.W., Whitman, A.G., Hamden, K.E., Bryan, B.A., Cook, P.P., McCubrey, J.A., 2005. B-Raf-dependent expression of vascular endothelial growth factor-A in Kaposi sarcoma-associated herpesvirus-infected human B cells. Blood 105, 4516-4522.

Akula, S.M., Ford, P.W., Whitman, A.G., Hamden, K.E., Shelton, J.G., McCubrey, J.A., 2004. Raf promotes human herpesvirus-8 (HHV-8/KSHV) infection. Oncogene 23, 5227-5241.

Akula, S.M., Naranatt, P.P., Walia, N.S., Wang, F.Z., Fegley, B., Chandran, B., 2003. Kaposi's sarcoma-associated herpesvirus (human herpesvirus 8) infection of human fibroblast cells occurs through endocytosis. J Virol 77, 7978-7990.

Akula, S.M., Pramod, N.P., Wang, F.Z., Chandran, B., 2001a. Human herpesvirus 8 envelope-associated glycoprotein B interacts with heparan sulfate-like moieties. Virology 284, 235-249.

Akula, S.M., Pramod, N.P., Wang, F.Z., Chandran, B., 2002. Integrin alpha3beta1 (CD 49c/29) is a cellular receptor for Kaposi's sarcoma-associated herpesvirus (KSHV/HHV-8) entry into the target cells. Cell 108, 407-419.

Akula, S.M., Wang, F.Z., Vieira, J., Chandran, B., 2001b. Human herpesvirus 8 interaction with target cells involves heparan sulfate. Virology 282, 245-255.

Alber, D., Staeheli, P., 1996. Partial inhibition of vesicular stomatitis virus by the interferon-induced human 9-27 protein. J Interferon Cytokine Res 16, 375-380.

Amini-Bavil-Olyaee, S., Choi, Y.J., Lee, J.H., Shi, M., Huang, I.C., Farzan, M., Jung, J.U., 2013. The antiviral effector IFITM3 disrupts intracellular cholesterol homeostasis to block viral entry. Cell Host Microbe 13, 452-464.

Ancicova, L., Wagnerova, M., Janulikova, J., Chalupkova, A., Hrabovska, Z., Kostolansky, F., Vareckova, E., Mistrikova, J., 2015. Simultaneous infection with gammaherpes and influenza viruses enhances the host immune defense. Acta virologica 59, 369-379.

Arias, C., Weisburd, B., Stern-Ginossar, N., Mercier, A., Madrid, A.S., Bellare, P., Holdorf, M., Weissman, J.S., Ganem, D., 2014. KSHV 2.0: a comprehensive annotation of the Kaposi's sarcoma-associated herpesvirus genome using next-generation sequencing reveals novel genomic and functional features. PLoS Pathog 10, e1003847.

Bai, Z., Huang, Y., Li, W., Zhu, Y., Jung, J.U., Lu, C., Gao, S.J., 2014. Genomewide mapping and screening of Kaposi's sarcoma-associated herpesvirus (KSHV) 3' untranslated regions identify bicistronic and polycistronic viral transcripts as frequent targets of KSHV microRNAs. J Virol 88, 377-392.

Baigude, H., Rana, T.M., 2014. Strategies to antagonize miRNA functions in vitro and in vivo. Nanomedicine (Lond) 9, 2545-2555.

Bailey, C.C., Zhong, G., Huang, I.C., Farzan, M., 2014. IFITM-Family Proteins: The Cell's First Line of Antiviral Defense. Annu Rev Virol 1, 261-283.

Barnes, B.J., Moore, P.A., Pitha, P.M., 2001. Virus-specific activation of a novel interferon regulatory factor, IRF-5, results in the induction of distinct interferon alpha genes. J Biol Chem 276, 23382-23390.

Barnes, D., Kunitomi, M., Vignuzzi, M., Saksela, K., Andino, R., 2008. Harnessing endogenous miRNAs to control virus tissue tropism as a strategy for developing attenuated virus vaccines. Cell Host Microbe 4, 239-248.

Bartel, D.P., 2004. MicroRNAs: genomics, biogenesis, mechanism, and function. Cell 116, 281-297.

Bartel, D.P., 2009. MicroRNAs: target recognition and regulatory functions. Cell 136, 215-233.

Barton, E., Mandal, P., Speck, S.H., 2011. Pathogenesis and host control of gammaherpesviruses: lessons from the mouse. Annu Rev Immunol 29, 351-397.

Bechtel, J.T., Winant, R.C., Ganem, D., 2005. Host and viral proteins in the virion of Kaposi's sarcoma-associated herpesvirus. J Virol 79, 4952-4964.

Bellare, P., Ganem, D., 2009. Regulation of KSHV lytic switch protein expression by a virus-encoded microRNA: an evolutionary adaptation that fine-tunes lytic reactivation. Cell Host Microbe 6, 570-575.

Bentz, G.L., Liu, R., Hahn, A.M., Shackelford, J., Pagano, J.S., 2010. Epstein-Barr virus BRLF1 inhibits transcription of IRF3 and IRF7 and suppresses induction of interferon-beta. Virology 402, 121-128.

Bofill-De Ros, X., Rovira-Rigau, M., Fillat, C., 2017. Implications of MicroRNAs in Oncolytic Virotherapy. Front Oncol 7, 142.

Borg, D., Hedner, C., Gaber, A., Nodin, B., Fristedt, R., Jirstrom, K., Eberhard, J., Johnsson, A., 2016. Expression of IFITM1 as a prognostic biomarker in resected gastric and esophageal adenocarcinoma. Biomark Res 4, 10.

Boss, I.W., Renne, R., 2010. Viral miRNAs: tools for immune evasion. Curr Opin Microbiol 13, 540-545.

Braicu, C., Calin, G.A., Berindan-Neagoe, I., 2013. MicroRNAs and cancer therapy - from bystanders to major players. Curr Med Chem 20, 3561-3573.

Brass, A.L., Huang, I.C., Benita, Y., John, S.P., Krishnan, M.N., Feeley, E.M., Ryan, B.J., Weyer, J.L., van der Weyden, L., Fikrig, E., Adams, D.J., Xavier, R.J., Farzan, M., Elledge, S.J., 2009. The IFITM proteins mediate cellular resistance to influenza A H1N1 virus, West Nile virus, and dengue virus. Cell 139, 1243-1254.

Brostoff, T., Pesavento, P.A., Barker, C.M., Kenney, J.L., Dietrich, E.A., Duggal, N.K., Bosco-Lauth, A.M., Brault, A.C., 2016. MicroRNA reduction of neuronal West Nile virus replication attenuates and affords a protective immune response in mice. Vaccine 34, 5366-5375.

Bruscella, P., Bottini, S., Baudesson, C., Pawlotsky, J.M., Feray, C., Trabucchi, M., 2017. Viruses and miRNAs: More Friends than Foes. Front Microbiol 8, 824.

Bryan, B.A., Dyson, O.F., Akula, S.M., 2006. Identifying cellular genes crucial for the reactivation of Kaposi's sarcoma-associated herpesvirus latency. J Gen Virol 87, 519-529.

Bryan, B.A., Dyson, O.F., McCubrey, J.A., Akula, S.M., 2005. Biology of Kaposi's sarcoma-associated herpesvirus. Front Biosci 10, 2882-2891.

Cai, Q., Verma, S.C., Choi, J.Y., Ma, M., Robertson, E.S., 2010a. Kaposi's sarcoma-associated herpesvirus inhibits interleukin-4-mediated STAT6 phosphorylation to regulate apoptosis and maintain latency. J Virol 84, 11134-11144.

Cai, Q., Verma, S.C., Lu, J., Robertson, E.S., 2010b. Molecular biology of Kaposi's sarcoma-associated herpesvirus and related oncogenesis. Adv Virus Res 78, 87-142.

Cai, X., Hagedorn, C.H., Cullen, B.R., 2004. Human microRNAs are processed from capped, polyadenylated transcripts that can also function as mRNAs. RNA 10, 1957-1966.

Cai, X., Lu, S., Zhang, Z., Gonzalez, C.M., Damania, B., Cullen, B.R., 2005. Kaposi's sarcoma-associated herpesvirus expresses an array of viral microRNAs in latently infected cells. Proc Natl Acad Sci U S A 102, 5570-5575.

Cai, X., Schafer, A., Lu, S., Bilello, J.P., Desrosiers, R.C., Edwards, R., Raab-Traub, N., Cullen, B.R., 2006. Epstein-Barr virus microRNAs are evolutionarily conserved and differentially expressed. PLoS Pathog 2, e23.

Cancian, L., Hansen, A., Boshoff, C., 2013. Cellular origin of Kaposi's sarcoma and Kaposi's sarcoma-associated herpesvirus-induced cell reprogramming. Trends Cell Biol 23, 421-432.

Cao, Y., Minhas, V., Tan, X., Huang, J., Wang, B., Zhu, M., Gao, Y., Zhao, T., Yang, L., Wood, C., 2014. High prevalence of early childhood infection by Kaposi's sarcoma-associated herpesvirus in a minority population in China. Clin Microbiol Infect 20, 475-481.

Carroll, P.A., Kenerson, H.L., Yeung, R.S., Lagunoff, M., 2006. Latent Kaposi's sarcoma-associated herpesvirus infection of endothelial cells activates hypoxia-induced factors. J Virol 80, 10802-10812.

Catrina Ene, A.M., Borze, I., Guled, M., Costache, M., Leen, G., Sajin, M., Ionica, E., Chitu, A., Knuutila, S., 2014. MicroRNA expression profiles in Kaposi's sarcoma. Pathol Oncol Res 20, 153-159.

Cavallin, L.E., Goldschmidt-Clermont, P., Mesri, E.A., 2014. Molecular and cellular mechanisms of KSHV oncogenesis of Kaposi's sarcoma associated with HIV/AIDS. PLoS Pathog 10, e1004154.

Chakraborty, S., Veettil, M.V., Chandran, B., 2012. Kaposi's Sarcoma Associated Herpesvirus Entry into Target Cells. Front Microbiol 3, 6.

Chandran, B., 2010. Early events in Kaposi's sarcoma-associated herpesvirus infection of target cells. J Virol 84, 2188-2199.

Chandrasekharan, J.A., Huang, X.M., Hwang, A.C., Sharma-Walia, N., 2016. Altering the Anti-inflammatory Lipoxin Microenvironment: a New Insight into Kaposi's Sarcoma-Associated Herpesvirus Pathogenesis. J Virol 90, 11020-11031.

Chang, P.C., Kung, H.J., 2014. SUMO and KSHV Replication. Cancers (Basel) 6, 1905-1924.

Chang, Y., Cesarman, E., Pessin, M.S., Lee, F., Culpepper, J., Knowles, D.M., Moore, P.S., 1994. Identification of herpesvirus-like DNA sequences in AIDS-associated Kaposi's sarcoma. Science 266, 1865-1869.

Chang, Y., Moore, P., 2014. Twenty years of KSHV. Viruses 6, 4258-4264.

Chen, H.S., Lu, F., Lieberman, P.M., 2013. Epigenetic regulation of EBV and KSHV latency. Curr Opin Virol 3, 251-259.

Chen, M., Sun, F., Han, L., Qu, Z., 2016. Kaposi's sarcoma herpesvirus (KSHV) microRNA K12-1 functions as an oncogene by activating NF-kappaB/IL-6/STAT3 signaling. Oncotarget 7, 33363-33373.

Chen, X., 2005. MicroRNA biogenesis and function in plants. FEBS Lett 579, 5923-5931.

Chen, Y., Shen, A., Rider, P.J., Yu, Y., Wu, K., Mu, Y., Hao, Q., Liu, Y., Gong, H., Zhu, Y., Liu, F., Wu, J., 2011. A liver-specific microRNA binds to a highly conserved RNA sequence of hepatitis B virus and negatively regulates viral gene expression and replication. FASEB J 25, 4511-4521.

Chendrimada, T.P., Gregory, R.I., Kumaraswamy, E., Norman, J., Cooch, N., Nishikura, K., Shiekhattar, R., 2005. TRBP recruits the Dicer complex to Ago2 for microRNA processing and gene silencing. Nature 436, 740-744.

Cheng, F., Pekkonen, P., Laurinavicius, S., Sugiyama, N., Henderson, S., Gunther, T., Rantanen, V., Kaivanto, E., Aavikko, M., Sarek, G., Hautaniemi, S., Biberfeld, P., Aaltonen, L., Grundhoff, A., Boshoff, C., Alitalo, K., Lehti, K., Ojala, P.M., 2011. KSHV-initiated notch activation leads to membrane-type-1 matrix metalloproteinase-dependent lymphatic endothelial-to-mesenchymal transition. Cell Host Microbe 10, 577-590.

Cho, H.J., Jeong, S.G., Park, J.E., Han, J.A., Kang, H.R., Lee, D., Song, M.J., 2013. Antiviral activity of angelicin against gammaherpesviruses. Antiviral Res 100, 75-83.

Choi, H.S., Jain, V., Krueger, B., Marshall, V., Kim, C.H., Shisler, J.L., Whitby, D., Renne, R., 2015. Kaposi's Sarcoma-Associated Herpesvirus (KSHV) Induces the Oncogenic miR-17-92 Cluster and Down-Regulates TGF-beta Signaling. PLoS Pathog 11, e1005255.

Christopher, A.F., Kaur, R.P., Kaur, G., Kaur, A., Gupta, V., Bansal, P., 2016. MicroRNA therapeutics: Discovering novel targets and developing specific therapy. Perspect Clin Res 7, 68-74.

Chugh, P.E., Sin, S.H., Ozgur, S., Henry, D.H., Menezes, P., Griffith, J., Eron, J.J., Damania, B., Dittmer, D.P., 2013. Systemically circulating viral and tumor-derived microRNAs in KSHV-associated malignancies. PLoS Pathog 9, e1003484.

Cipkova-Jarcuskova, J., Chalupkova, A., Hrabovska, Z., Wagnerova, M., Mistrikova, J., 2013. Biological and pathogenetic characterization of different isolates of murine gammaherpesvirus 68 (MHV-68) in the context of study of human oncogenic gammaherpesviruses. Acta virologica 57, 105-112.

Cock, J.M., Sterck, L., Rouze, P., Scornet, D., Allen, A.E., Amoutzias, G., Anthouard, V., Artiguenave, F., Aury, J.M., Badger, J.H., Beszteri, B., Billiau, K., Bonnet, E., Bothwell, J.H., Bowler, C., Boyen, C., Brownlee, C., Carrano, C.J., Charrier, B., Cho, G.Y., Coelho, S.M., Collen, J., Corre, E., Da Silva, C., Delage, L., Delaroque, N., Dittami, S.M., Doulbeau, S., Elias, M., Farnham, G., Gachon, C.M., Gschloessl, B., Heesch, S., Jabbari, K., Jubin, C., Kawai, H., Kimura, K., Kloareg, B., Kupper, F.C., Lang, D., Le Bail, A., Leblanc, C., Lerouge, P., Lohr, M., Lopez, P.J., Martens, C., Maumus, F., Michel, G., Miranda-Saavedra, D., Morales, J., Moreau, H., Motomura, T., Nagasato, C., Napoli, C.A., Nelson, D.R., Nyvall-Collen, P., Peters, A.F., Pommier, C., Potin, P., Poulain, J., Quesneville, H., Read, B., Rensing, S.A., Ritter, A., Rousvoal, S., Samanta, M., Samson, G., Schroeder, D.C., Segurens, B., Strittmatter, M., Tonon, T., Tregear, J.W., Valentin, K., von Dassow, P., Yamagishi, T., Van de Peer, Y., Wincker, P., 2010. The Ectocarpus genome and the independent evolution of multicellularity in brown algae. Nature 465, 617-621.

Coen, N., Duraffour, S., Snoeck, R., Andrei, G., 2014. KSHV targeted therapy: an update on inhibitors of viral lytic replication. Viruses 6, 4731-4759.

Cohen, A., Brodie, C., Sarid, R., 2006. An essential role of ERK signalling in TPA-induced reactivation of Kaposi's sarcoma-associated herpesvirus. J Gen Virol 87, 795-802.

Colantonio, A.D., Epeldegui, M., Jesiak, M., Jachimowski, L., Blom, B., Uittenbogaart, C.H., 2011. IFN-alpha is constitutively expressed in the human thymus, but not in peripheral lymphoid organs. PLoS One 6, e24252.

Coll, O., Villalba, A., Bussotti, G., Notredame, C., Gebauer, F., 2010. A novel, noncanonical mechanism of cytoplasmic polyadenylation operates in Drosophila embryogenesis. Genes Dev 24, 129-134.

Cosmopoulos, K., Pegtel, M., Hawkins, J., Moffett, H., Novina, C., Middeldorp, J., Thorley-Lawson, D.A., 2009. Comprehensive profiling of Epstein-Barr virus microRNAs in nasopharyngeal carcinoma. J Virol 83, 2357-2367.

Cui, C., Griffiths, A., Li, G., Silva, L.M., Kramer, M.F., Gaasterland, T., Wang, X.J., Coen, D.M., 2006. Prediction and identification of herpes simplex virus 1-encoded microRNAs. J Virol 80, 5499-5508.

Cullen, B.R., 2010. Five questions about viruses and microRNAs. PLoS Pathog 6, e1000787.

Cullen, B.R., 2011. Viruses and microRNAs: RISCy interactions with serious consequences. Genes Dev 25, 1881-1894.

Cullen, B.R., 2013. How do viruses avoid inhibition by endogenous cellular microRNAs? PLoS Pathog 9, e1003694.

Cuperus, J.T., Fahlgren, N., Carrington, J.C., 2011. Evolution and functional diversification of MIRNA genes. Plant Cell 23, 431-442.

Curreli, F., Cerimele, F., Muralidhar, S., Rosenthal, L.J., Cesarman, E., Friedman-Kien, A.E., Flore, O., 2002. Transcriptional downregulation of ORF50/Rta by methotrexate inhibits the switch of Kaposi's sarcoma-associated herpesvirus/human herpesvirus 8 from latency to lytic replication. J Virol 76, 5208-5219.

de Jong, Y.P., Jacobson, I.M., 2014. Antisense therapy for hepatitis C virus infection. J Hepatol 60, 227-228.

Deblandre, G.A., Marinx, O.P., Evans, S.S., Majjaj, S., Leo, O., Caput, D., Huez, G.A., Wathelet, M.G., 1995. Expression cloning of an interferon-inducible 17-kDa membrane protein implicated in the control of cell growth. J Biol Chem 270, 23860-23866.

Dedicoat, M., Newton, R., Alkharsah, K.R., Sheldon, J., Szabados, I., Ndlovu, B., Page, T., Casabonne, D., Gilks, C.F., Cassol, S.A., Whitby, D., Schulz, T.F., 2004. Mother-to-child transmission of human herpesvirus-8 in South Africa. J Infect Dis 190, 1068-1075.

Direkze, S., Laman, H., 2004. Regulation of growth signalling and cell cycle by Kaposi's sarcoma-associated herpesvirus genes. Int J Exp Pathol 85, 305-319.

Dittmer, D.P., Richards, K.L., Damania, B., 2012. Treatment of Kaposi sarcoma-associated herpesvirus-associated cancers. Front Microbiol 3, 141.

Dolken, L., Malterer, G., Erhard, F., Kothe, S., Friedel, C.C., Suffert, G., Marcinowski, L., Motsch, N., Barth, S., Beitzinger, M., Lieber, D., Bailer, S.M., Hoffmann, R., Ruzsics, Z., Kremmer, E., Pfeffer, S., Zimmer, R., Koszinowski, U.H., Grasser, F., Meister, G., Haas, J., 2010. Systematic analysis of viral and cellular microRNA targets in cells latently

infected with human gamma-herpesviruses by RISC immunoprecipitation assay. Cell Host Microbe 7, 324-334.

Donlin, L.T., Jayatilleke, A., Giannopoulou, E.G., Kalliolias, G.D., Ivashkiv, L.B., 2014. Modulation of TNF-induced macrophage polarization by synovial fibroblasts. J Immunol 193, 2373-2383.

Dourmishev, L.A., Dourmishev, A.L., Palmeri, D., Schwartz, R.A., Lukac, D.M., 2003. Molecular genetics of Kaposi's sarcoma-associated herpesvirus (human herpesvirus-8) epidemiology and pathogenesis. Microbiol Mol Biol Rev 67, 175-212, table of contents.

Drury, R.E., O'Connor, D., Pollard, A.J., 2017. The Clinical Application of MicroRNAs in Infectious Disease. Front Immunol 8, 1182.

Dukers, N.H., Rezza, G., 2003. Human herpesvirus 8 epidemiology: what we do and do not know. AIDS 17, 1717-1730.

Dyson, O.F., Oxendine, T.L., Hamden, K.E., Ford, P.W., Akula, S.M., 2008. Differential regulation of the attachment of Kaposi's sarcoma-associated herpesvirus (KSHV)-infected human B cells to extracellular matrix by KSHV-encoded gB and cellular alphaV integrins. Cell Microbiol 10, 1546-1558.

Dyson, O.F., Traylen, C.M., Akula, S.M., 2010. Cell membrane-bound Kaposi's sarcoma-associated herpesvirus-encoded glycoprotein B promotes virus latency by regulating expression of cellular Egr-1. J Biol Chem 285, 37491-37502.

Dyson, O.F., Walker, L.R., Whitehouse, A., Cook, P.P., Akula, S.M., 2012. Resveratrol Inhibits KSHV Reactivation by Lowering the Levels of Cellular EGR-1. PLoS One 7, e33364.

Eckenfelder, A., Segeral, E., Pinzon, N., Ulveling, D., Amadori, C., Charpentier, M., Nidelet, S., Concordet, J.P., Zagury, J.F., Paillart, J.C., Berlioz-Torrent, C., Seitz, H., Emiliani, S., Gallois-Montbrun, S., 2017. Argonaute proteins regulate HIV-1 multiply spliced RNA and viral production in a Dicer independent manner. Nucleic Acids Res 45, 4158-4173.

El Assal, R., Gurkan, U.A., Chen, P., Juillard, F., Tocchio, A., Chinnasamy, T., Beauchemin, C., Unluisler, S., Canikyan, S., Holman, A., Srivatsa, S., Kaye, K.M., Demirci, U., 2016. 3-D Microwell Array System for Culturing Virus Infected Tumor Cells. Sci Rep 6, 39144.

Emuss, V., Lagos, D., Pizzey, A., Gratrix, F., Henderson, S.R., Boshoff, C., 2009. KSHV manipulates Notch signaling by DLL4 and JAG1 to alter cell cycle genes in lymphatic endothelia. PLoS Pathog 5, e1000616.

Engels, E.A., Biggar, R.J., Hall, H.I., Cross, H., Crutchfield, A., Finch, J.L., Grigg, R., Hylton, T., Pawlish, K.S., McNeel, T.S., Goedert, J.J., 2008. Cancer risk in people infected with human immunodeficiency virus in the United States. Int J Cancer 123, 187-194.

Ensoli, B., Sgadari, C., Barillari, G., Sirianni, M.C., Sturzl, M., Monini, P., 2001. Biology of Kaposi's sarcoma. Eur J Cancer 37, 1251-1269.

Eulalio, A., Schulte, L., Vogel, J., 2012. The mammalian microRNA response to bacterial infections. RNA Biol 9, 742-750.

Evans, S.S., Lee, D.B., Han, T., Tomasi, T.B., Evans, R.L., 1990. Monoclonal antibody to the interferon-inducible protein Leu-13 triggers aggregation and inhibits proliferation of leukemic B cells. Blood 76, 2583-2593.

Fatahzadeh, M., 2012. Kaposi sarcoma: review and medical management update. Oral Surg Oral Med Oral Pathol Oral Radiol 113, 2-16.

Feeley, E.M., Sims, J.S., John, S.P., Chin, C.R., Pertel, T., Chen, L.M., Gaiha, G.D., Ryan, B.J., Donis, R.O., Elledge, S.J., Brass, A.L., 2011. IFITM3 inhibits influenza A virus infection by preventing cytosolic entry. PLoS Pathog 7, e1002337.

Ferreira, D.M., Afonso, M.B., Rodrigues, P.M., Simao, A.L., Pereira, D.M., Borralho, P.M., Rodrigues, C.M., Castro, R.E., 2014. c-Jun N-terminal kinase 1/c-Jun activation of the p53/microRNA 34a/sirtuin 1 pathway contributes to apoptosis induced by deoxycholic acid in rat liver. Mol Cell Biol 34, 1100-1120.

Flano, E., Husain, S.M., Sample, J.T., Woodland, D.L., Blackman, M.A., 2000. Latent murine gamma-herpesvirus infection is established in activated B cells, dendritic cells, and macrophages. J Immunol 165, 1074-1081.

Flowers, C.C., Flowers, S.P., Nabel, G.J., 1998. Kaposi's sarcoma-associated herpesvirus viral interferon regulatory factor confers resistance to the antiproliferative effect of interferon-alpha. Mol Med 4, 402-412.

Ford, P.W., Bryan, B.A., Dyson, O.F., Weidner, D.A., Chintalgattu, V., Akula, S.M., 2006. Raf/MEK/ERK signalling triggers reactivation of Kaposi's sarcoma-associated herpesvirus latency. J Gen Virol 87, 1139-1144.

Forster, S.C., Tate, M.D., Hertzog, P.J., 2015. MicroRNA as Type I Interferon-Regulated Transcripts and Modulators of the Innate Immune Response. Front Immunol 6, 334.

Franceschi, S., Lise, M., Clifford, G.M., Rickenbach, M., Levi, F., Maspoli, M., Bouchardy, C., Dehler, S., Jundt, G., Ess, S., Bordoni, A., Konzelmann, I., Frick, H., Dal Maso, L., Elzi, L., Furrer, H., Calmy, A., Cavassini, M., Ledergerber, B., Keiser, O., Swiss, H.I.V.C.S., 2010. Changing patterns of cancer incidence in the early- and late-HAART periods: the Swiss HIV Cohort Study. Br J Cancer 103, 416-422.

Frappier, L., 2015. Regulation of herpesvirus reactivation by host microRNAs. J Virol 89, 2456-2458.

Friedman, R.L., Manly, S.P., McMahon, M., Kerr, I.M., Stark, G.R., 1984. Transcriptional and posttranscriptional regulation of interferon-induced gene expression in human cells. Cell 38, 745-755.

Gabarre, J., Bossi, P., 2003. [HAART and changes of epidemiology, treatment and prognosis of HIV-positive patients with Kaposi's sarcoma and lymphoma]. Bull Cancer 90, 419-425.

Gallaher, A.M., Das, S., Xiao, Z., Andresson, T., Kieffer-Kwon, P., Happel, C., Ziegelbauer, J., 2013. Proteomic screening of human targets of viral microRNAs reveals functions associated with immune evasion and angiogenesis. PLoS Pathog 9, e1003584.

Ganem, D., 1998. Human herpesvirus 8 and its role in the genesis of Kaposi's sarcoma. Curr Clin Top Infect Dis 18, 237-251.

Ganem, D., 2010. KSHV and the pathogenesis of Kaposi sarcoma: listening to human biology and medicine. J Clin Invest 120, 939-949.

Gantier, M.P., Sadler, A.J., Williams, B.R., 2007. Fine-tuning of the innate immune response by microRNAs. Immunol Cell Biol 85, 458-462.

Gantt, S., Cattamanchi, A., Krantz, E., Magaret, A., Selke, S., Kuntz, S.R., Huang, M.L., Corey, L., Wald, A., Casper, C., 2014. Reduced human herpesvirus-8 oropharyngeal shedding associated with protease inhibitor-based antiretroviral therapy. J Clin Virol 60, 127-132.

Giffin, L., West, J.A., Damania, B., 2015. Kaposi's Sarcoma-Associated Herpesvirus Interleukin-6 Modulates Endothelial Cell Movement by Upregulating Cellular Genes Involved in Migration. MBio 6, e01499-01415.

Girardi, E., Miesen, P., Pennings, B., Frangeul, L., Saleh, M.C., van Rij, R.P., 2017. Histone-derived piRNA biogenesis depends on the ping-pong partners Piwi5 and Ago3 in Aedes aegypti. Nucleic Acids Res.

Glenewinkel, F., Cohen, M.J., King, C.R., Kaspar, S., Bamberg-Lemper, S., Mymryk, J.S., Becker, W., 2016. The adaptor protein DCAF7 mediates the interaction of the adenovirus E1A oncoprotein with the protein kinases DYRK1A and HIPK2. Sci Rep 6, 28241.

Gottwein, E., 2012. Kaposi's Sarcoma-Associated Herpesvirus microRNAs. Front Microbiol 3, 165.

Gottwein, E., 2013. Roles of microRNAs in the life cycles of mammalian viruses. Curr Top Microbiol Immunol 371, 201-227.

Gottwein, E., Cai, X., Cullen, B.R., 2006. Expression and function of microRNAs encoded by Kaposi's sarcoma-associated herpesvirus. Cold Spring Harb Symp Quant Biol 71, 357-364.

Gottwein, E., Corcoran, D.L., Mukherjee, N., Skalsky, R.L., Hafner, M., Nusbaum, J.D., Shamulailatpam, P., Love, C.L., Dave, S.S., Tuschl, T., Ohler, U., Cullen, B.R., 2011. Viral microRNA targetome of KSHV-infected primary effusion lymphoma cell lines. Cell Host Microbe 10, 515-526.

Gourzones, C., Jimenez, A.S., Busson, P., 2012. Profiling of Epstein-Barr virus-encoded microRNAs in nasopharyngeal carcinoma reveals potential biomarkers and oncomirs. Cancer 118, 4634; author reply 4634-4635.

Greene, W., Kuhne, K., Ye, F., Chen, J., Zhou, F., Lei, X., Gao, S.J., 2007. Molecular biology of KSHV in relation to AIDS-associated oncogenesis. Cancer Treat Res 133, 69-127.

Gu, S., Jin, L., Zhang, F., Sarnow, P., Kay, M.A., 2009. Biological basis for restriction of microRNA targets to the 3' untranslated region in mammalian mRNAs. Nat Struct Mol Biol 16, 144-150.

Guo, J., Hui, D.J., Merrick, W.C., Sen, G.C., 2000. A new pathway of translational regulation mediated by eukaryotic initiation factor 3. Embo j 19, 6891-6899.

Guo, Y., Li, W., Qin, J., Lu, C., Fan, W., 2017. Kaposi's sarcoma-associated herpesvirus (KSHV)-encoded microRNAs promote matrix metalloproteinases (MMPs) expression and pro-angiogenic cytokine secretion in endothelial cells. J Med Virol 89, 1274-1280.

Ha, M., Kim, V.N., 2014. Regulation of microRNA biogenesis. Nat Rev Mol Cell Biol 15, 509-524.

Hahn, A.S., Kaufmann, J.K., Wies, E., Naschberger, E., Panteleev-Ivlev, J., Schmidt, K., Holzer, A., Schmidt, M., Chen, J., Konig, S., Ensser, A., Myoung, J., Brockmeyer, N.H., Sturzl, M., Fleckenstein, B., Neipel, F., 2012. The ephrin receptor tyrosine kinase A2 is a cellular receptor for Kaposi's sarcoma-associated herpesvirus. Nat Med 18, 961-966.

Hajnicka, V., Kudelova, M., Stibraniova, I., Slovak, M., Bartikova, P., Halasova, Z., Pancik, P., Belvoncikova, P., Vrbova, M., Holikova, V., Hails, R.S., Nuttall, P.A., 2017. Tick-Borne Transmission of Murine Gammaherpesvirus 68. Frontiers in cellular and infection microbiology 7, 458.

Hamden, K.E., Ford, P.W., Whitman, A.G., Dyson, O.F., Cheng, S.Y., McCubrey, J.A., Akula, S.M., 2004. Raf-induced vascular endothelial growth factor augments Kaposi's sarcoma-associated herpesvirus infection. J Virol 78, 13381-13390.

Hamden, K.E., Whitman, A.G., Ford, P.W., Shelton, J.G., McCubrey, J.A., Akula, S.M., 2005. Raf and VEGF: emerging therapeutic targets in Kaposi's sarcoma-associated herpesvirus infection and angiogenesis in hematopoietic and nonhematopoietic tumors. Leukemia 19, 18-26.

Hammond, S.M., 2015. An overview of microRNAs. Adv Drug Deliv Rev 87, 3-14.

Han, J., Lee, Y., Yeom, K.H., Nam, J.W., Heo, I., Rhee, J.K., Sohn, S.Y., Cho, Y., Zhang, B.T., Kim, V.N., 2006. Molecular basis for the recognition of primary microRNAs by the Drosha-DGCR8 complex. Cell 125, 887-901.

Happel, C., Ramalingam, D., Ziegelbauer, J.M., 2016. Virus-Mediated Alterations in miRNA Factors and Degradation of Viral miRNAs by MCPIP1. PLoS Biol 14, e2000998.

Hashimoto, Y., Akiyama, Y., Yuasa, Y., 2013. Multiple-to-multiple relationships between microRNAs and target genes in gastric cancer. PLoS ONE 8, e62589.

Havens, M.A., Reich, A.A., Duelli, D.M., Hastings, M.L., 2012. Biogenesis of mammalian microRNAs by a non-canonical processing pathway. Nucleic Acids Res 40, 4626-4640.

He, G., Sun, D., Ou, Z., Ding, A., 2012. The protein Zfand5 binds and stabilizes mRNAs with AU-rich elements in their 3'-untranslated regions. J Biol Chem 287, 24967-24977.

Heiss, B.L., Maximova, O.A., Pletnev, A.G., 2011. Insertion of microRNA targets into the flavivirus genome alters its highly neurovirulent phenotype. J Virol 85, 1464-1472.

Hengge, U.R., Ruzicka, T., Tyring, S.K., Stuschke, M., Roggendorf, M., Schwartz, R.A., Seeber, S., 2002. Update on Kaposi's sarcoma and other HHV8 associated diseases. Part 1: epidemiology, environmental predispositions, clinical manifestations, and therapy. Lancet Infect Dis 2, 281-292.

Henry, J.C., Azevedo-Pouly, A.C., Schmittgen, T.D., 2011. MicroRNA replacement therapy for cancer. Pharm Res 28, 3030-3042.

Hensler, H.R., Tomaszewski, M.J., Rappocciolo, G., Rinaldo, C.R., Jenkins, F.J., 2014. Human herpesvirus 8 glycoprotein B binds the entry receptor DC-SIGN. Virus Res 190, 97-103.

Herrera-Carrillo, E., Berkhout, B., 2017. Dicer-independent processing of small RNA duplexes: mechanistic insights and applications. Nucleic Acids Res 45, 10369-10379.

Hertel, L., 2011. Herpesviruses and intermediate filaments: close encounters with the third type. Viruses 3, 1015-1040.

Hickford, D., Frankenberg, S., Shaw, G., Renfree, M.B., 2012. Evolution of vertebrate interferon inducible transmembrane proteins. BMC Genomics 13, 155.

Hong, Y.K., Foreman, K., Shin, J.W., Hirakawa, S., Curry, C.L., Sage, D.R., Libermann, T., Dezube, B.J., Fingeroth, J.D., Detmar, M., 2004. Lymphatic reprogramming of blood vascular endothelium by Kaposi sarcoma-associated herpesvirus. Nat Genet 36, 683-685.

Huang, I.C., Bailey, C.C., Weyer, J.L., Radoshitzky, S.R., Becker, M.M., Chiang, J.J., Brass, A.L., Ahmed, A.A., Chi, X., Dong, L., Longobardi, L.E., Boltz, D., Kuhn, J.H., Elledge, S.J., Bavari, S., Denison, M.R., Choe, H., Farzan, M., 2011. Distinct patterns of IFITM-

mediated restriction of filoviruses, SARS coronavirus, and influenza A virus. PLoS Pathog 7, e1001258.

Hussain, M., Frentiu, F.D., Moreira, L.A., O'Neill, S.L., Asgari, S., 2011. Wolbachia uses host microRNAs to manipulate host gene expression and facilitate colonization of the dengue vector Aedes aegypti. Proc Natl Acad Sci U S A 108, 9250-9255.

Hussein, H.A., Walker, L.R., Abdel-Raouf, U.M., Desouky, S.A., Montasser, A.K., Akula, S.M., 2015. Beyond RGD: virus interactions with integrins. Arch Virol 160, 2669-2681.

Hussein, H.A.M., Akula, S.M., 2017a. miRNA-36 inhibits KSHV, EBV, HSV-2 infection of cells via stifling expression of interferon induced transmembrane protein 1 (IFITM1). Sci Rep 7, 17972.

Hussein, H.A.M., Akula, S.M., 2017b. Profiling of cellular microRNA responses during the early stages of KSHV infection. Arch Virol 162, 3293-3303.

Hussein, H.A.M., Akula, S.M., 2017c. Profiling of cellular microRNA responses during the early stages of KSHV infection. Arch Virol.

Hussein, H.A.M., Walker, L.R., Akula, S.M., 2016. KSHV gB associated RGD interactions promote attachment of cells by inhibiting the potential migratory signals induced by the disintegrin-like domain. BMC Cancer 16, 148.

Hutvagner, G., Zamore, P.D., 2002a. A microRNA in a multiple-turnover RNAi enzyme complex. Science 297, 2056-2060.

Hutvagner, G., Zamore, P.D., 2002b. RNAi: nature abhors a double-strand. Curr Opin Genet Dev 12, 225-232.

Ibrahim, A.F., Weirauch, U., Thomas, M., Grunweller, A., Hartmann, R.K., Aigner, A., 2011. MicroRNA replacement therapy for miR-145 and miR-33a is efficacious in a model of colon carcinoma. Cancer Res 71, 5214-5224.

Ivashkiv, L.B., Donlin, L.T., 2014. Regulation of type I interferon responses. Nat Rev Immunol 14, 36-49.

Iwasaki, Y.W., Siomi, M.C., Siomi, H., 2015. PIWI-Interacting RNA: Its Biogenesis and Functions. Annu Rev Biochem 84, 405-433.

Jain, S., McGinnes, L.W., Morrison, T.G., 2008. Overexpression of thiol/disulfide isomerases enhances membrane fusion directed by the Newcastle disease virus fusion protein. J Virol 82, 12039-12048.

Janssen, H.L., Kauppinen, S., Hodges, M.R., 2013a. HCV infection and miravirsen. N Engl J Med 369, 878.

Janssen, H.L., Reesink, H.W., Lawitz, E.J., Zeuzem, S., Rodriguez-Torres, M., Patel, K., van der Meer, A.J., Patick, A.K., Chen, A., Zhou, Y., Persson, R., King, B.D., Kauppinen, S., Levin, A.A., Hodges, M.R., 2013b. Treatment of HCV infection by targeting microRNA. N Engl J Med 368, 1685-1694.

Jenner, R.G., Boshoff, C., 2002. The molecular pathology of Kaposi's sarcoma-associated herpesvirus. Biochim Biophys Acta 1602, 1-22.

Jia, X., Nie, Q., Zhang, X., Nolan, L.K., Lamont, S.J., 2017. Novel MicroRNA Involved in Host Response to Avian Pathogenic Escherichia coli Identified by Deep Sequencing and Integration Analysis. Infect Immun 85.

Jin, B., Jin, H., Wang, J., 2017. Silencing of Interferon-Induced Transmembrane Protein 1 (IFITM1) Inhibits Proliferation, Migration, and Invasion in Lung Cancer Cells. Oncol Res.

Jin, H.Y., Gonzalez-Martin, A., Miletic, A.V., Lai, M., Knight, S., Sabouri-Ghomi, M., Head, S.R., Macauley, M.S., Rickert, R.C., Xiao, C., 2015. Transfection of microRNA Mimics Should Be Used with Caution. Front Genet 6, 340.

Jones, T., Ye, F., Bedolla, R., Huang, Y., Meng, J., Qian, L., Pan, H., Zhou, F., Moody, R., Wagner, B., Arar, M., Gao, S.J., 2012. Direct and efficient cellular transformation of primary rat mesenchymal precursor cells by KSHV. J Clin Invest 122, 1076-1081.

Jopling, C.L., Yi, M., Lancaster, A.M., Lemon, S.M., Sarnow, P., 2005. Modulation of hepatitis C virus RNA abundance by a liver-specific MicroRNA. Science 309, 1577-1581.

Jurak, I., Kramer, M.F., Mellor, J.C., van Lint, A.L., Roth, F.P., Knipe, D.M., Coen, D.M., 2010. Numerous conserved and divergent microRNAs expressed by herpes simplex viruses 1 and 2. J Virol 84, 4659-4672.

Kaleeba, J.A., Berger, E.A., 2006. Broad target cell selectivity of Kaposi's sarcoma-associated herpesvirus glycoprotein-mediated cell fusion and virion entry. Virology 354, 7-14.

Kaneko, H., Kawana, T., Ishioka, K., Fukushima, E., Suzutani, T., 2008. Discrimination of herpes simplex virus type 2 strains by nucleotide sequence variations. J Clin Microbiol 46, 780-784.

Kang, H., Wiedmer, A., Yuan, Y., Robertson, E., Lieberman, P.M., 2011a. Coordination of KSHV latent and lytic gene control by CTCF-cohesin mediated chromosome conformation. PLoS Pathog 7, e1002140.

Kang, J.G., Majerciak, V., Uldrick, T.S., Wang, X., Kruhlak, M., Yarchoan, R., Zheng, Z.M., 2011b. Kaposi's sarcoma-associated herpesviral IL-6 and human IL-6 open reading frames contain miRNA binding sites and are subject to cellular miRNA regulation. J Pathol 225, 378-389.

Kelly, E.J., Nace, R., Barber, G.N., Russell, S.J., 2010. Attenuation of vesicular stomatitis virus encephalitis through microRNA targeting. J Virol 84, 1550-1562.

Kertesz, M., Iovino, N., Unnerstall, U., Gaul, U., Segal, E., 2007. The role of site accessibility in microRNA target recognition. Nat Genet 39, 1278-1284.

Keshavarzi, M., Sorayayi, S., Jafar Rezaei, M., Mohammadi, M., Ghaderi, A., Rostamzadeh, A., Masoudifar, A., Mirzaei, H., 2017. MicroRNAs-Based Imaging Techniques in Cancer Diagnosis and Therapy. J Cell Biochem.

Ketting, R.F., 2010. MicroRNA biogenesis and function. An overview. Adv Exp Med Biol 700, 1-14.

Khvorova, A., Reynolds, A., Jayasena, S.D., 2003. Functional siRNAs and miRNAs exhibit strand bias. Cell 115, 209-216.

Kincaid, R.P., Sullivan, C.S., 2012. Virus-encoded microRNAs: an overview and a look to the future. PLoS Pathog 8, e1003018.

Klipper-Aurbach, Y., Wasserman, M., Braunspiegel-Weintrob, N., Borstein, D., Peleg, S., Assa, S., Karp, M., Benjamini, Y., Hochberg, Y., Laron, Z., 1995. Mathematical formulae for the prediction of the residual beta cell function during the first two years of disease in children and adolescents with insulin-dependent diabetes mellitus. Med Hypotheses 45, 486-490.

Kozomara, A., Griffiths-Jones, S., 2011. miRBase: integrating microRNA annotation and deep-sequencing data. Nucleic Acids Res 39, D152-157.

Kozomara, A., Griffiths-Jones, S., 2014. miRBase: annotating high confidence microRNAs using deep sequencing data. Nucleic Acids Res 42, D68-73.

Krause, C.J., Popp, O., Thirunarayanan, N., Dittmar, G., Lipp, M., Muller, G., 2016. MicroRNA-34a promotes genomic instability by a broad suppression of genome maintenance mechanisms downstream of the oncogene KSHV-vGPCR. Oncotarget 7, 10414-10432.

Krishnan, H.H., Naranatt, P.P., Smith, M.S., Zeng, L., Bloomer, C., Chandran, B., 2004. Concurrent expression of latent and a limited number of lytic genes with immune modulation and antiapoptotic function by Kaposi's sarcoma-associated herpesvirus early during infection of primary endothelial and fibroblast cells and subsequent decline of lytic gene expression. J Virol 78, 3601-3620.

Krishnan, H.H., Sharma-Walia, N., Zeng, L., Gao, S.J., Chandran, B., 2005. Envelope glycoprotein gB of Kaposi's sarcoma-associated herpesvirus is essential for egress from infected cells. J Virol 79, 10952-10967.

Krol, J., Loedige, I., Filipowicz, W., 2010. The widespread regulation of microRNA biogenesis, function and decay. Nat Rev Genet 11, 597-610.

Kumar, B., Chandran, B., 2016. KSHV Entry and Trafficking in Target Cells-Hijacking of Cell Signal Pathways, Actin and Membrane Dynamics. Viruses 8.

Kurokawa, A., Narukawa, M., Ohmoto, M., Yoshimoto, J., Abe, K., Misaka, T., 2015. Expression of the synaptic exocytosis-regulating molecule complexin 2 in taste buds and its participation in peripheral taste transduction. J Neurochem 133, 806-814.

La Ferla, L., Pinzone, M.R., Nunnari, G., Martellotta, F., Lleshi, A., Tirelli, U., De Paoli, P., Berretta, M., Cacopardo, B., 2013. Kaposi' s sarcoma in HIV-positive patients: the state of art in the HAART-era. Eur Rev Med Pharmacol Sci 17, 2354-2365.

Labo, N., Miley, W., Marshall, V., Gillette, W., Esposito, D., Bess, M., Turano, A., Uldrick, T., Polizzotto, M.N., Wyvill, K.M., Bagni, R., Yarchoan, R., Whitby, D., 2014. Heterogeneity and breadth of host antibody response to KSHV infection demonstrated by systematic analysis of the KSHV proteome. PLoS Pathog 10, e1004046.

Lagos-Quintana, M., Rauhut, R., Yalcin, A., Meyer, J., Lendeckel, W., Tuschl, T., 2002. Identification of tissue-specific microRNAs from mouse. Curr Biol 12, 735-739.

Lagos, D., Pollara, G., Henderson, S., Gratrix, F., Fabani, M., Milne, R.S., Gotch, F., Boshoff, C., 2010. miR-132 regulates antiviral innate immunity through suppression of the p300 transcriptional co-activator. Nat Cell Biol 12, 513-519.

Landgraf, P., Rusu, M., Sheridan, R., Sewer, A., Iovino, N., Aravin, A., Pfeffer, S., Rice, A., Kamphorst, A.O., Landthaler, M., Lin, C., Socci, N.D., Hermida, L., Fulci, V., Chiaretti, S., Foa, R., Schliwka, J., Fuchs, U., Novosel, A., Muller, R.U., Schermer, B., Bissels, U., Inman, J., Phan, Q., Chien, M., Weir, D.B., Choksi, R., De Vita, G., Frezzetti, D., Trompeter, H.I., Hornung, V., Teng, G., Hartmann, G., Palkovits, M., Di Lauro, R., Wernet, P., Macino, G., Rogler, C.E., Nagle, J.W., Ju, J., Papavasiliou, F.N., Benzing, T., Lichter, P., Tam, W., Brownstein, M.J., Bosio, A., Borkhardt, A., Russo, J.J., Sander, C., Zavolan, M., Tuschl, T., 2007. A mammalian microRNA expression atlas based on small RNA library sequencing. Cell 129, 1401-1414.

Leang, R.S., Wu, T.T., Hwang, S., Liang, L.T., Tong, L., Truong, J.T., Sun, R., 2011. The anti-interferon activity of conserved viral dUTPase ORF54 is essential for an effective MHV-68 infection. PLoS Pathog 7, e1002292.

Leber, M.F., Bossow, S., Leonard, V.H., Zaoui, K., Grossardt, C., Frenzke, M., Miest, T., Sawall, S., Cattaneo, R., von Kalle, C., Ungerechts, G., 2011. MicroRNA-sensitive oncolytic measles viruses for cancer-specific vector tropism. Mol Ther 19, 1097-1106.

Lee, R.C., Feinbaum, R.L., Ambros, V., 1993. The C. elegans heterochronic gene lin-4 encodes small RNAs with antisense complementarity to lin-14. Cell 75, 843-854.

Lee, Y., Kim, M., Han, J., Yeom, K.H., Lee, S., Baek, S.H., Kim, V.N., 2004. MicroRNA genes are transcribed by RNA polymerase II. EMBO J 23, 4051-4060.

Lei, X., Bai, Z., Ye, F., Xie, J., Kim, C.G., Huang, Y., Gao, S.J., 2010. Regulation of NF-kappaB inhibitor IkappaBalpha and viral replication by a KSHV microRNA. Nat Cell Biol 12, 193-199.

Lewin, A.R., Reid, L.E., McMahon, M., Stark, G.R., Kerr, I.M., 1991. Molecular analysis of a human interferon-inducible gene family. Eur J Biochem 199, 417-423.

Lewis, B.P., Burge, C.B., Bartel, D.P., 2005. Conserved seed pairing, often flanked by adenosines, indicates that thousands of human genes are microRNA targets. Cell 120, 15-20.

Li, K., Markosyan, R.M., Zheng, Y.M., Golfetto, O., Bungart, B., Li, M., Ding, S., He, Y., Liang, C., Lee, J.C., Gratton, E., Cohen, F.S., Liu, S.L., 2013a. IFITM proteins restrict viral membrane hemifusion. PLoS Pathog 9, e1003124.

Li, P., Shi, M.L., Shen, W.L., Zhang, Z., Xie, D.J., Zhang, X.Y., He, C., Zhang, Y., Zhao, Z.H., 2017. Coordinated regulation of IFITM1, 2 and 3 genes by an IFN-responsive enhancer through long-range chromatin interactions. Biochim Biophys Acta 1860, 885-893.

Li, W., Jia, X., Shen, C., Zhang, M., Xu, J., Shang, Y., Zhu, K., Hu, M., Yan, Q., Qin, D., Lee, M.S., Zhu, J., Lu, H., Krueger, B.J., Renne, R., Gao, S.J., Lu, C., 2016a. A KSHV microRNA enhances viral latency and induces angiogenesis by targeting GRK2 to activate the CXCR2/AKT pathway. Oncotarget 7, 32286-32305.

Li, W., Yan, Q., Ding, X., Shen, C., Hu, M., Zhu, Y., Qin, D., Lu, H., Krueger, B.J., Renne, R., Gao, S.J., Lu, C., 2016b. The SH3BGR/STAT3 Pathway Regulates Cell Migration and Angiogenesis Induced by a Gammaherpesvirus MicroRNA. PLoS Pathog 12, e1005605.

Li, Y., Masaki, T., Yamane, D., McGivern, D.R., Lemon, S.M., 2013b. Competing and noncompeting activities of miR-122 and the 5' exonuclease Xrn1 in regulation of hepatitis C virus replication. Proc Natl Acad Sci U S A 110, 1881-1886.

Lieber, D., Haas, J., 2011. Viruses and microRNAs: a toolbox for systematic analysis. Wiley Interdiscip Rev RNA 2, 787-801.

Lim, S.T., Rubin, N., Said, J., Levine, A.M., 2005. Primary effusion lymphoma: successful treatment with highly active antiretroviral therapy and rituximab. Ann Hematol 84, 551-552.

Lin, Y.T., Kincaid, R.P., Arasappan, D., Dowd, S.E., Hunicke-Smith, S.P., Sullivan, C.S., 2010. Small RNA profiling reveals antisense transcription throughout the KSHV genome and novel small RNAs. RNA 16, 1540-1558.

Lindsay, M.A., 2008. microRNAs and the immune response. Trends Immunol 29, 343-351.

Liu, C., Kelnar, K., Liu, B., Chen, X., Calhoun-Davis, T., Li, H., Patrawala, L., Yan, H., Jeter, C., Honorio, S., Wiggins, J.F., Bader, A.G., Fagin, R., Brown, D., Tang, D.G., 2011. The microRNA miR-34a inhibits prostate cancer stem cells and metastasis by directly repressing CD44. Nat Med 17, 211-215.

Liu, F., Du, Y., Feng, W.H., 2017a. New perspective of host microRNAs in the control of PRRSV infection. Vet Microbiol.

Liu, F., Zhou, Z.H., 2007. Comparative virion structures of human herpesviruses.

Liu, X., Happel, C., Ziegelbauer, J.M., 2017b. Kaposi's Sarcoma-Associated Herpesvirus MicroRNAs Target GADD45B To Protect Infected Cells from Cell Cycle Arrest and Apoptosis. J Virol 91.

Liu, Y., Zhou, Y., Wu, J., Zheng, P., Li, Y., Zheng, X., Puthiyakunnon, S., Tu, Z., Chen, X.G., 2015. The expression profile of Aedes albopictus miRNAs is altered by dengue virus serotype-2 infection. Cell Biosci 5, 16.

Lu, F., Stedman, W., Yousef, M., Renne, R., Lieberman, P.M., 2010. Epigenetic regulation of Kaposi's sarcoma-associated herpesvirus latency by virus-encoded microRNAs that target Rta and the cellular Rbl2-DNMT pathway. J Virol 84, 2697-2706.

Lu, J., Pan, Q., Rong, L., He, W., Liu, S.L., Liang, C., 2011. The IFITM proteins inhibit HIV-1 infection. J Virol 85, 2126-2137.

Lui, A.J., Geanes, E.S., Ogony, J., Behbod, F., Marquess, J., Valdez, K., Jewell, W., Tawfik, O., Lewis-Wambi, J., 2017. IFITM1 suppression blocks proliferation and invasion of aromatase inhibitor-resistant breast cancer in vivo by JAK/STAT-mediated induction of p21. Cancer Lett 399, 29-43.

Lukac, D.M., Renne, R., Kirshner, J.R., Ganem, D., 1998. Reactivation of Kaposi's sarcoma-associated herpesvirus infection from latency by expression of the ORF 50 transactivator, a homolog of the EBV R protein. Virology 252, 304-312.

Macfarlane, L.A., Murphy, P.R., 2010. MicroRNA: Biogenesis, Function and Role in Cancer. Curr Genomics 11, 537-561.

Maisch, T., Kropff, B., Sinzger, C., Mach, M., 2002. Upregulation of CD40 expression on endothelial cells infected with human cytomegalovirus. J Virol 76, 12803-12812.

Makharoblidze, E., Goishvili, N., McHedlishvili, M., Jangavadze, M., 2015. Primary Kaposi's sarcoma of the heart in non-immunodeficient patient: case report and literature review. Diagn Pathol 10, 111.

Mbulaiteye, S.M., Biggar, R.J., Pfeiffer, R.M., Bakaki, P.M., Gamache, C., Owor, A.M., Katongole-Mbidde, E., Ndugwa, C.M., Goedert, J.J., Whitby, D., Engels, E.A., 2005. Water, socioeconomic factors, and human herpesvirus 8 infection in Ugandan children and their mothers. J Acquir Immune Defic Syndr 38, 474-479.

Mbulaiteye, S.M., Pfeiffer, R.M., Engels, E.A., Marshall, V., Bakaki, P.M., Owor, A.M., Ndugwa, C.M., Katongole-Mbidde, E., Goedert, J.J., Biggar, R.J., Whitby, D., 2004. Detection of kaposi sarcoma-associated herpesvirus DNA in saliva and buffy-coat samples from children with sickle cell disease in Uganda. J Infect Dis 190, 1382-1386.

Mencia, A., Modamio-Hoybjor, S., Redshaw, N., Morin, M., Mayo-Merino, F., Olavarrieta, L., Aguirre, L.A., del Castillo, I., Steel, K.P., Dalmay, T., Moreno, F., Moreno-Pelayo, M.A., 2009. Mutations in the seed region of human miR-96 are responsible for nonsyndromic progressive hearing loss. Nat Genet 41, 609-613.

Meshesha, M.K., Veksler-Lublinsky, I., Isakov, O., Reichenstein, I., Shomron, N., Kedem, K., Ziv-Ukelson, M., Bentwich, Z., Avni, Y.S., 2012. The microRNA Transcriptome of Human Cytomegalovirus (HCMV). Open Virol J 6, 38-48.

Mesri, E.A., Cesarman, E., Arvanitakis, L., Rafii, S., Moore, M.A., Posnett, D.N., Knowles, D.M., Asch, A.S., 1996. Human herpesvirus-8/Kaposi's sarcoma-associated herpesvirus is a new transmissible virus that infects B cells. J Exp Med 183, 2385-2390.

Mesri, E.A., Feitelson, M.A., Munger, K., 2014. Human viral oncogenesis: a cancer hallmarks analysis. Cell Host Microbe 15, 266-282.

Montgomery, R.L., Yu, G., Latimer, P.A., Stack, C., Robinson, K., Dalby, C.M., Kaminski, N., van Rooij, E., 2014. MicroRNA mimicry blocks pulmonary fibrosis. EMBO Mol Med 6, 1347-1356.

Morrison, B.J., Labo, N., Miley, W.J., Whitby, D., 2015. Serodiagnosis for tumor viruses. Semin Oncol 42, 191-206.

Mudhasani, R., Tran, J.P., Retterer, C., Radoshitzky, S.R., Kota, K.P., Altamura, L.A., Smith, J.M., Packard, B.Z., Kuhn, J.H., Costantino, J., Garrison, A.R., Schmaljohn, C.S., Huang, I.C., Farzan, M., Bavari, S., 2013. IFITM-2 and IFITM-3 but not IFITM-1 restrict Rift Valley fever virus. J Virol 87, 8451-8464.

Muller, M.R., Rao, A., 2010. NFAT, immunity and cancer: a transcription factor comes of age. Nat Rev Immunol 10, 645-656.

Muller, S., Rycak, L., Winter, P., Kahl, G., Koch, I., Rotter, B., 2013. omiRas: a Web server for differential expression analysis of miRNAs derived from small RNA-Seq data. Bioinformatics 29, 2651-2652.

Murphy, C., Hawkes, E., Chionh, F., Chong, G., 2017. Durable remission of both multicentric Castleman's disease and Kaposi's sarcoma with valganciclovir, rituximab and liposomal doxorubicin in an HHV-8-positive, HIV-negative patient. J Clin Pharm Ther 42, 111-114.

Murphy, E., Vanicek, J., Robins, H., Shenk, T., Levine, A.J., 2008. Suppression of immediate-early viral gene expression by herpesvirus-coded microRNAs: implications for latency. Proc Natl Acad Sci U S A 105, 5453-5458.

Myoung, J., Ganem, D., 2011. Infection of lymphoblastoid cell lines by Kaposi's sarcoma-associated herpesvirus: critical role of cell-associated virus. J Virol 85, 9767-9777.

Nachmani, D., Stern-Ginossar, N., Sarid, R., Mandelboim, O., 2009. Diverse herpesvirus microRNAs target the stress-induced immune ligand MICB to escape recognition by natural killer cells. Cell Host Microbe 5, 376-385.

Naranatt, P.P., Akula, S.M., Zien, C.A., Krishnan, H.H., Chandran, B., 2003. Kaposi's sarcoma-associated herpesvirus induces the phosphatidylinositol 3-kinase-PKC-zeta-MEK-ERK signaling pathway in target cells early during infection: implications for infectivity. J Virol 77, 1524-1539.

Naranatt, P.P., Krishnan, H.H., Svojanovsky, S.R., Bloomer, C., Mathur, S., Chandran, B., 2004. Host gene induction and transcriptional reprogramming in Kaposi's sarcoma-associated herpesvirus (KSHV/HHV-8)-infected endothelial, fibroblast, and B cells: insights into modulation events early during infection. Cancer Res 64, 72-84.

Narayana, S.K., Helbig, K.J., McCartney, E.M., Eyre, N.S., Bull, R.A., Eltahla, A., Lloyd, A.R., Beard, M.R., 2015. The Interferon-induced Transmembrane Proteins, IFITM1, IFITM2, and IFITM3 Inhibit Hepatitis C Virus Entry. J Biol Chem 290, 25946-25959.

Nathans, R., Chu, C.Y., Serquina, A.K., Lu, C.C., Cao, H., Rana, T.M., 2009. Cellular microRNA and P bodies modulate host-HIV-1 interactions. Mol Cell 34, 696-709.

Neipel, F., Fleckenstein, B., 1999. The role of HHV-8 in Kaposi's sarcoma. Semin Cancer Biol 9, 151-164.

Nemerow, G.R., Cheresh, D.A., 2002. Herpesvirus hijacks an integrin. Nat Cell Biol 4, E69-71.

Nethe, M., Berkhout, B., van der Kuyl, A.C., 2005. Retroviral superinfection resistance. Retrovirology 2, 52.

Nian, Q., Chi, J., Xiao, Q., Wei, C., Costeas, P., Yang, Z., Liu, L., Wang, L., 2015. SPARC ectopic overexpression inhibits growth and promotes programmed cell death in acute myeloid leukemia transformed from myelodysplastic syndrome cells, alone and in combination with Ara-C treatment. Oncol Rep 34, 1406-1414.

Ning, M.S., Kim, A.S., Prasad, N., Levy, S.E., Zhang, H., Andl, T., 2014. Characterization of the Merkel Cell Carcinoma miRNome. J Skin Cancer 2014, 289548.

Ninova, M., Ronshaugen, M., Griffiths-Jones, S., 2016. MicroRNA evolution, expression, and function during short germband development in Tribolium castaneum. Genome Res 26, 85-96.

Noh, K., Kim, M., Kim, Y., Kim, H., Byun, J., Park, Y., Lee, H., Lee, Y.S., Choe, J., Kim, Y.M., Jeoung, D., 2017. miR-122-SOCS1-JAK2 axis regulates allergic inflammation and allergic inflammation-promoted cellular interactions. Oncotarget 8, 63155-63176.

Norman, K.L., Sarnow, P., 2010. Modulation of hepatitis C virus RNA abundance and the isoprenoid biosynthesis pathway by microRNA miR-122 involves distinct mechanisms. J Virol 84, 666-670.

Nourse, J.P., Crooks, P., Keane, C., Nguyen-Van, D., Mujaj, S., Ross, N., Jones, K., Vari, F., Han, E., Trappe, R., Fink, S., Gandhi, M.K., 2012. Expression profiling of Epstein-Barr virus-encoded microRNAs from paraffin-embedded formalin-fixed primary Epstein-Barr virus-positive B-cell lymphoma samples. J Virol Methods 184, 46-54.

O'Hara, A.J., Vahrson, W., Dittmer, D.P., 2008. Gene alteration and precursor and mature microRNA transcription changes contribute to the miRNA signature of primary effusion lymphoma. Blood 111, 2347-2353.

O'Hara, A.J., Wang, L., Dezube, B.J., Harrington, W.J., Jr., Damania, B., Dittmer, D.P., 2009. Tumor suppressor microRNAs are underrepresented in primary effusion lymphoma and Kaposi sarcoma. Blood 113, 5938-5941.

Ohsaki, E., Ueda, K., 2012. Kaposi's Sarcoma-Associated Herpesvirus Genome Replication, Partitioning, and Maintenance in Latency. Front Microbiol 3, 7.

Okada, C., Yamashita, E., Lee, S.J., Shibata, S., Katahira, J., Nakagawa, A., Yoneda, Y., Tsukihara, T., 2009. A high-resolution structure of the pre-microRNA nuclear export machinery. Science 326, 1275-1279.

Orom, U.A., Nielsen, F.C., Lund, A.H., 2008. MicroRNA-10a binds the 5'UTR of ribosomal protein mRNAs and enhances their translation. Mol Cell 30, 460-471.

Ostermann, E., Tuddenham, L., Macquin, C., Alsaleh, G., Schreiber-Becker, J., Tanguy, M., Bahram, S., Pfeffer, S., Georgel, P., 2012. Deregulation of type I IFN-dependent genes correlates with increased susceptibility to cytomegalovirus acute infection of dicer mutant mice. PLoS One 7, e43744.

Otsuka, M., Jing, Q., Georgel, P., New, L., Chen, J., Mols, J., Kang, Y.J., Jiang, Z., Du, X., Cook, R., Das, S.C., Pattnaik, A.K., Beutler, B., Han, J., 2007. Hypersusceptibility to vesicular stomatitis virus infection in Dicer1-deficient mice is due to impaired miR24 and miR93 expression. Immunity 27, 123-134.

Padua, D., Mahurkar-Joshi, S., Law, I.K., Polytarchou, C., Vu, J.P., Pisegna, J.R., Shih, D., Iliopoulos, D., Pothoulakis, C., 2016. A long noncoding RNA signature for ulcerative colitis identifies IFNG-AS1 as an enhancer of inflammation. Am J Physiol Gastrointest Liver Physiol 311, G446-457.

Pan, H., Xie, J., Ye, F., Gao, S.J., 2006. Modulation of Kaposi's sarcoma-associated herpesvirus infection and replication by MEK/ERK, JNK, and p38 multiple mitogen-activated protein kinase pathways during primary infection. J Virol 80, 5371-5382.

Paraskevopoulou, M.D., Georgakilas, G., Kostoulas, N., Vlachos, I.S., Vergoulis, T., Reczko, M., Filippidis, C., Dalamagas, T., Hatzigeorgiou, A.G., 2013. DIANA-microT web server v5.0: service integration into miRNA functional analysis workflows. Nucleic Acids Res 41, W169-173.

Park, J.K., Kogure, T., Nuovo, G.J., Jiang, J., He, L., Kim, J.H., Phelps, M.A., Papenfuss, T.L., Croce, C.M., Patel, T., Schmittgen, T.D., 2011. miR-221 silencing blocks hepatocellular carcinoma and promotes survival. Cancer Res 71, 7608-7616.

Pecot, C.V., Rupaimoole, R., Yang, D., Akbani, R., Ivan, C., Lu, C., Wu, S., Han, H.D., Shah, M.Y., Rodriguez-Aguayo, C., Bottsford-Miller, J., Liu, Y., Kim, S.B., Unruh, A., Gonzalez-Villasana, V., Huang, L., Zand, B., Moreno-Smith, M., Mangala, L.S., Taylor, M., Dalton, H.J., Sehgal, V., Wen, Y., Kang, Y., Baggerly, K.A., Lee, J.S., Ram, P.T., Ravoori, M.K., Kundra, V., Zhang, X., Ali-Fehmi, R., Gonzalez-Angulo, A.M., Massion, P.P., Calin, G.A., Lopez-Berestein, G., Zhang, W., Sood, A.K., 2013. Tumour angiogenesis regulation by the miR-200 family. Nat Commun 4, 2427.

Pedersen, I.M., Cheng, G., Wieland, S., Volinia, S., Croce, C.M., Chisari, F.V., David, M., 2007. Interferon modulation of cellular microRNAs as an antiviral mechanism. Nature 449, 919-922.

Perez, J.T., Pham, A.M., Lorini, M.H., Chua, M.A., Steel, J., tenOever, B.R., 2009. MicroRNA-mediated species-specific attenuation of influenza A virus. Nat Biotechnol 27, 572-576.

Perreira, J.M., Chin, C.R., Feeley, E.M., Brass, A.L., 2013. IFITMs restrict the replication of multiple pathogenic viruses. J Mol Biol 425, 4937-4955.

Pfeffer, S., Sewer, A., Lagos-Quintana, M., Sheridan, R., Sander, C., Grasser, F.A., van Dyk, L.F., Ho, C.K., Shuman, S., Chien, M., Russo, J.J., Ju, J., Randall, G., Lindenbach, B.D., Rice, C.M., Simon, V., Ho, D.D., Zavolan, M., Tuschl, T., 2005. Identification of microRNAs of the herpesvirus family. Nat Methods 2, 269-276.

Pfeffer, S., Zavolan, M., Grasser, F.A., Chien, M., Russo, J.J., Ju, J., John, B., Enright, A.J., Marks, D., Sander, C., Tuschl, T., 2004. Identification of virus-encoded microRNAs. Science 304, 734-736.

Polizzotto, M.N., Uldrick, T.S., Hu, D., Yarchoan, R., 2012. Clinical Manifestations of Kaposi Sarcoma Herpesvirus Lytic Activation: Multicentric Castleman Disease (KSHV-MCD) and the KSHV Inflammatory Cytokine Syndrome. Front Microbiol 3, 73.

Pramanik, D., Campbell, N.R., Karikari, C., Chivukula, R., Kent, O.A., Mendell, J.T., Maitra, A., 2011. Restitution of tumor suppressor microRNAs using a systemic nanovector inhibits pancreatic cancer growth in mice. Mol Cancer Ther 10, 1470-1480.

Pugalagiri, P., Muller, S., Cox, D.P., Kessler, H.P., Wright, J.M., Cheng, Y.S., 2013. Lymphangioma-like Kaposi sarcoma of the oral mucosa. Oral Surg Oral Med Oral Pathol Oral Radiol 116, 84-90.

Qin, J., Li, W., Gao, S.J., Lu, C., 2017a. KSHV microRNAs: Tricks of the Devil. Trends Microbiol.

Qin, J., Li, W., Gao, S.J., Lu, C., 2017b. KSHV microRNAs: Tricks of the Devil. Trends Microbiol 25, 648-661.

Qin, Z., Kearney, P., Plaisance, K., Parsons, C.H., 2010. Pivotal advance: Kaposi's sarcoma-associated herpesvirus (KSHV)-encoded microRNA specifically induce IL-6 and IL-10 secretion by macrophages and monocytes. J Leukoc Biol 87, 25-34.

Qin, Z., Peruzzi, F., Reiss, K., Dai, L., 2014. Role of host microRNAs in Kaposi's sarcoma-associated herpesvirus pathogenesis. Viruses 6, 4571-4580.

Raposo, R.A., de Mulder Rougvie, M., Paquin-Proulx, D., Brailey, P.M., Cabido, V.D., Zdinak, P.M., Thomas, A.S., Huang, S.H., Beckerle, G.A., Jones, R.B., Nixon, D.F., 2017. IFITM1 targets HIV-1 latently infected cells for antibody-dependent cytolysis. JCI insight 2, e85811.

Rappocciolo, G., Hensler, H.R., Jais, M., Reinhart, T.A., Pegu, A., Jenkins, F.J., Rinaldo, C.R., 2008. Human herpesvirus 8 infects and replicates in primary cultures of activated B lymphocytes through DC-SIGN. J Virol 82, 4793-4806.

Rappocciolo, G., Jenkins, F.J., Hensler, H.R., Piazza, P., Jais, M., Borowski, L., Watkins, S.C., Rinaldo, C.R., Jr., 2006. DC-SIGN is a receptor for human herpesvirus 8 on dendritic cells and macrophages. J Immunol 176, 1741-1749.

Reid, G., Kao, S.C., Pavlakis, N., Brahmbhatt, H., MacDiarmid, J., Clarke, S., Boyer, M., van Zandwijk, N., 2016. Clinical development of TargomiRs, a miRNA mimic-based treatment for patients with recurrent thoracic cancer. Epigenomics 8, 1079-1085.

Reid, L.E., Brasnett, A.H., Gilbert, C.S., Porter, A.C., Gewert, D.R., Stark, G.R., Kerr, I.M., 1989. A single DNA response element can confer inducibility by both alpha- and gamma-interferons. Proc Natl Acad Sci U S A 86, 840-844.

Renwick, N., Weverling, G.J., Brouwer, J., Bakker, M., Schulz, T.F., Goudsmit, J., 2002. Vascular endothelial growth factor levels in serum do not increase following HIV type 1 and HHV8 seroconversion and lack correlation with AIDS-related Kaposi's sarcoma. AIDS Res Hum Retroviruses 18, 695-698.

Reuter, J.S., Mathews, D.H., 2010. RNAstructure: software for RNA secondary structure prediction and analysis. BMC Bioinformatics 11, 129.

Robinson, A.R., Kwek, S.S., Hagemeier, S.R., Wille, C.K., Kenney, S.C., 2011. Cellular transcription factor Oct-1 interacts with the Epstein-Barr virus BRLF1 protein to promote disruption of viral latency. J Virol 85, 8940-8953.

Rougvie, A.E., 2001. Control of developmental timing in animals. Nat Rev Genet 2, 690-701.

Samols, M.A., Hu, J., Skalsky, R.L., Renne, R., 2005. Cloning and identification of a microRNA cluster within the latency-associated region of Kaposi's sarcoma-associated herpesvirus. J Virol 79, 9301-9305.

Samols, M.A., Skalsky, R.L., Maldonado, A.M., Riva, A., Lopez, M.C., Baker, H.V., Renne, R., 2007. Identification of cellular genes targeted by KSHV-encoded microRNAs. PLoS Pathog 3, e65.

Samuel, C.E., 2001. Antiviral actions of interferons. Clin Microbiol Rev 14, 778-809, table of contents.

Sanchez-Mut, J.V., Aso, E., Panayotis, N., Lott, I., Dierssen, M., Rabano, A., Urdinguio, R.G., Fernandez, A.F., Astudillo, A., Martin-Subero, J.I., Balint, B., Fraga, M.F., Gomez, A., Gurnot, C., Roux, J.C., Avila, J., Hensch, T.K., Ferrer, I., Esteller, M., 2013. DNA methylation map of mouse and human brain identifies target genes in Alzheimer's disease. Brain 136, 3018-3027.

Schalling, M., Ekman, M., Kaaya, E.E., Linde, A., Biberfeld, P., 1995. A role for a new herpes virus (KSHV) in different forms of Kaposi's sarcoma. Nat Med 1, 707-708.

Schmittgen, T.D., Livak, K.J., 2008. Analyzing real-time PCR data by the comparative C(T) method. Nature protocols 3, 1101-1108.

Schneider, W.M., Chevillotte, M.D., Rice, C.M., 2014. Interferon-stimulated genes: a complex web of host defenses. Annu Rev Immunol 32, 513-545.

Schoggins, J.W., Rice, C.M., 2011. Interferon-stimulated genes and their antiviral effector functions. Curr Opin Virol 1, 519-525.

Schwartz, R.A., 2004. Kaposi's sarcoma: an update. J Surg Oncol 87, 146-151.

Seimandi, M., Lemaire, G., Pillon, A., Perrin, A., Carlavan, I., Voegel, J.J., Vignon, F., Nicolas, J.C., Balaguer, P., 2005. Differential responses of PPARalpha, PPARdelta, and PPARgamma reporter cell lines to selective PPAR synthetic ligands. Anal Biochem 344, 8-15.

Shao, P., Qu, W.K., Wang, C.Y., Tian, Y., Ye, M.L., Sun, D.G., Sui, J.D., Wang, L.M., Fan, R., Gao, Z.M., 2017. MicroRNA-205-5p regulates the chemotherapeutic resistance of hepatocellular carcinoma cells by targeting PTEN/JNK/ANXA3 pathway. Am J Transl Res 9, 4300-4307.

Shapiro, J.S., Varble, A., Pham, A.M., Tenoever, B.R., 2010. Noncanonical cytoplasmic processing of viral microRNAs. RNA 16, 2068-2074.

Sharma-Walia, N., Krishnan, H.H., Naranatt, P.P., Zeng, L., Smith, M.S., Chandran, B., 2005. ERK1/2 and MEK1/2 induced by Kaposi's sarcoma-associated herpesvirus (human herpesvirus 8) early during infection of target cells are essential for expression of viral genes and for establishment of infection. J Virol 79, 10308-10329.

Sharma-Walia, N., Raghu, H., Sadagopan, S., Sivakumar, R., Veettil, M.V., Naranatt, P.P., Smith, M.M., Chandran, B., 2006. Cyclooxygenase 2 induced by Kaposi's sarcoma-associated herpesvirus early during in vitro infection of target cells plays a role in the maintenance of latent viral gene expression. J Virol 80, 6534-6552.

Sharp, T.V., Boshoff, C., 2000. Kaposi's sarcoma-associated herpesvirus: from cell biology to pathogenesis. IUBMB Life 49, 97-104.

Sharp, T.V., Wang, H.W., Koumi, A., Hollyman, D., Endo, Y., Ye, H., Du, M.Q., Boshoff, C., 2002. K15 protein of Kaposi's sarcoma-associated herpesvirus is latently expressed and binds to HAX-1, a protein with antiapoptotic function. J Virol 76, 802-816.

Shiryaev, A., Kostenko, S., Dumitriu, G., Moens, U., 2012. Septin 8 is an interaction partner and in vitro substrate of MK5. World J Biol Chem 3, 98-109.

Shrivastava, S., Steele, R., Ray, R., Ray, R.B., 2015. MicroRNAs: Role in Hepatitis C Virus pathogenesis. Genes Dis 2, 35-45.

Sibley, C.R., Seow, Y., Saayman, S., Dijkstra, K.K., El Andaloussi, S., Weinberg, M.S., Wood, M.J., 2012. The biogenesis and characterization of mammalian microRNAs of mirtron origin. Nucleic Acids Res 40, 438-448.

Simas, J.P., Efstathiou, S., 1998. Murine gammaherpesvirus 68: a model for the study of gammaherpesvirus pathogenesis. Trends Microbiol 6, 276-282.

Skalsky, R.L., Cullen, B.R., 2010. Viruses, microRNAs, and host interactions. Annu Rev Microbiol 64, 123-141.

Slonchak, A., Hussain, M., Torres, S., Asgari, S., Khromykh, A.A., 2014. Expression of mosquito microRNA Aae-miR-2940-5p is downregulated in response to West Nile virus infection to restrict viral replication. J Virol 88, 8457-8467.

Smith, R.A., Young, J., Weis, J.J., Weis, J.H., 2006. Expression of the mouse fragilis gene products in immune cells and association with receptor signaling complexes. Genes Immun 7, 113-121.

Song, M.S., Salmena, L., Pandolfi, P.P., 2012. The functions and regulation of the PTEN tumour suppressor. Nat Rev Mol Cell Biol 13, 283-296.

Song, S.N., Tomosugi, N., Kawabata, H., Ishikawa, T., Nishikawa, T., Yoshizaki, K., 2010. Down-regulation of hepcidin resulting from long-term treatment with an anti-IL-6 receptor antibody (tocilizumab) improves anemia of inflammation in multicentric Castleman disease. Blood 116, 3627-3634.

Soulier, J., Grollet, L., Oksenhendler, E., Cacoub, P., Cazals-Hatem, D., Babinet, P., d'Agay, M.F., Clauvel, J.P., Raphael, M., Degos, L., et al., 1995. Kaposi's sarcoma-associated herpesvirus-like DNA sequences in multicentric Castleman's disease. Blood 86, 1276-1280.

Spear, P.G., Longnecker, R., 2003. Herpesvirus entry: an update. J Virol 77, 10179-10185.

Stanescu, L., Foarfa, C., Georgescu, A.C., Georgescu, I., 2007. Kaposi's sarcoma associated with AIDS. Rom J Morphol Embryol 48, 181-187.

Stark, T.J., Arnold, J.D., Spector, D.H., Yeo, G.W., 2012. High-resolution profiling and analysis of viral and host small RNAs during human cytomegalovirus infection. J Virol 86, 226-235.

Steer, B., Adler, B., Jonjic, S., Stewart, J.P., Adler, H., 2010. A gammaherpesvirus complement regulatory protein promotes initiation of infection by activation of protein kinase Akt/PKB. PLoS One 5, e11672.

Steitz, J., Borah, S., Cazalla, D., Fok, V., Lytle, R., Mitton-Fry, R., Riley, K., Samji, T., 2011. Noncoding RNPs of viral origin. Cold Spring Harb Perspect Biol 3.

Stiglincova, V., Chalupkova, A., Hrabovska, Z., Cipkova, J., Wagnerova, M., Mistrikova, J., 2011. Vertical transmission of murine gammaherpesvirus 68 in mice. Acta virologica 55, 55-59.

Stringer, S.E., Gallagher, J.T., 1997. Specific binding of the chemokine platelet factor 4 to heparan sulfate. J Biol Chem 272, 20508-20514.

Suffert, G., Malterer, G., Hausser, J., Viiliainen, J., Fender, A., Contrant, M., Ivacevic, T., Benes, V., Gros, F., Voinnet, O., Zavolan, M., Ojala, P.M., Haas, J.G., Pfeffer, S., 2011. Kaposi's sarcoma herpesvirus microRNAs target caspase 3 and regulate apoptosis. PLoS Pathog 7, e1002405.

Sun, H., Zhou, Z., Dong, Y., Yang, A., Jiang, J., Chen, Z., Guan, X., Wang, B., Gao, S., Jiang, B., 2016. Expression analysis of microRNAs related to the skin ulceration syndrome of sea cucumber Apostichopus japonicus. Fish Shellfish Immunol 49, 205-212.

Sun, R., Lin, S.F., Staskus, K., Gradoville, L., Grogan, E., Haase, A., Miller, G., 1999. Kinetics of Kaposi's sarcoma-associated herpesvirus gene expression. J Virol 73, 2232-2242.

Swaminathan, G., Martin-Garcia, J., Navas-Martin, S., 2013. RNA viruses and microRNAs: challenging discoveries for the 21st century. Physiol Genomics 45, 1035-1048.

Szajerka, T., Jablecki, J., 2007. Kaposi's sarcoma revisited. AIDS Rev 9, 230-236.

Takeuchi, O., Akira, S., 2010. Pattern recognition receptors and inflammation. Cell 140, 805-820.

Tamburro, K.M., Yang, D., Poisson, J., Fedoriw, Y., Roy, D., Lucas, A., Sin, S.H., Malouf, N., Moylan, V., Damania, B., Moll, S., van der Horst, C., Dittmer, D.P., 2012. Vironome of Kaposi sarcoma associated herpesvirus-inflammatory cytokine syndrome in an AIDS patient reveals co-infection of human herpesvirus 8 and human herpesvirus 6A. Virology 433, 220-225.

Tan, X., Gao, Y., Nan, Y., Zhang, J., Di, C., Wang, X., Lian, F., Cao, Y., Hu, Y., Xu, L., Ma, H., Hong, Y., Liu, T., Wu, Y., Xu, X., Yan, Y., Yang, L., 2015. Cellular MicroRNA Let-7a Suppresses KSHV Replication through Targeting MAP4K4 Signaling Pathways. PLoS ONE 10, e0132148.

Tanaka, S.S., Yamaguchi, Y.L., Tsoi, B., Lickert, H., Tam, P.P., 2005. IFITM/Mil/fragilis family proteins IFITM1 and IFITM3 play distinct roles in mouse primordial germ cell homing and repulsion. Dev Cell 9, 745-756.

Tang, G., Tang, X., 2013. Short tandem target mimic: a long journey to the engineered molecular landmine for selective destruction/blockage of microRNAs in plants and animals. J Genet Genomics 40, 291-296.

Tang, S., Patel, A., Krause, P.R., 2009. Novel less-abundant viral microRNAs encoded by herpes simplex virus 2 latency-associated transcript and their roles in regulating ICP34.5 and ICP0 mRNAs. J Virol 83, 1433-1442.

Taylor, G.S., Blackbourn, D.J., 2011. Infectious agents in human cancers: lessons in immunity and immunomodulation from gammaherpesviruses EBV and KSHV. Cancer Lett 305, 263-278.

tenOever, B.R., 2013. RNA viruses and the host microRNA machinery. Nat Rev Microbiol 11, 169-180.

Teruel-Montoya, R., Kong, X., Abraham, S., Ma, L., Kunapuli, S.P., Holinstat, M., Shaw, C.A., McKenzie, S.E., Edelstein, L.C., Bray, P.F., 2014. MicroRNA expression differences in human hematopoietic cell lineages enable regulated transgene expression. PLoS One 9, e102259.

Titze-de-Almeida, R., David, C., Titze-de-Almeida, S.S., 2017. The Race of 10 Synthetic RNAi-Based Drugs to the Pharmaceutical Market. Pharm Res 34, 1339-1363.

Toth, Z., Brulois, K., Jung, J.U., 2013. The chromatin landscape of Kaposi's sarcoma-associated herpesvirus. Viruses 5, 1346-1373.

Trang, P., Wiggins, J.F., Daige, C.L., Cho, C., Omotola, M., Brown, D., Weidhaas, J.B., Bader, A.G., Slack, F.J., 2011. Systemic delivery of tumor suppressor microRNA mimics using a neutral lipid emulsion inhibits lung tumors in mice. Mol Ther 19, 1116-1122.

Traylen, C.M., Patel, H.R., Fondaw, W., Mahatme, S., Williams, J.F., Walker, L.R., Dyson, O.F., Arce, S., Akula, S.M., 2011. Virus reactivation: a panoramic view in human infections. Future Virol 6, 451-463.

Treiber, T., Treiber, N., Meister, G., 2012. Regulation of microRNA biogenesis and function. Thromb Haemost 107, 605-610.

Trionfini, P., Benigni, A., 2017. MicroRNAs as Master Regulators of Glomerular Function in Health and Disease. J Am Soc Nephrol.

Trobaugh, D.W., Gardner, C.L., Sun, C., Haddow, A.D., Wang, E., Chapnik, E., Mildner, A., Weaver, S.C., Ryman, K.D., Klimstra, W.B., 2014. RNA viruses can hijack vertebrate microRNAs to suppress innate immunity. Nature 506, 245-248.

Tsai, Y.H., Wu, M.F., Wu, Y.H., Chang, S.J., Lin, S.F., Sharp, T.V., Wang, H.W., 2009. The M type K15 protein of Kaposi's sarcoma-associated herpesvirus regulates microRNA expression via its SH2-binding motif to induce cell migration and invasion. J Virol 83, 622-632.

Tuddenham, L., Jung, J.S., Chane-Woon-Ming, B., Dolken, L., Pfeffer, S., 2012. Small RNA deep sequencing identifies microRNAs and other small noncoding RNAs from human herpesvirus 6B. J Virol 86, 1638-1649.

Uldrick, T.S., Whitby, D., 2011. Update on KSHV epidemiology, Kaposi Sarcoma pathogenesis, and treatment of Kaposi Sarcoma. Cancer Lett 305, 150-162.

Umbach, J.L., Cullen, B.R., 2010. In-depth analysis of Kaposi's sarcoma-associated herpesvirus microRNA expression provides insights into the mammalian microRNA-processing machinery. J Virol 84, 695-703.

Umbach, J.L., Wang, K., Tang, S., Krause, P.R., Mont, E.K., Cohen, J.I., Cullen, B.R., 2010. Identification of viral microRNAs expressed in human sacral ganglia latently infected with herpes simplex virus 2. J Virol 84, 1189-1192.

Uppal, T., Banerjee, S., Sun, Z., Verma, S.C., Robertson, E.S., 2014. KSHV LANA--the master regulator of KSHV latency. Viruses 6, 4961-4998.

Uppal, T., Jha, H.C., Verma, S.C., Robertson, E.S., 2015. Chromatinization of the KSHV Genome During the KSHV Life Cycle. Cancers (Basel) 7, 112-142.

van der Ree, M.H., de Vree, J.M., Stelma, F., Willemse, S., van der Valk, M., Rietdijk, S., Molenkamp, R., Schinkel, J., van Nuenen, A.C., Beuers, U., Hadi, S., Harbers, M., van der Veer, E., Liu, K., Grundy, J., Patick, A.K., Pavlicek, A., Blem, J., Huang, M., Grint, P., Neben, S., Gibson, N.W., Kootstra, N.A., Reesink, H.W., 2017. Safety, tolerability, and antiviral effect of RG-101 in patients with chronic hepatitis C: a phase 1B, double-blind, randomised controlled trial. Lancet 389, 709-717.

Van Peer, G., Lefever, S., Anckaert, J., Beckers, A., Rihani, A., Van Goethem, A., Volders, P.J., Zeka, F., Ongenaert, M., Mestdagh, P., Vandesompele, J., 2014. miRBase Tracker: keeping track of microRNA annotation changes. Database (Oxford) 2014.

Vasudevan, S., Steitz, J.A., 2007. AU-rich-element-mediated upregulation of translation by FXR1 and Argonaute 2. Cell 128, 1105-1118.

Vejnar, C.E., Zdobnov, E.M., 2012. MiRmap: comprehensive prediction of microRNA target repression strength. Nucleic Acids Res 40, 11673-11683.

Vodovar, N., Bronkhorst, A.W., van Cleef, K.W., Miesen, P., Blanc, H., van Rij, R.P., Saleh, M.C., 2012. Arbovirus-derived piRNAs exhibit a ping-pong signature in mosquito cells. PLoS ONE 7, e30861.

Vogler, M., Walter, H.S., Dyer, M.J.S., 2017. Targeting anti-apoptotic BCL2 family proteins in haematological malignancies - from pathogenesis to treatment. Br J Haematol.

Walker, L.R., Hussein, H.A., Akula, S.M., 2014. Disintegrin-like domain of glycoprotein B regulates Kaposi's sarcoma-associated herpesvirus infection of cells. J Gen Virol.

Walker, L.R., Hussein, H.A., Akula, S.M., 2016. Subcellular fractionation method to study endosomal trafficking of Kaposi's sarcoma-associated herpesvirus. Cell & bioscience 6, 1.

Wang, D., Shanina, I., Toyofuku, W.M., Horwitz, M.S., Scott, M.D., 2015. Inhibition of Autoimmune Diabetes in NOD Mice by miRNA Therapy. PLoS ONE 10, e0145179.

Wang, H.W., Trotter, M.W., Lagos, D., Bourboulia, D., Henderson, S., Makinen, T., Elliman, S., Flanagan, A.M., Alitalo, K., Boshoff, C., 2004. Kaposi sarcoma herpesvirus-induced cellular reprogramming contributes to the lymphatic endothelial gene expression in Kaposi sarcoma. Nat Genet 36, 687-693.

Wang, Z., Tan, Y., Yu, W., Zheng, S., Zhang, S., Sun, L., Ding, K., 2017. Small role with big impact: miRNAs as communicators in the cross-talk between cancer-associated fibroblasts and cancer cells. Int J Biol Sci 13, 339-348.

Warren, C.J., Griffin, L.M., Little, A.S., Huang, I.C., Farzan, M., Pyeon, D., 2014. The antiviral restriction factors IFITM1, 2 and 3 do not inhibit infection of human papillomavirus, cytomegalovirus and adenovirus. PLoS One 9, e96579.

Weidner, J.M., Jiang, D., Pan, X.B., Chang, J., Block, T.M., Guo, J.T., 2010. Interferon-induced cell membrane proteins, IFITM3 and tetherin, inhibit vesicular stomatitis virus infection via distinct mechanisms. J Virol 84, 12646-12657.

West, J.A., Damania, B., 2010. Kaposi's sarcoma-associated herpesvirus and innate immunity. Future Virol 5, 185-196.

Westmoreland, S.V., Mansfield, K.G., 2008. Comparative pathobiology of Kaposi sarcoma-associated herpesvirus and related primate rhadinoviruses. Comp Med 58, 31-42.

Whitby, D., Luppi, M., Barozzi, P., Boshoff, C., Weiss, R.A., Torelli, G., 1998. Human herpesvirus 8 seroprevalence in blood donors and lymphoma patients from different regions of Italy. J Natl Cancer Inst 90, 395-397.

White, D.W., Suzanne Beard, R., Barton, E.S., 2012. Immune modulation during latent herpesvirus infection. Immunol Rev 245, 189-208.

Wiebusch, L., Uecker, R., Hagemeier, C., 2003. Human cytomegalovirus prevents replication licensing by inhibiting MCM loading onto chromatin. EMBO Rep 4, 42-46.

Wienholds, E., Plasterk, R.H., 2005. MicroRNA function in animal development. FEBS Lett 579, 5911-5922.

Wightman, B., Ha, I., Ruvkun, G., 1993. Posttranscriptional regulation of the heterochronic gene lin-14 by lin-4 mediates temporal pattern formation in C. elegans. Cell 75, 855-862.

Wilkins, C., Woodward, J., Lau, D.T., Barnes, A., Joyce, M., McFarlane, N., McKeating, J.A., Tyrrell, D.L., Gale, M., Jr., 2013. IFITM1 is a tight junction protein that inhibits hepatitis C virus entry. Hepatology 57, 461-469.

Williams, S.C., 2013. First IL-6-blocking drug nears approval for rare blood disorder. Nat Med 19, 1193.

Wong, A.M., Kong, K.L., Tsang, J.W., Kwong, D.L., Guan, X.Y., 2012. Profiling of Epstein-Barr virus-encoded microRNAs in nasopharyngeal carcinoma reveals potential biomarkers and oncomirs. Cancer 118, 698-710.

Wu, J., Mao, X., Cai, T., Luo, J., Wei, L., 2006a. KOBAS server: a web-based platform for automated annotation and pathway identification. Nucleic Acids Res 34, W720-724.

Wu, T.T., Qian, J., Ang, J., Sun, R., 2012. Vaccine prospect of Kaposi sarcoma-associated herpesvirus. Curr Opin Virol 2, 482-488.

Wu, W., Vieira, J., Fiore, N., Banerjee, P., Sieburg, M., Rochford, R., Harrington, W., Jr., Feuer, G., 2006b. KSHV/HHV-8 infection of human hematopoietic progenitor (CD34+) cells: persistence of infection during hematopoiesis in vitro and in vivo. Blood 108, 141-151.

Wu, X., Yang, J., Na, T., Zhang, K., Davidoff, A.M., Yuan, B.Z., Wang, Y., 2017. RIG-I and IL-6 are negative-feedback regulators of STING induced by double-stranded DNA. PLoS One 12, e0182961.

Wu, X.J., Pu, X.M., Zhao, Z.F., Zhao, Y.N., Kang, X.J., Wu, W.D., Zou, Y.M., Wu, C.Y., Qu, Y.Y., Zhang, D.Z., Feng, Y.Y., Liu, J.Y., 2015. The expression profiles of microRNAs in Kaposi's sarcoma. Tumour Biol 36, 437-446.

Wu, Y.H., Hu, T.F., Chen, Y.C., Tsai, Y.N., Tsai, Y.H., Cheng, C.C., Wang, H.W., 2011. The manipulation of miRNA-gene regulatory networks by KSHV induces endothelial cell motility. Blood 118, 2896-2905.

Xie, J., Pan, H., Yoo, S., Gao, S.J., 2005. Kaposi's sarcoma-associated herpesvirus induction of AP-1 and interleukin 6 during primary infection mediated by multiple mitogen-activated protein kinase pathways. J Virol 79, 15027-15037.

Yan, Q., Li, W., Tang, Q., Yao, S., Lv, Z., Feng, N., Ma, X., Bai, Z., Zeng, Y., Qin, D., Lu, C., 2013. Cellular microRNAs 498 and 320d regulate herpes simplex virus 1 induction of Kaposi's sarcoma-associated herpesvirus lytic replication by targeting RTA. PLoS One 8, e55832.

Yan, Q., Ma, X., Shen, C., Cao, X., Feng, N., Qin, D., Zeng, Y., Zhu, J., Gao, S.J., Lu, C., 2014. Inhibition of Kaposi's sarcoma-associated herpesvirus lytic replication by HIV-1 Nef and cellular microRNA hsa-miR-1258. J Virol 88, 4987-5000.

Yan, Q., Shen, C., Qin, J., Li, W., Hu, M., Lu, H., Qin, D., Zhu, J., Gao, S.J., Lu, C., 2016. HIV-1 Vpr Inhibits Kaposi's Sarcoma-Associated Herpesvirus Lytic Replication by Inducing MicroRNA miR-942-5p and Activating NF-kappaB Signaling. J Virol 90, 8739-8753.

Yang, J.S., Lai, E.C., 2011. Alternative miRNA biogenesis pathways and the interpretation of core miRNA pathway mutants. Mol Cell 43, 892-903.

Yang, W.S., Hsu, H.W., Campbell, M., Cheng, C.Y., Chang, P.C., 2015. K-bZIP Mediated SUMO-2/3 Specific Modification on the KSHV Genome Negatively Regulates Lytic Gene Expression and Viral Reactivation. PLoS Pathog 11, e1005051.

Ye, H., Ling, S., Castillo, A.C., Thomas, B., Long, B., Qian, J., Perez-Polo, J.R., Ye, Y., Chen, X., Birnbaum, Y., 2013. Nebivolol induces distinct changes in profibrosis microRNA expression compared with atenolol, in salt-sensitive hypertensive rats. Hypertension 61, 1008-1013.

Yount, J.S., Moltedo, B., Yang, Y.Y., Charron, G., Moran, T.M., Lopez, C.B., Hang, H.C., 2010. Palmitoylome profiling reveals S-palmitoylation-dependent antiviral activity of IFITM3. Nat Chem Biol 6, 610-614.

Yu, J., Li, M., Wilkins, J., Ding, S., Swartz, T.H., Esposito, A.M., Zheng, Y.M., Freed, E.O., Liang, C., Chen, B.K., Liu, S.L., 2015a. IFITM Proteins Restrict HIV-1 Infection by Antagonizing the Envelope Glycoprotein. Cell Rep 13, 145-156.

Yu, J., Li, M., Wilkins, J., Ding, S., Swartz, T.H., Esposito, A.M., Zheng, Y.M., Freed, E.O., Liang, C., Chen, B.K., Liu, S.L., 2015b. IFITM Proteins Restrict HIV-1 Infection by Antagonizing the Envelope Glycoprotein. Cell Rep 13, 145-156.

Zhang, L., Wei, P., Shen, X., Zhang, Y., Xu, B., Zhou, J., Fan, S., Hao, Z., Shi, H., Zhang, X., Kong, R., Xu, L., Gao, J., Zou, D., Liang, C., 2015. MicroRNA Expression Profile in Penile Cancer Revealed by Next-Generation Small RNA Sequencing. PLoS ONE 10, e0131336.

Zhang, Y., Fan, M., Geng, G., Liu, B., Huang, Z., Luo, H., Zhou, J., Guo, X., Cai, W., Zhang, H., 2014. A novel HIV-1-encoded microRNA enhances its viral replication by targeting the TATA box region. Retrovirology 11, 23.

Zhao, X., Guo, F., Liu, F., Cuconati, A., Chang, J., Block, T.M., Guo, J.T., 2014. Interferon induction of IFITM proteins promotes infection by human coronavirus OC43. Proc Natl Acad Sci U S A 111, 6756-6761.

Zhi, H., Zahoor, M.A., Shudofsky, A.M., Giam, C.Z., 2015. KSHV vCyclin counters the senescence/G1 arrest response triggered by NF-kappaB hyperactivation. Oncogene 34, 496-505.

Zhong, W., Wang, H., Herndier, B., Ganem, D., 1996. Restricted expression of Kaposi sarcoma-associated herpesvirus (human herpesvirus 8) genes in Kaposi sarcoma. Proc Natl Acad Sci U S A 93, 6641-6646.

Zhou, P., Xu, W., Peng, X., Luo, Z., Xing, Q., Chen, X., Hou, C., Liang, W., Zhou, J., Wu, X., Songyang, Z., Jiang, S., 2013. Large-scale screens of miRNA-mRNA interactions unveiled that the 3'UTR of a gene is targeted by multiple miRNAs. PLoS One 8, e68204.

Zhu, L., Puri, V., Chandran, B., 1999. Characterization of human herpesvirus-8 K8.1A/B glycoproteins by monoclonal antibodies. Virology 262, 237-249.